

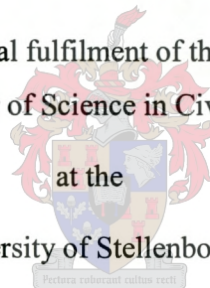
INCIPIENT MOTION IN COBBLE/BOULDER BED RIVERS

MENNO GAZENDAM

Thesis presented in partial fulfilment of the requirements for the
Degree of Master of Science in Civil Engineering

at the

University of Stellenbosch



Promotor: Professor A Rooseboom

December 2005

DECLARATION

I, the undersigned, hereby declare that the work contained in this thesis is my own original work and that I have not previously in its entirety or in part submitted it at any university for a degree.

ABSTRACT

This study sets out to describe the incipient motion process in cobble/boulder bed rivers in terms of the unit applied power approach. This objective has been met through the collection of data on stone movement from a total of thirteen flood events observed in two undisturbed rivers in the Western Cape, namely the Molenaars and Berg Rivers.

The data were plotted on the original modified Liu diagram for incipient motion and it was found that the threshold of movement for the smaller stones did not conform with the portion of the Liu diagram which represents fully turbulent flow (i.e. where $\sqrt{gD_s}/V_{ss} = 0.12$ for $Re_* > 13$). It was concluded that the only reason that could explain this deviation is the fact that the original modified Liu diagram had been derived for uniform particle size beds while the data of the Molenaars and Berg Rivers represent non-uniform particle size beds. This was proved through re-deriving the y-axis function of the original modified Liu diagram to include a factor that makes provision for the roughness of a non-uniform particle size bed. It was found that the average absolute roughness of the non-uniform particle size beds in the Molenaars and Berg Rivers is reasonably well approximated by a value of $k=d_{84}$.

Design curves (in terms of the original modified Liu diagram parameters) for intensity of motion were also produced. Although it is not possible to read off accurate percentages of movement values directly from these curves, it should be possible to deduce reasonably accurate values in practical situations.

OPSOMMING

Die studie poog om die begin van beweging proses in klip/rotsbed riviere te beskryf in terme van die eenheids aangewende drywing metode. Hierdie doel is bereik deur die insameling van klipbewegingdata in 'n totaal van dertien vloedgebeurtenisse in twee ongerepte riviere in die Wes-Kaap, naamlik die Molenaars en Bergriviere.

Die data was geplot op die oorspronklike aangepaste Liu diagram vir begin van beweging en dit was gevind dat die grens van beweging vir die kleiner klippe nie ooreenstem met die gedeelte van die Liu diagram wat volle turbulente vloei verteenwoordig nie (waar $\sqrt{gDs}/V_{ss} = 0.12$ vir $Re_* > 13$). Daar was tot die gevolgtrekking gekom dat die enigste rede wat die afwyking kan beskryf is die feit dat die oorspronklike aangepaste Liu diagram afgelei was vir uniforme partikelgrootte beddens terwyl die data van die Molenaars and Bergriviere nie-uniforme partikelgrootte beddens verteenwoordig. Dit was bewys deur die herafleiding van die y-as funksie van die oorspronklike aangepaste Liu diagram om 'n faktor in te sluit wat voorsiening maak vir die ruheid van 'n nie-uniforme partikelgrootte bed. Dit was gevind dat die gemiddelde absolute ruheid van die nie-uniforme partikelgrootte beddens in die Molenaars en Bergriviere word redelik goed benaderd met 'n waarde van $k=d_{84}$.

Ontwerpkurwes (in terme van die oorspronklike aangepaste Liu diagram parameters) vir intensiteit van beweging was ook ontwikkel. Alhoewel dit nie moontlik is om baie akkurate persentasies van beweging af te lees van die kurwes nie, is dit moontlik om akkuraat genoeg waardes te verkry in praktiese situasies.

ACKNOWLEDGEMENTS

I wish to record my sincere gratitude to the following:

My supervisor, Professor Albert Rooseboom, for his guidance, patience and willingness to teach.

Geordie Ractliffe who oversaw the data collection.

James Cullis, project leader, who compiled most of the data as well as for numerous conversations discussing the project.

Everyone who assisted in gathering data, which involved many hours standing in a cold mountain stream in the middle of winter.

The Water Research Commission for financial support.

All my family and friends that supported and helped me in many different ways.

To God, for giving us inquisitive minds to try and find order in the nature he created.

TABLE OF CONTENTS

	Page
<i>Declaration</i>	<i>i</i>
<i>Abstract</i>	<i>ii</i>
<i>Opsomming</i>	<i>iii</i>
<i>Acknowledgements</i>	<i>iv</i>
<i>Table of contents</i>	<i>v</i>
<i>List of Symbols</i>	<i>viii</i>
<i>List of Tables</i>	<i>ix</i>
<i>List of Figures</i>	<i>x</i>
<i>List of Appendices</i>	<i>xiii</i>

1 INTRODUCTION

1.1	Background	1
1.2	Objectives and Methodology	4
1.3	Thesis Layout	5

2 LITERATURE REVIEW

2.1	Incipient motion theories	6
	(i) Critical shear stress	6
	(ii) Critical velocity	10
	(iii) Critical flow discharge	11
	(iv) Critical Froude numbers	12
	(v) Transport distances	12
	(vi) Probability models	13

(vii) Stream power	15
2.2 Conclusions	21
3 DATA COLLECTION	
3.1 Site selection	22
3.2 Site setup	25
(i) Surveys	25
(ii) Stones	25
(iii) Water levels	26
3.3 Base flow conditions	28
3.4 Flood events data	28
3.5 Collection of incipient motion data	36
4 CRITICAL CONDITIONS	
4.1 Original modified Liu-diagram	40
4.2 Influence of embedded stones	44
4.3 Influence of non-uniformity under fully developed turbulent conditions	46
4.4 Influence of laminar zones on incipient motion	56
4.5 Conclusions	58
5 INTENSITY OF MOVEMENT GRAPHS	
5.1 Introduction	61
5.2 Intensity of movement	61

(i)	Original modified Liu-diagram	61
(ii)	Incipient motion in terms of DRIFT classification	68
5.3	Conclusions	70
6	COMBINED CONCLUSIONS AND RECOMMENDATIONS	
6.1	Combined conclusions	72
6.2	Recommendations	73
7	REFERENCES	

LIST OF SYMBOLS

a, b	: constants
A	: cross sectional flow area
A_s	: grain area
C_D	: drag coefficient
d	: particle diameter
d_x	: particle size for which x % is smaller
D	: flow depth
Fr	: Froude number
g	: gravitational acceleration
k	: absolute bed roughness
Q	: discharge (m^3/s)
Re_*	: Reynold's number
R'	: proportion of the hydraulic radius appropriate to sediment transport
s	: energy gradient \approx channel gradient (uniform conditions)
S_f	: energy gradient
u	: mean velocity
u_*	: shear velocity
V_{ss}	: settling velocity
V_s	: grain volume
y	: flow depth
z	: bed elevation above datum
ϕ	: angle of repose
Φ	: dimensionless bedload function
ρ	: density of water
ρ_s	: particle density
τ	: shear stress
τ_0	: shear stress at bed
ν	: kinematic viscosity

LIST OF TABLES

	Page
Table 2.1: Different empirical equation coefficients	8
Table 3.1: Classification of bed particle sizes	23
Table 3.2: DRIFT classification of floods for H1H018 and G1H004 in terms of average daily flows (m^3/s) (Brown and King, 2002; Howard, 2004).....	30
Table 3.3: Flood events observed at the Molenaars study site	33
Table 3.4: Flood events observed at the Berg study site.....	33
Table 3.5: Stone movement in the Molenaars River during 2003 flood events	36
Table 3.6: Stone movement in the Molenaars River during 2004 flood events	37
Table 3.7: Stone movement in the Berg River during 2004 flood event	38
Table 5.1: Flood events observed at the Molenaars study site	67
Table 5.2: Flood events observed at the Berg study site.....	68

LIST OF FIGURES

	Page
Figure 1.1: The relationship between percentage of natural flow and river condition (Brown and King, 2000)	3
Figure 2.1: Shields' diagram	7
Figure 2.2: Empirical equations (Lorang and Hauer, 2003)	9
Figure 2.3: Shear stress for motion of sediments.....	10
Figure 2.4: Hjulstrom curves for critical hydraulic conditions in uniform particle size sand beds.....	11
Figure 2.5: Einstein bedload model	14
Figure 2.6: Modified Liu diagram (Rooseboom, 1992).....	20
Figure 3.1: Location of study sites.....	22
Figure 3.2: Molenaars River study site (looking downstream).....	23
Figure 3.3: Berg River study site (looking upstream).....	24
Figure 3.4: Study site set up.....	25
Figure 3.5: Example of a marked stone	26
Figure 3.6: Plastic stage pipe used to measure flood levels.....	27
Figure 3.7: Plastic stage pipe used to measure flood levels (during flood conditions)	27
Figure 3.8: The Molenaars study site in flood	29
Figure 3.9: Flood events observed on the Molenaars River (H1H018) in 2003.....	31
Figure 3.10: Flood events observed on the Molenaars River (H1H018) in 2004.....	31
Figure 3.11: Flood events observed on the Berg River (G1H004) in 2004	32
Figure 3.12: Water level profiles for the Molenaars study site in 2003	34

Figure 3.13: Water level profiles for the Molenaars study site in 2004 34

Figure 3.14: Water level profiles for the Berg study site in 2004..... 35

Figure 3.15: Level of disturbance in the Molenaars River during 2003 flood events 37

Figure 3.16: Levels of disturbance in the Molenaars River during 2004 flood events..... 38

Figure 3.17: Level of disturbance in the Berg River during 2004 flood events 39

Figure 4.1: Original modified Liu diagram (Rooseboom, 1992)..... 40

Figure 4.2: Molenaars 2003 data plotted in the original modified Liu diagram..... 41

Figure 4.3: Molenaars 2004 data plotted in the original modified Liu diagram..... 41

Figure 4.4: Berg 2004 data plotted in the original modified Liu diagram..... 42

Figure 4.5: Molenaars 2003 data, excluding data for embedded stones, plotted on the original modified Liu diagram 45

Figure 4.6: Molenaars 2004 data, excluding data for embedded stones, plotted on the original modified Liu diagram 45

Figure 4.7: Berg 2004 data, excluding data on embedded stones, plotted on the original modified Liu diagram 46

Figure 4.8: Two-dimensional representation of the eddy formation process in a uniform particle size bed..... 49

Figure 4.9: Two-dimensional representation of the eddy formation process in a non-uniform particle size bed..... 50

Figure 4.10: Stone d in a uniform particle size bed with a fixed \sqrt{gDs} 52

Figure 4.11: Stone d in a non-uniform particle size bed with a fixed \sqrt{gDs} 52

Figure 4.12: Stone d in a non-uniform particle size bed with an increased \sqrt{gDs} 53

Figure 4.13: Liu diagram, adapted for non-uniformity, $k=d84$ Molenaars 2003..... 54

Figure 4.14: Liu diagram, adapted for non-uniformity, $k=d84$, Molenaars 2004..... 55

Figure 4.15: Liu diagram, adapted for non-uniformity, $k=d84$, Berg 2004..... 55

Figure 4.16: Transition zones	56
Figure 4.17: Critical conditions for sediment particles (Liu diagram) with river flood data and bedforms added (Rooseboom and Le Grange, 2000).....	57
Figure 5.1: Max Applied Power/Required Power per stone size class for Molenaars 2003 Flood 6	62
Figure 5.2: Molenaars 2003 data, floods separated, plotted in the original modified Liu diagram	63
Figure 5.3: Molenaars 2004 data, floods separated, plotted in the original modified Liu diagram	64
Figure 5.4: Berg 2004 data, floods separated, plotted in the original modified Liu diagram	64
Figure 5.5: Envelope curves for intensity of movement, Molenaars 2003	65
Figure 5.6: Envelope curves for intensity of movement, Molenaars 2004	66
Figure 5.7: Envelope curves for intensity of movement, Berg 2004	66
Figure 5.8: DRIFT flood classification vs. Intensity of movement (excluding non-embedded stones).....	69
Figure 5.9: DRIFT flood classification vs. Intensity of movement (all stones)	70

LIST OF APPENDICES

APPENDIX A: Detail of study sites

APPENDIX B: Base flow conditions

APPENDIX C: Field notes from flood event data collection

APPENDIX D: Stone movement for individual flood events

1 INTRODUCTION

1.1 Background

In pristine cobble/boulder bed rivers the channel bed configuration is maintained by a range of flows which are characteristic of the natural flow regime and which typically incorporate flows of different timing, duration, magnitude and frequency. The health of these channel beds is crucial to a multitude of aquatic organisms that are dependent on the bed for their survival. The channel bed of cobble/boulder a bed river is often referred to as a faunal reservoir, as it provides the source for recolonization of a stream when aquatic populations are depleted by adverse conditions. A variety of factors control the abundance, distribution and productivity of aquatic organisms in rivers. These include competition for space, predation, chemical water quality, nutrient supplies, flow patterns, as well as flow variability and together they describe the biological, chemical and physical habitat (Gordon *et al.*, 1992).

Depending on the biological species and life-cycle, the channel bed provides refuge from floods, shelter during droughts and extreme temperatures and interstitial spaces in which to lay and incubate eggs. Sufficient flow through the interstitial spaces allows the replenishment of nutrients and oxygen while metabolic wastes are continuously removed. The cobbles and boulders also assist with the periodic physical breakdown of organic detritus and provide a mechanism for entrainment of organic matter in the spaces between larger bed elements. This disturbance or breakdown process is an essential organizing factor in many ecosystems (Picket and White 1985).

The construction of dams, leads to alterations in the natural flow regime, flooding magnitude, frequency and the sediment transport capacity in the river channels downstream. This has a definite, often negative, impact on the dynamics of substrate movement and maintenance, which in turn affects the faunal and floral aquatic environment. Traditionally chemical water quality has been viewed as the most important factor affecting the degradation of aquatic ecosystems (Hugues *et al.*, 1990). However,

the physical habitat and its modifications have recently been identified as key elements in stream ecosystem functioning (Lamouroux *et al.*, 1995).

The process of determination of the amount of water which is required for environmental needs, is known as “Environmental Flow Assessment” (EFA). Following the EFA, a modified flow regime is prescribed for the river. The amount of water required in the modified flow regime is that which is deemed to be necessary for maintaining the river in a pre-determined condition and is known as the “Environmental Flow Requirement” (EFR). EFR’s are based on an understanding (Brown and King, 2000) of how flow changes relate to changes in river condition, in order to describe flow that will:

- minimize or mitigate the impacts of new water-resource development
- restore systems impacted by past developments
- allow calculation of the costs of compensating people affected by such impacts.

In order to maintain a healthy and productive substrate environment in cobble and boulder bed rivers it is necessary that the environmental flow requirement (EFR) accommodates a substrate maintenance flow component. The specification of this substrate maintenance flow component must provide information on the amount and frequency of managed flows which are required to maintain a river in a pre-determined, environmentally acceptable condition. The availability of water, especially in a water scarce country such as South Africa, the cost of water that is released and lost for storage and the financial implications associated with the installation of outlet structures at reservoirs, emphasize the need to specify substrate maintenance flows as accurately as possible.

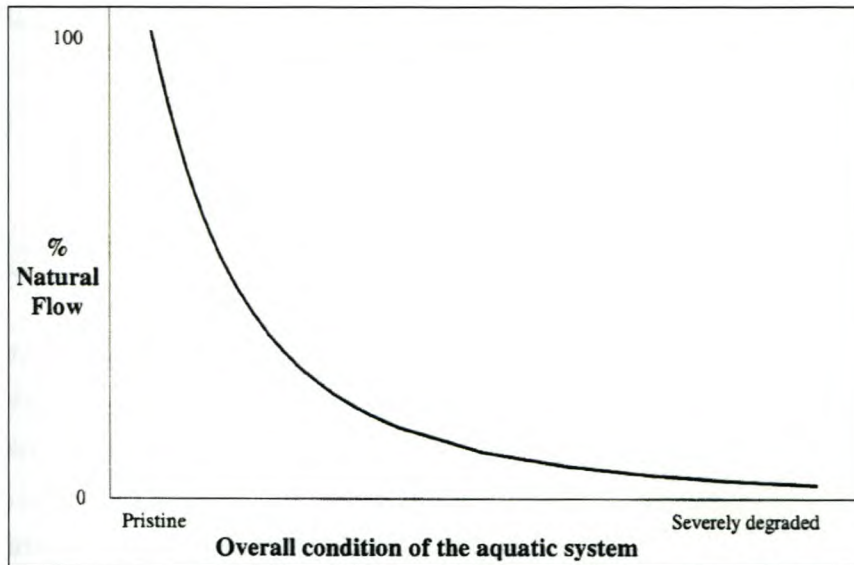


Figure 1.1: The relationship between percentage of natural flow and river condition (Brown and King, 2000)

Various factors complicate the determination of a substrate maintenance flow component. There is very little scientifically based data available regarding the impacts (both positive and negative) of different levels of substrate disturbance on the aquatic environment, from the scale of an individual disturbance event to that of the disturbance regime. Furthermore, it is necessary to contend with the complexity of flow and sediment transport processes in cobble/boulder bed rivers. This includes the effects of large scale roughness, macro scale bedforms (pool-riffle structures), the heterogeneous nature of the substrate particles and the effects of shielding or hydraulic protection on critical conditions for sediment movement.

With the increasing development of water infrastructure in mountain regions, knowledge of the hydraulic characteristics of rivers in the upper catchment areas has become very important, especially for determining environmental flow requirements. Due to their characteristic morphological and associated hydraulic attributes, the physical habitats within these rivers are extremely diverse, both on spatial and temporal scales. They are characterized by high gradients, great variability in sediment size and relatively low flow depths. The bed configuration typically contains a series of pools, steps, rapids, riffles

and plane bed beds, while energy losses are high as a result of turbulence and local hydraulic jumps (Jonker, 2003). Thus, in order to facilitate the specification of substrate maintenance flows in cobble/boulder bed rivers, which can be incorporated into either an environmental flow requirement or river rehabilitation programs, knowledge of the relationship between substrate disturbance, the aquatic environment and discharge is critical.

1.2 Objectives and Methodology

This thesis forms part of a bigger research project^[1] sponsored by the Water Research Commission, of which the main aims are:

- To define and quantify ecologically significant substrate disturbance levels in cobble and boulder bed rivers.
- To develop theoretically-based hydraulic models that will address the relationship between discharge and substrate disturbance in cobble and boulder bed rivers.
- To develop guidelines for the specification of substrate maintenance flow components in cobble and boulder bed rivers.

In order to establish the relationship between substrate disturbance, the aquatic environment and discharge, detailed knowledge is required of different levels of bed disturbance in cobble/boulder bed rivers. Disturbances within these rivers can broadly be categorized in terms of the following levels of disturbance:

- No bed movement, where no sediment is being transported.
- Incipient motion, where the bed elements just start to move.
- Full bed movement, where all the particles along the bed surface are being transported.

^[1] WRC Project K5/1411, Determination of Substrate Maintenance Flows in Cobble and Boulder Bed Rivers, Ecological and Hydraulic Considerations.

The incipient motion condition is also referred to as the critical condition. Not only does incipient motion describe the movement threshold for sediment but it also serves to define the deposition threshold whereby sediment ceases to be transported. Thus a key in understanding the different levels of movement lies in the proper understanding of the incipient motion condition.

The following objectives were formulated for this thesis:

- *To describe incipient motion in cobble/boulder bed rivers.*
- *To produce graphs that will aid in the prediction of sediment movement in cobble/boulder bed rivers.*

The incipient motion process will be described by addressing the factors relating to the onset of incipient motion in the two streams studied.

1.3 Thesis Layout

Chapter 2 provides a literature overview of past and current methods for describing incipient motion. The data collection process is described in Chapter 3. In Chapter 4 the hydraulic relationships associated with incipient motion are addressed. Chapter 5 explains the process of producing graphs for practical use in predicting different levels of entrainment. Final conclusions and recommendations are contained in Chapters 6 and references are listed in Chapter 7. Appendices follow at the end.

2 LITERATURE REVIEW

2.1 Incipient motion theories

(i) Critical shear stress

Critical shear stress is defined as the maximum shear stress exerted on the bed that will not cause erosion of the sediment forming the bed. The retarding effect that limits the movement of one fluid element relative to another is traditionally represented by so called shear stress. This shear stress (τ) is shown by the following,

$$\tau = \rho g(D - y)s \quad (2.1)$$

where D is the distance from the water level, y the distance from the bed, ρ the density of water and s the channel gradient.. Thus the maximum shear stress will prevail at the bed which is denoted by τ_o .

In field studies the critical shear stress has been estimated from the largest grain observed in motion (Andrews, 1983; Carling, 1983; Hammond *et al.*, 1984). Mixed-size sediment transport rates, from which incipient motion may be estimated, have been measured in several laboratory studies (Day, 1984; Dhamotharan *et al.*, 1980; Misri *et al.*, 1984) and in the field (Milhouse, 1973; Parker *et al.*). Experiments focusing on part of the problem, the pivoting angle of individual size fractions, have been undertaken by Li and Komar (1986).

The simplest shear stress model, the empirical power law, relating τ_o (shear stress at the bed) and d (diameter of stone) as

$$d_{50} = a\tau_o^b \quad (2.2)$$

where b is the regression line slope and a is the y-intercept for a log-plot of τ_o (shear stress at the bed) versus d_{50} . Knowing the shear stress at the bed (τ_o) allows one to solve

for the diameter of stones that will move (with the aid of equation 2.2 and the constants known) and from knowing the diameter (d) of a stone that moved the critical bed shear stress can be determined. However, the relationship is restrictive, applying only to a limited range of grain sizes and flow conditions where grain density and other entrainment parameters are known or are assumed to be constant (Carling, 1983).

Shields (1936) showed that the particle entrainment was related to a form of Reynolds' Number, based on the shear velocity u_* ($=\sqrt{\tau_0/\rho}$) i.e. $Re_* = \rho u_* D / \mu$. Shields plotted the results of his experiments in the form of an entrainment function (which is depicted by the y-axis and equals $\tau_0/(\rho_s - \rho)gD$) against Re_* .

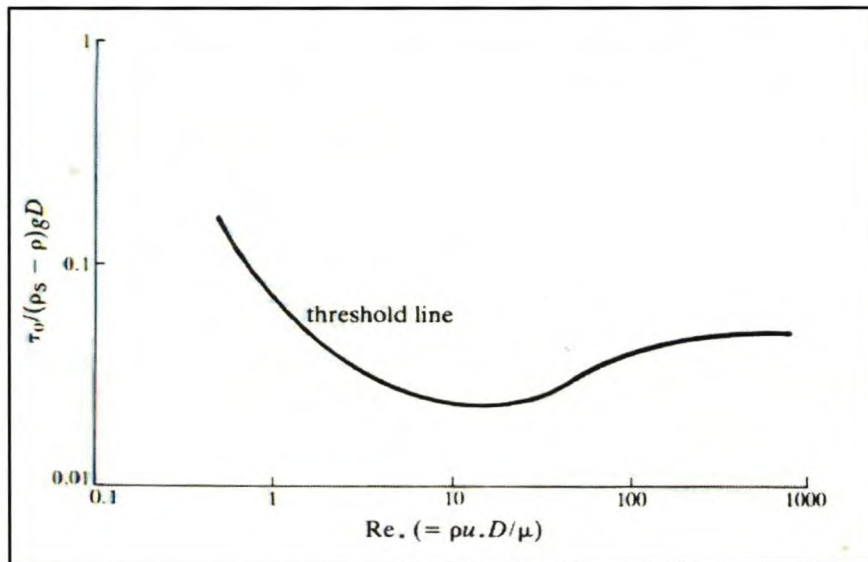


Figure 2.1: Shields' diagram

Power analysis by Rooseboom (1992) (Chapter 2.1.7) proves that the x-axis represents Laminar power/Turbulent power. The Shields equation was originally tested in a flume using spheres of uniform size and found to approach a constant value (y-axis) of 0.06 for coarse grained sediment with $d > 6\text{mm}$ (Shields, 1936, Bagnold, 1966, and Allen, 1970). In natural streams, however, there is a high variance in the estimated values of τ_0 as a result of the non-uniformity of the bed particles.

An investigation of critical hydraulic conditions in gravel-bed rivers with naturally sorted bed material described by Andrews (1983) showed that the critical shear stress τ_0 could be given by an equation of the type shown in equation 2.3. As with the power law relationship this equation also allows calculation of a critical diameter once the shear stress is known or vice versa.

$$\tau_0 = a \left(\frac{d_i}{d_{50}} \right)^b \quad (2.3)$$

In this type of equation, the coefficient a represents Shields' entrainment function in homogeneous sediment conditions when $(d_i/d_{50})=1$. The (d_i/d_{50}) term attempts to provide a measure of the hydraulic protection that a stone of a certain diameter experiences due to its relative size in the bed. Several studies confirm the validity of this approach even though the values of the coefficients differ vastly. Table 2.1 shows these respective studies and their coefficients.

a	b	d_{50}	d_i/d_{50} range	Study
0.088	-0.98		0.045-4.2	Parker <i>et al.</i> (1982)
0.083	-0.87	0.13-2.5 5.4-7.4	0.3-4.2	Andrews (1983)
0.045	-0.68	2	0.4-5.9	Milhous (1973) in Komar (1987)
0.045	-0.68	2	0.5-10	Carling (1983)
0.045	-0.71	0.75	0.67-5.33	Hammond <i>et al.</i> (1984)
0.089	-0.74	2.3-9.8	0.1-2	Ashworth and Ferguson (1989)
0.047	-0.88	7.3	0.04-1.2	Ferguson <i>et al.</i> (1989)
0.049	-0.69	1.8-3.2	0.15-3.12	Ashworth <i>et al.</i> (1992)

Table 2.1: Different empirical equation coefficients

The difference in coefficients might be attributed to the fact that size distributions along individual reaches respond uniquely to a given distribution of particles, packing and turbulence characteristic of flow (Komar & Carling, 1991).

Several empirical flow equations are plotted in Figure 2.2. Differences in the slopes and intercepts of regression lines are obvious.

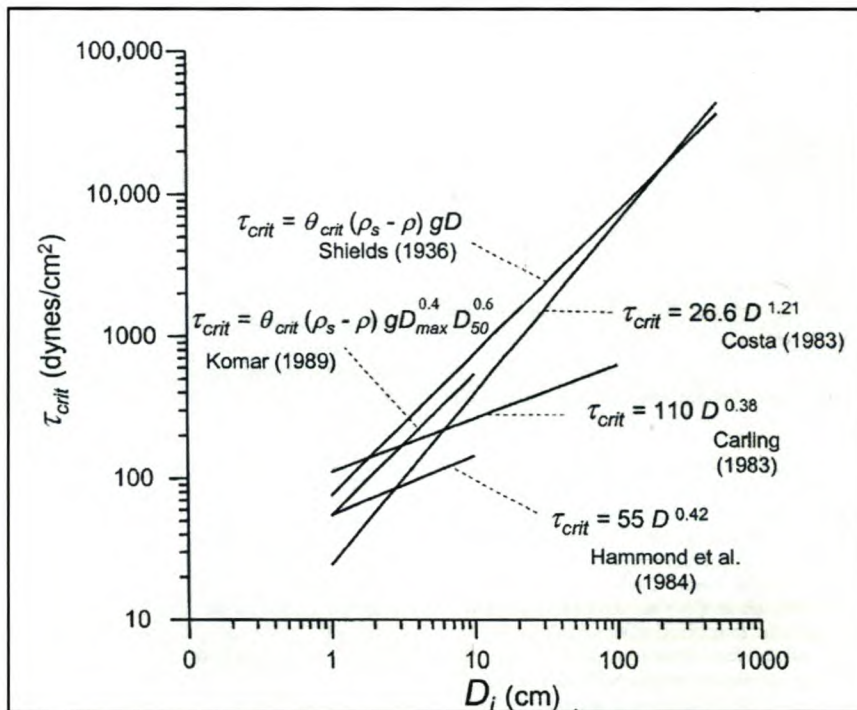


Figure 2.2: Empirical equations (Lorang and Hauer, 2003)

According to Wiberg and Smith (1987) a particle in a poorly sorted bed can have critical shear stresses that differ significantly from the critical shear stress associated with that particle when placed on a well sorted bed of the same size. In Chapter 4 this is shown to be true for applied stream power as well. Wiberg and Smith (1987) indicate that this difference is primarily due to the relative protrusion of a particle into the flow along with differences in the particle angle of repose, or bed pocket geometry that results from having a mixture of grain sizes on the bed. This led them to Figure 2.3 to determine critical shear stress for a specific particle. The graph contains incipient motion curves for

different ratios of grain diameter to bed roughness length, D/k_s , where bed roughness length refers to the diameter of the eddy sizes that can fit in between the bed particles. Critical shear stress is indicated with τ_* and the Reynolds' Number with Re_* .

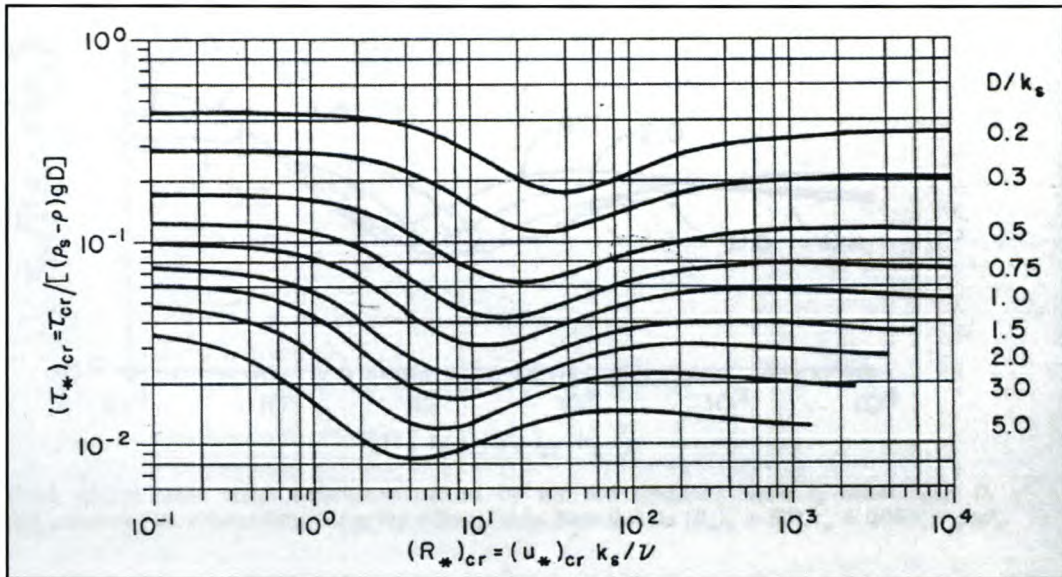


Figure 2.3: Shear stress for motion of sediments

Wilcock & Southard (1988) found that the sorting of the mixture had little effect on the critical shear stress of individual fractions, once the median size (d_{50}) of the mixture and a fraction's relative size (d_i/d_{50}) are accounted for. Their data showed a consistent relationship between the critical shear stress of individual fractions and each fraction's relative grain size, despite a broad variation in the available data of mixture sorting, grain size distribution shape, mean grain size, and grain shape.

(ii) Critical velocity

Critical velocity is defined as the maximum velocity of the stream that will not cause erosion of the sediment forming the bed. Extensive empirical data exists relating maximum velocities to various soil and vegetation conditions. Hjulstrom (1939) developed the graph in Figure 2.4, which relates average critical velocity to particle size.

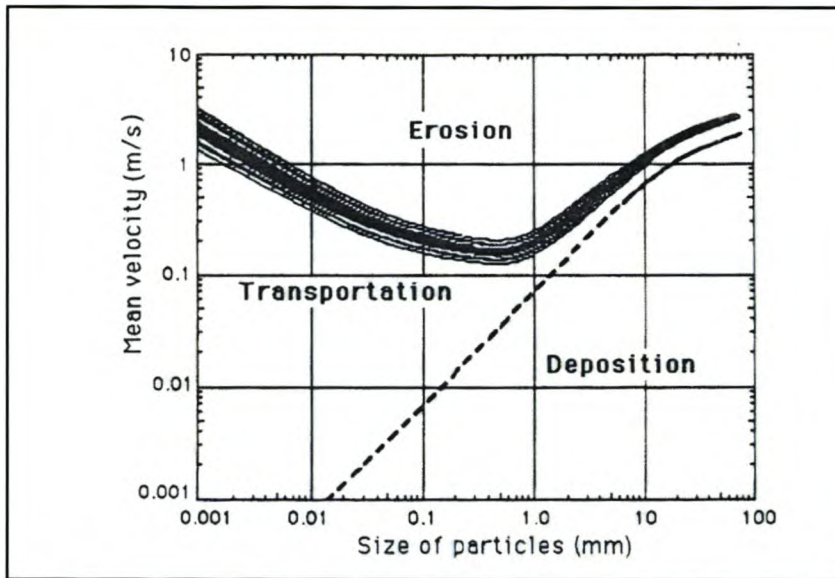


Figure 2.4: Hjulstrom curves for critical hydraulic conditions in uniform particle size sand beds

However, this simple method (critical velocity) for design does not consider the channel shape or flow depth. At the same mean velocity, channels of different shapes or depths may have quite different forces acting on the boundaries.

(iii) Critical flow discharge

Bathurst (1987) argues that on steep slopes the critical conditions for movement are best predicted by an approach based on water discharge rather than the Shields shear stress. He therefore adopted the Schoklitch (1962) approach to prediction of critical flow conditions, based on water discharge rather than shear stress. Using flume data for bed materials with relatively uniform size distributions he developed the empirical relationship:

$$q_{cr} = 0.15g^{0.5}d^{1.5}s^{-1.12} \quad (2.4)$$

where q_{cr} = critical water discharge per unit width; and s = bed slope. The equation was derived for the range of slopes $0.0025 < s < 0.2$ and particle sizes $3 < d < 44$ mm and for ratios

of depth to particle size as low as 1. The above equation was used in conjunction with the following equation to determine the critical flow condition for each particle size:

$$q_{ci} = q_{cr} (d_i/d_r)^b \quad (2.5)$$

where $b = 1.5(d_{84}/d_{16})^{-1}$, d_r is set equal to d_{50} , q_{ci} = the critical unit discharge for movement of particle d_i , q_{cr} = the critical unit discharge for the reference particle size d_r which is unaffected by the hiding/exposure effect and b = an exponent. Calibration of the above equation was carried out empirically using field data.

(iv) Critical Froude numbers

Aguirre-Pe *et al.* (2003) states that for ratios of flow depth to bed particle diameter less than ten (flow on very rough boundaries) neither the Reynolds number of the solid loose particles at a stream bed nor the Shields parameter are adequate variables to predict critical flow conditions for the initiation of motion. A particle densimetric Froude number $F^* = u/[(r-1)gd]^{1/2}$ is proposed as an alternative criterion to predict hydraulic conditions for the initiation of motion. Where u = mean velocity, r = ratio of sediment and fluid densities, g = acceleration due to gravity, and d = characteristic diameter of bed particle.

(v) Transport distances

D'Agostino *et al.* (1999 (a),(b)) used the ratio of transport distances and stone diameter to establish a criterion to define the incipient motion condition. The incipient motion condition of a grain size class is assumed to be given by an average distance of movement less than the diameter d_i representative of the diameter class itself. The average lengths of movement for different size stones were recorded. Where this average length was found to be less than the diameter of the stone itself, the stone diameter and the flood size were grouped together. Using the flood size and stone diameter, the boundary shear stress was obtained indirectly from flood size values by employing momentum conservation on a fluid control volume in uniform flow.

(vi) Probability models

Einstein (1942), in light of the fact that the incidence of an eddy capable of transporting a particular grain is some statistical function of time, proposed a probabilistic model of bedload for the case of even beds of grains. The basic ideas underlying Einstein's equation are the following:

For an individual grain, migration will take place in a series of jumps (Figure 2.5) of length $L = K_L D$. During a time T a series of n such jumps will occur, so that the particle will travel a total distance nL .

The probability, ρ , that a grain will be eroded during the typical period, T , must be some function of the immersed self-weight of the particle and the fluid force acting on the particle. The immersed self-weight is $(\rho_s - \rho)g(K_V d^3)$, and the lift force is $C_L \rho (K_A d^2) u^2 / 2$, where the grain area $A_s = K_A d^2$ and the grain volume $V_s = K_V d^3$. Therefore,

$$\rho = f\left(\frac{(\rho_s - \rho)g(K_V d^3)}{C_L \rho (K_A d^2) u^2 / 2}\right) \quad (2.6)$$

u is a 'typical' velocity at the sub-layer proposed by,

$$u \approx 11.6u_* \approx 11.6\sqrt{gR's} \quad (2.6a)$$

where R' is that proportion of the hydraulic radius appropriate to sediment transport. Equation 2.6 is usually expressed as

$$p = f\{B_* \cdot \Psi\} \quad (2.6b)$$

where

$$B_s = \frac{K_v}{C_L K_A^{1.35/2}} \quad (2.6c)$$

$$\Psi = \frac{(\rho_s - \rho)d}{\rho R's} \quad (2.6d)$$

The number of grains of a given size in area A ($K_L D \times 1$) is $K_L D / K_A D^2$, therefore the number of grains dislodged during time T will be $\rho K_L D / K_A D^2$. The volume of grains crossing a given boundary must therefore be

$$\frac{\rho K_L d}{K_A d^2} K_v d^3 = \frac{\rho K_L K_v d^2}{K_A} \quad (2.7)$$

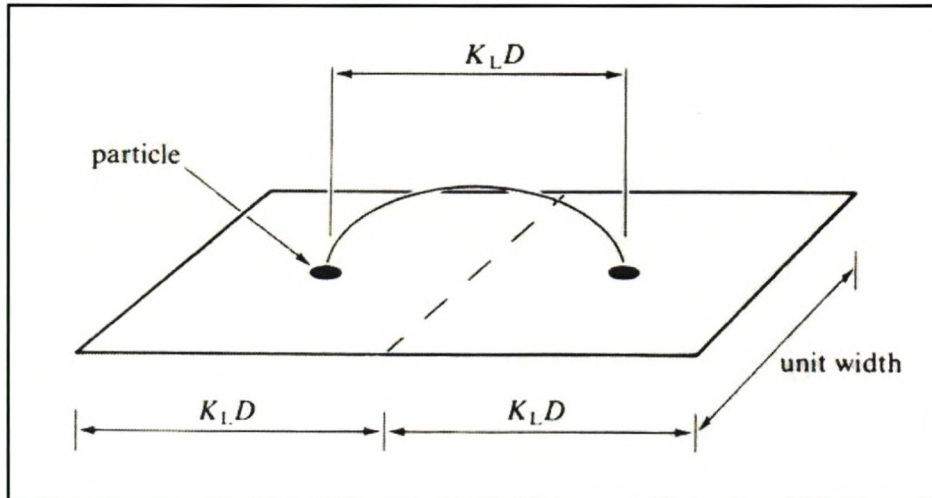


Figure 2.5: Einstein bedload model

The volume must also be given by $q_s T$. If the time T is some function of particle size and fall velocity, say $T = K_T d / V_{ss}$, then

$$q_s T = q_s \frac{K_T d}{V_{ss}} \quad (2.8)$$

Equating 2.7 and 2.8

$$\frac{q_s K_T d}{V_{ss}} = \frac{\rho K_L K_V d^2}{K_A} \quad (2.9)$$

therefore

$$\rho = \frac{q_s K_T K_A}{V_{ss} K_L K_V d} \quad (2.10)$$

Equating 2.6 and 2.10, leads, with some rearrangement, to

$$\Phi = q_s \sqrt{\frac{\rho}{(\rho_s - \rho)d^3}} = f(B_*, \Psi) \quad (2.11)$$

where Φ is a dimensionless bedload function and B_* and Ψ have been defined above.

Following Einstein, a number of researchers investigated the relationship between Φ and Ψ . A typical result is due to Brown (in Rouse, 1950),

$$\Phi = 40(1/\Psi)^3$$

which is valid for $\Phi > 0.04$. As Φ (and therefore q_s) $\rightarrow 0.1/\Psi \rightarrow 0.056$, which corresponds to the Shields threshold condition where Shield's entrainment function reveals a value of 0.056 (see Figure 2.1).

(vii) Stream power

The movement of bed particles (or water) requires expenditure of energy, which is provided in streams by the release of potential energy as water travels down a slope. The

rate of energy dissipation is a measure of the stream power of a reach and specifically describes the amount (per unit volume) of power made available by the decrease in potential energy of flowing water (Jonker 2002) to maintain motion. This motion can be purely that of the fluid, or it can be of a fluid / solid mixture (Armitage & McGahey 2003). A number of researchers have preferred to use unit stream power as an indicator of sediment motion, although this application is not generally described in standard hydraulic introductory texts (e.g. Gordon *et al.* 2004).

Armitage & McGahey (2003) argue that the quantity represented by unit stream power is more directly related to the entrainment threshold, because it can be computed at any point in the water column, and because turbulence is directly related to dissipation of energy. Rooseboom (1998) argues that the application of the law of conservation of stream power (over that for example of momentum which is the basis for equations of critical shear stress) has advantages in that it involves scalar quantities (unlike the momentum-impulse law), its terms are directly time-dependent and account for the roughness (k) of the bed directly. Further, Rooseboom (1998) showed that the stream power equations uniquely give theoretical and numerical support to the empirically derived functions of the Liu Diagram for incipient motion (Liu, 1957), and provides a complete mathematical description of the Liu diagram..

Rooseboom (1974) defined the law of conservation of power under conditions of steady, uniform flow as

$$\int_{y_0}^D \rho g s v dy = \int_{y_0}^D \tau \frac{dv}{dy} dy \quad (2.12)$$

with ρ : fluid density (kg/m^3)
 g : gravitational acceleration (m/s^2)
 s : energy gradient \approx channel gradient

v : velocity at distance y above the bed (m/s) ($\approx \frac{1}{\kappa} \sqrt{gDs} \ln \frac{y}{y_0}$)

D : flow depth (m)

y_0 : $\approx k/30$; ordinate where velocity is mathematically equal to zero (m)

τ : shear stress at distance y above the bed (N/m^2)

κ : von Karman coefficient ($\approx \frac{1}{\sqrt{2\pi}}$)

The parameter ρgsv in equation 2.12 represents the amount of unit power made available by the flowing stream, whereas the parameter $\tau \frac{dv}{dy}$ represents the power applied per unit volume to maintain motion.

Where alternative modes of flow exist, that mode of flow which requires the least amount of unit power will be followed and it therefore follows that fluid flowing over moveable material would only transport the material, if it will result in a decrease in the amount of unit power being applied (Rooseboom 1974; 1998). As the power applied along the bed of a river varies depending on whether laminar or turbulent flow conditions prevail at the bed, the critical condition for sediment movement also depends on whether flow condition at the bed is laminar or turbulent.

Under conditions of laminar or smooth turbulent flow, Rooseboom (1974) showed that the unit stream power applied along the bed equals

$$\frac{(\rho g s D)^2}{\rho \nu} \quad (2.13)$$

with ν : kinematic viscosity (m^2/s)

The applied power required per unit volume to entrain a particle with density ρ_s and settling velocity V_{ss} in a fluid with density ρ , equals

$$(\rho_s - \rho)gV_{ss} \quad (2.14)$$

Stokes's law (Graf 1971), defines the settling velocity of a particle with diameter d under viscous conditions as

$$(V_{ss})_{LAM} \propto d^2 g \frac{\rho - \rho_s}{\rho \nu} \quad (2.15)$$

The critical condition for the movement of sediment particles is reached when the power applied along the bed exceeds the power required to move the sediment particles out of their original positions. In laminar or smooth turbulent flow therefore, a relationship defining the threshold for sediment transport under viscous conditions can be defined from equation 2.13, 2.14 and 2.15. This relationship, calibrated with data by Grass (1970) and Yang (1973), was found to be:

$$\frac{\sqrt{gDs}}{V_{ss}} = \frac{1.6}{\frac{\sqrt{gDs}}{\nu} \cdot d} \quad (2.16)$$

for values of $\frac{\sqrt{gDs} \cdot d}{\nu} < 13$, i.e. with smooth turbulent or completely laminar flow over a smooth bed (Rooseboom 1974, 1998).

Under conditions of rough, turbulent flow, Rooseboom (1974; 1998) showed that the unit applied power near the bed at (y_0) , where $D - y_0 \approx D$, is

$$\tau \frac{dv}{dy} \approx \frac{30\rho g s D \sqrt{2\pi g s D}}{d} \quad (2.17)$$

Under turbulent conditions energy dissipation occurs through the formation of turbulent eddies and not at the molecular level as is the case under laminar or smooth turbulent flow conditions. Viscosity is therefore not significant, but rather the size of the turbulent eddies that form. The size of these eddies represent the absolute roughness (k) of the bed. In the case of a bed with a uniform size distribution the size of the turbulent eddies that fit between the particles can be considered to be equal to the diameter of the bed particles. Furthermore, under conditions of turbulent flow, the settling velocity as expressed by Graf (1971) equals

$$(V_{ss})_{\text{TURB}} = \sqrt{\frac{4(\rho_s - \rho)gd}{3C_d}} \quad (2.18)$$

with C_d : drag coefficient (assumed constant for larger diameters).

From equations 2.14, 2.17 and 2.18 the critical condition for the movement of sediment along an even bed in rough turbulent flow can thus be defined by

$$\frac{\sqrt{gDs}}{V_{ss}} = \text{Constant} \quad (2.19)$$

This relationship was calibrated with measured data from Yang (1973) and the value of the constant was found to be 0.12 for values of $\frac{\sqrt{gDs} \cdot d}{\nu} > 13$ (Rooseboom 1974; 1998)

Rooseboom (1992) used the above parameters in a modified Liu diagram to describe the hydraulic relationships for sediment at incipient motion conditions as depicted in Figure 2.6.

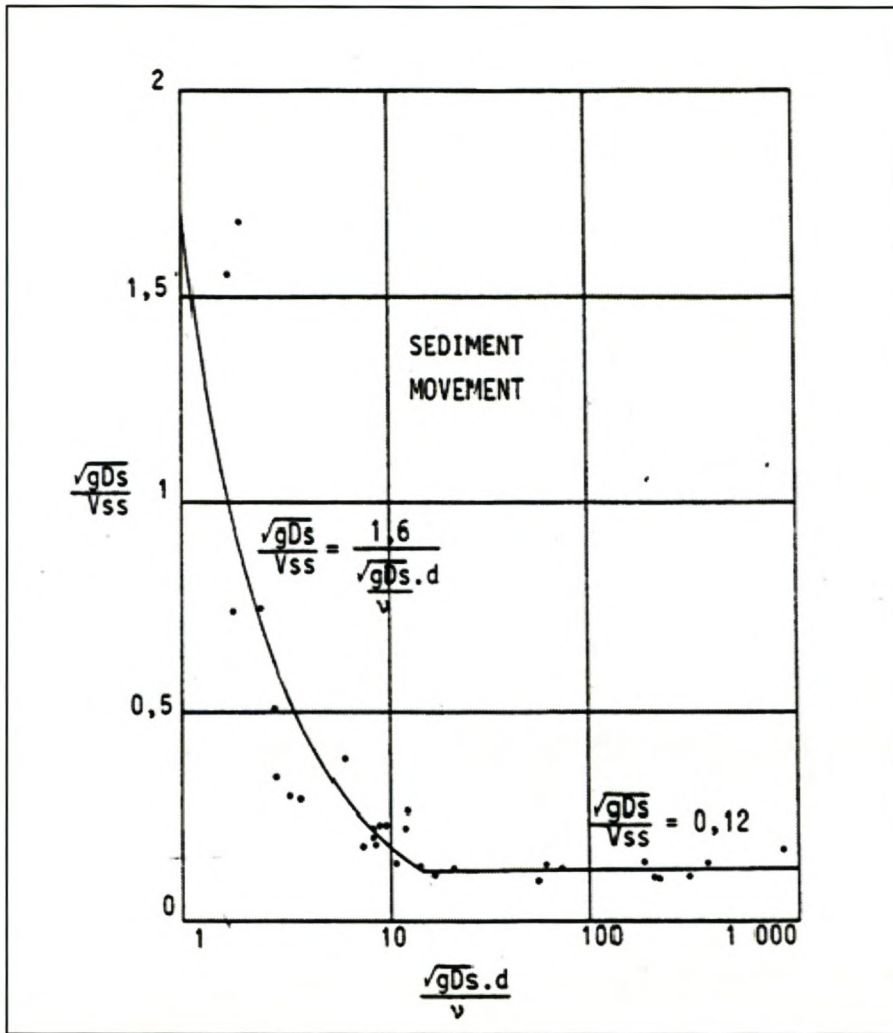


Figure 2.6: Modified Liu diagram (Rooseboom, 1992)

In the above figures the term $\frac{\sqrt{gDs}}{V_{ss}}$ can be interpreted as the ratio

$\left[\frac{\text{Unit applied power along bed}}{\text{Unit power required to suspend particles}} \right]$, which reflects the ratio of the stream's

capacity to entrain bed particles relative to the minimum power required to keep the particles in suspension (Rooseboom and Le Grange, 2000). On the other axis the term

$\frac{\sqrt{gDs} \cdot d}{\nu}$ can be interpreted as the ratio $\left[\frac{\text{Laminar power}}{\text{Turbulent power}} \right]$ because it indicates whether

the position of a data point on the modified Liu diagram is in a laminar flowing zone or a

turbulent flowing zone. The law of conservation of stream power states that the mode of flow which requires the least amount of unit power will be followed. Thus according to the ratio $\left[\frac{\text{Laminar power}}{\text{Turbulent power}} \right]$ if turbulent flow is prevailing at the bed a data point will plot to the right on the x-axis and if laminar flow is prevailing then it will plot to the left.

A plot above the threshold line in Figure 2.3 therefore implies that the unit power applied along the bed is greater than the unit power required to suspend particles, while the function on the x-axis may be regarded as a type of Reynolds number, which indicates whether laminar or turbulent conditions prevail at the bed.

2.2 Conclusions

The information in this chapter support the assertion that applied power approach has significant advantages over other sediment transport theories. The results from other methods are inconsistent due to their empirical nature. Thus the data collection will be done with the aim of using the applied stream power approach in predicting the movement of sediment in cobble/boulder bed rivers.

3 DATA COLLECTION

3.1 Site selection

Two study sites were selected for this project. Both of these sites are situated in the Western Cape about 25 km from each other. This area of the country (indicated in Figure 3.1) is characterized by high winter rainfall (mean annual precipitation of over 1000mm) in the mountain catchments.

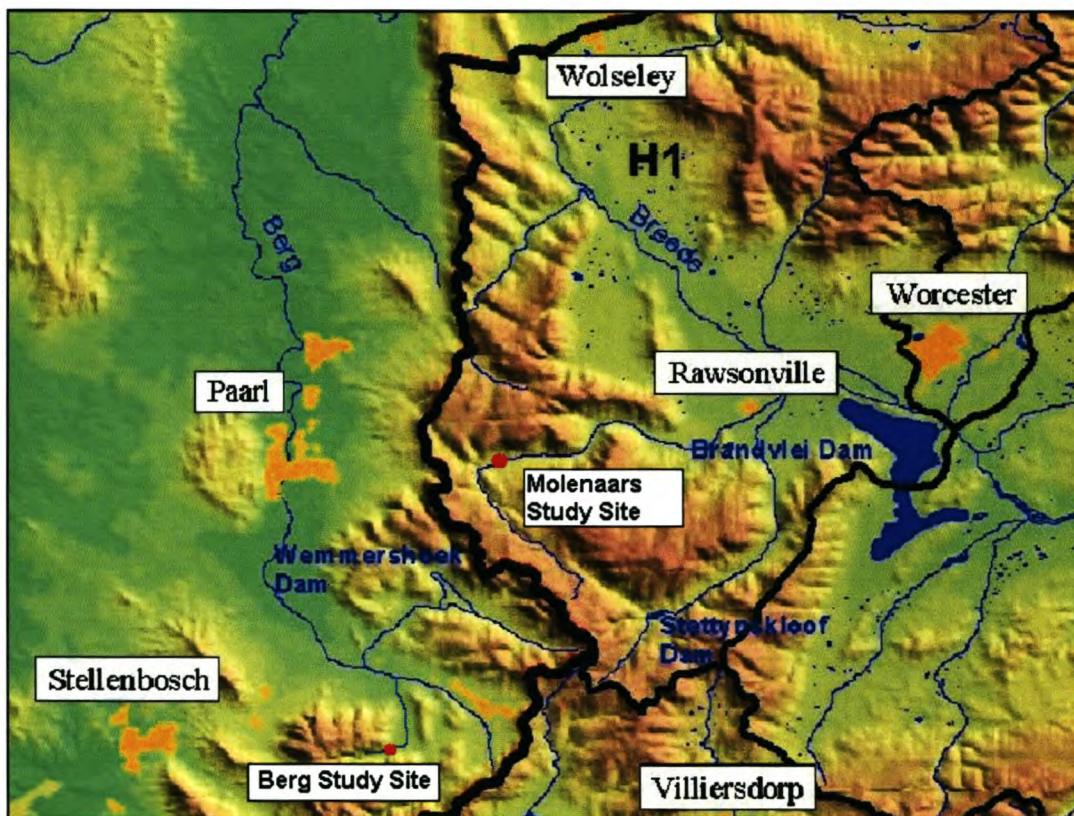


Figure 3.1: Location of study sites

Both sites are located in the headwaters of the Cape Fold mountains and are thus characterized by relatively steep gradients with bed particles predominantly derived from the Table Mountain group sandstones in the cobble to boulder bed range as defined by the Wentworth scale given in Table 3.1.

Class (Wentworth)	Diameter (mm)
Boulder	>256
Cobble	64 to 256
Gravel	2 to 64
Sand	0.0625 to 2
Silt	0.0039 to 0.0625
Clay	< 0.0039

Table 3.1: Classification of bed particle sizes

The first of these two study sites is located on the Molenaars River, about 2km east of the Huguenot Tunnel. This river has its origin in the Klein-Drakenstein Mountains and is one of the main tributaries of the Breede River, which is the largest river in the Western Cape and flows in an easterly direction into the Indian Ocean. The study reach was about 60m long with relatively well defined banks on both sides and consisted primarily of a riffle and rapid section ending in a large pool. The layout of the Molenaars River study site as well as the Thalweg profile and selection of cross sections, and the size distribution are shown in Appendix A1.



Figure 3.2: Molenaars River study site (looking downstream)

The second study site is located on the Berg River, which is the second largest river in the Western Cape and flows for the most part (including the area of the study reach) in a northerly direction and later in a westerly direction into the Atlantic Ocean. The site is situated near the origin of the Berg River which is found in the Franschhoek Mountains. The study site is located on a slight bend in the river and has a steep bank on the outside (left bank) and a lateral bar of deposited cobbles on the inside bank. A small rapid section dominates the top half of the site leading to a deeper pool in the lower half of the reach. The layout of the Berg River study site as well as the Thalweg profile and a selection of cross-sections and the stone size distribution are shown in Appendix A2



Figure 3.3: Berg River study site (looking upstream)

3.2 Site setup

(i) Surveys

A detailed land survey of the riverbed was conducted on both study sites. This consisted of surveying at 1m intervals along thirty transects which were spaced at 2m intervals. Also, an aerial photogrammatic survey was conducted on the Molenaars study site in 2003 which was used to create a detailed digital terrain map of the site. The map is considered to be accurate to 10cm.

(ii) Stones

The thirty transects were marked by steel pegs on each bank of the river. The stones to be studied were selected by stringing a tape between the pegs and selecting stones at two meter intervals across the transect. A total of 345 and 435 stones were selected for the Molenaars (2003 and 2004) and Berg River (2004) study sites respectively.



Figure 3.4: Study site set up

In order to locate the selected stones after a flood they were marked and numbered with paint, putty or a waterproof pen. The stones were marked on both sides to note if they were disturbed without necessarily being moved from its original position. Initially small magnets were attached to some of the stones as it was felt that this would have less of an impact on the potential for organisms to reconolise a marked stone than paint or an ink mark. This however was abandoned when it was found that too much natural magnetism in the stones existed to make it a reliable method for relocating stones after a flood event.



Figure 3.5: Example of a marked stone

(iii) Water levels

To measure the water levels during a flood eight clear plastic pipes, 2m long, were placed at intervals along both banks of the study reach. The pipes were attached to metal y-sections that were secured at the base with cemented stone foundations. Water entered the pipes through small holes drilled at the bottom and air escaped through similar holes at the top. A handful of cork flakes or finely cut dry grass was placed in each pipe which would rise with the water level in the pipe clinging to the sides when the water level

dropped down again. After each flood the height the cork or grass reached in the pipe would be measured to indicate the maximum water levels reached during the relevant flood.



Figure 3.6: Plastic stage pipe used to measure flood levels

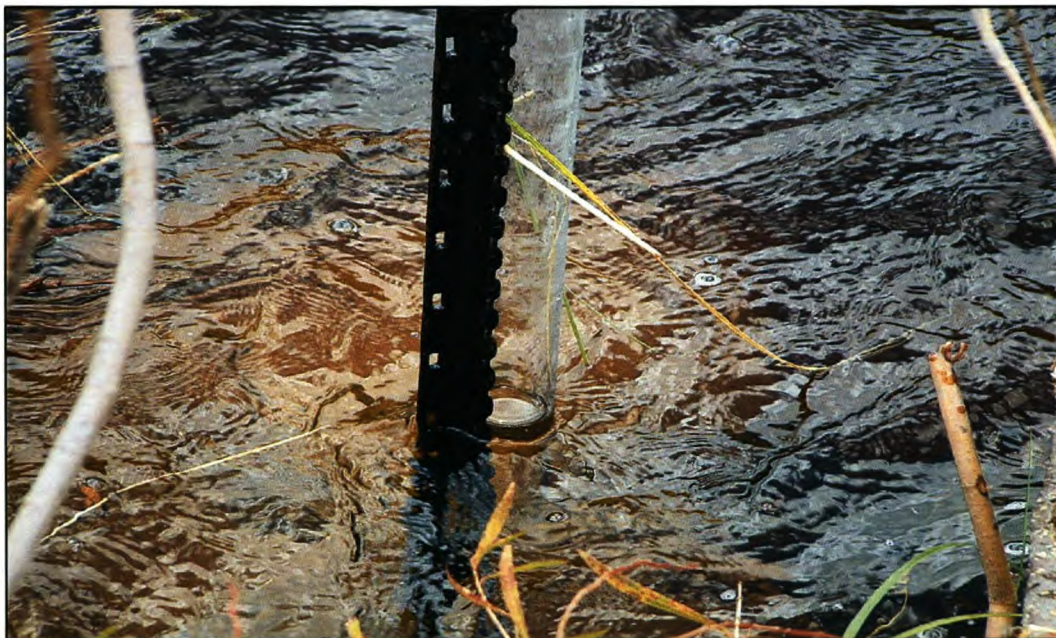


Figure 3.7: Plastic stage pipe used to measure flood levels (during flood conditions)

3.3 Base flow conditions

During the study site setup, base flow conditions were measured in terms of both hydraulic and ecological characteristics. Both sites were established at the start of the winter flood season in April/May under assumed winter base-flow conditions rather than summer low-flow conditions. The depth and average velocity were recorded above each of the marked stones. After sampling, the stones were returned to their original positions and the offset from the survey pegs recorded and used to determine the co-ordinates of each stone in a local co-ordinate system. Wherever possible the stones were removed from the bed and measured in terms of their three main axis. Invertebrate and periphyton samples were taken and the stones were returned to their original positions. If the stones could not be removed then their visible dimensions were measured and they were recorded as embedded. The bed level of each stone could then be determined according to the detailed survey. The hydraulic base flow conditions in terms of stone size, depth, velocity, Froude number, Reynolds number, stream power and bed shear stress are shown in Appendix B1 for the Molenaars and Appendix B2 for the Berg River site, as well as the base flow water level profiles.

3.4 Flood events data

The initial set of flood data was collected at the Molenaars study site during six flood events in the winter of 2003. During the winter of 2004 more data were collected at five floods both on the Molenaars and Berg River sites.



Figure 3.8: The Molenaars study site in flood

In terms of environmental flow requirements the DRIFT methodology is used to classify different flood sizes (King *et al.*, 2003). DRIFT divides the long-term average daily flow data into eight flood classes. The inter-annual flood events with a return period between two and fifty years are represented by DRIFT classes V to VIII. Classes I to IV represent the intra-annual flood events and the level is obtained by halving the two year return period flood to obtain the Class IV flood which on its turn is halved to obtain Class III, and so on. Howard (2004) determined the eight classes for gauge G1H004 on the Berg River and Brown and King (2002) for gauge H1H018 on the Molenaars River and these are shown in Table 3.2. The two gauges G1H004 and H1H018 are located immediately downstream of the Berg and Molenaars study sites respectively. Gauge G1H004 data caused concern (Howard 2004) regarding reliability of its flow record prior to 1980. Thus flood classification was based on both the longer record and the shorter record after 1980. For the purpose of classifying the floods studied during this project, the classification based on the shorter record was used due to its higher level of accuracy. It does however bring with it a greater level of uncertainty, especially with regards to the higher floods.

Class	Recurrence Interval	H1H018 (Molenaars)	G1H004 (Berg) (Short Record)	G1H004 (Berg) (Long Record)
I	Intra annual floods	5.0	3.6	4.3
II		16.0	7.2	9.5
III		31.0	14.5	19.1
IV		61.0	29.0	38.2
V	1 : 2 years	93.7	58.7	76.3
VI	1 : 5 years	146.0	75.3	118.0
VII	1 : 10 years	181.0	78.8	154.6
VIII	1 : 20 years	187.0	85.6	178.0

Table 3.2: DRIFT classification of floods for H1H018 and G1H004 in terms of average daily flows (m^3/s) (Brown and King, 2002; Howard, 2004)

Flood data recorded by the two gauges during the winters of 2003 and 2004 are shown in Figures 3.9, 3.10 and 3.11. These figures show the average daily flow and instantaneous flow rates recorded at the two gauges. The DRIFT flood classification levels are also shown and can be related to the average daily flow for each of the observed events to determine its class.

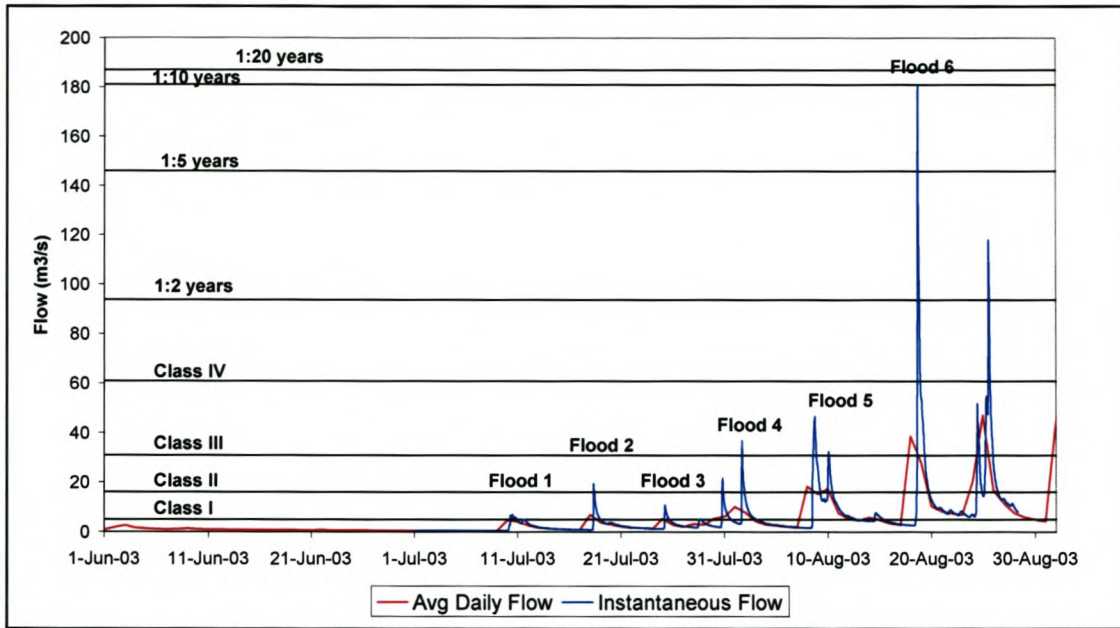


Figure 3.9: Flood events observed on the Molenaars River (H1H018) in 2003

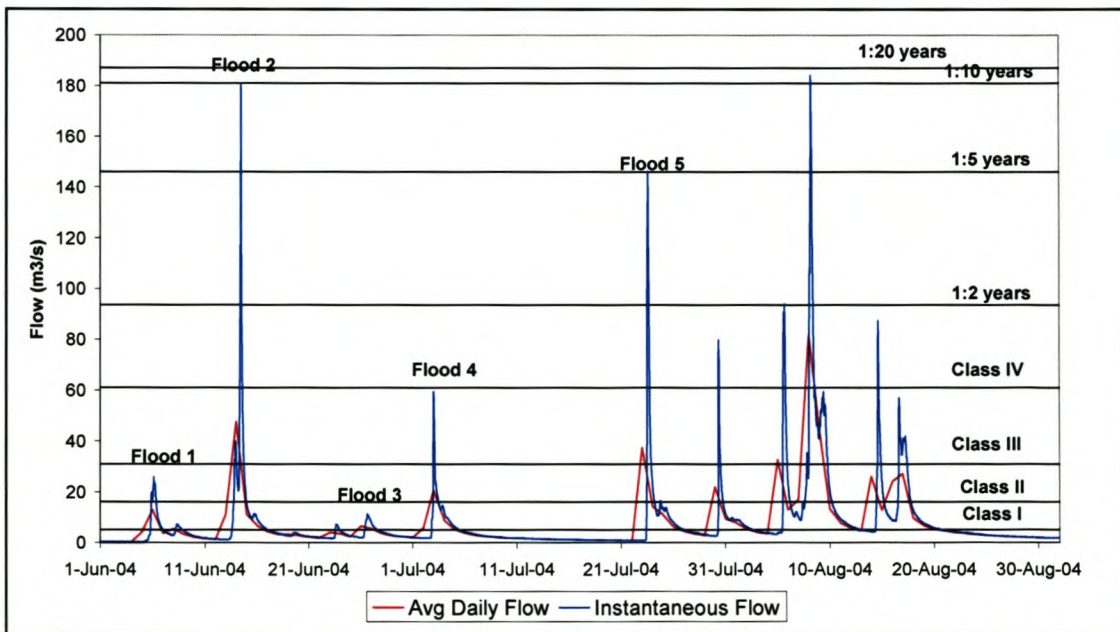


Figure 3.10: Flood events observed on the Molenaars River (H1H018) in 2004

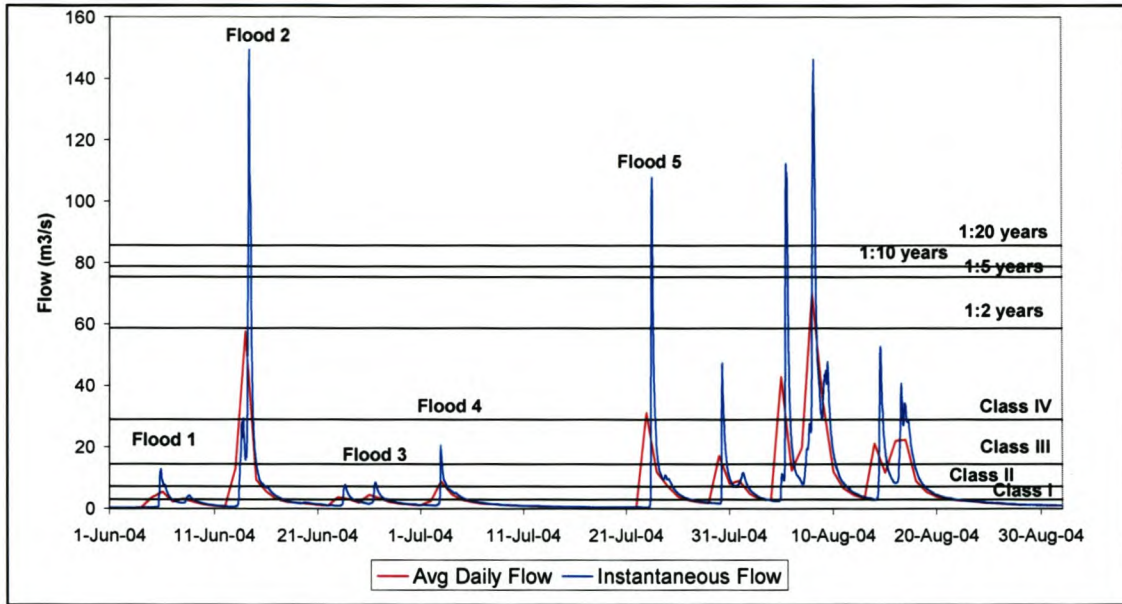


Figure 3.11: Flood events observed on the Berg River (G1H004) in 2004

In order to calculate the maximum flow rate experienced at the study reach during each flood, the instantaneous flood peak observed at the downstream gauge was reduced by the ratio of the catchment area upstream of the study site to the catchment area upstream of the gauge. Tables 3.3 and 3.4 depict the estimated maximum flow rate, average daily flow rate, flood volume (including base flow) and class of flood as determined from the average daily flow rate at the downstream gauge for all the observed flood events. The flood DRIFT classes (Tables 3.4 and 3.4) were determined with the values given in Table 3.2. If a flood size falls in the interval between a 1:2 year and half of a 1:2 year flood it is deemed a DRIFT class IV flood. If a flood size falls in the interval between half of a 1:2 year flood and a quarter of a 1:2 year flood it is deemed a DRIFT class III flood and so on for DRIFT class II and I floods.

Year	Event Number	Date	Duration (hours)	Max Flow (m ³ /s)	Avg. Daily Flow (m ³ /s)	Volume (Mm ³)	DRIFT Class
2003	1	10 th July	33	5.56	3.72	0.41	I
	2	18 th July	21	15.23	5.41	0.49	I
	3	25 th July	14	8.60	4.20	0.28	I
	4	1 st August	26	28.76	7.98	0.95	I
	5	8 th August	26	36.46	14.45	1.74	II
	6	18 th August	32	140.80	30.29	4.15	III
2004	1	6 th June	29	20.20	10.02	1.04	I
	2	14 th June	33	140.97	37.21	3.82	III
	3	26 th June	31	8.87	5.13	0.66	I
	4	3 rd July	21	46.38	16.08	1.35	II
	5	23 rd July	18	113.93	29.17	2.67	III

Table 3.3: Flood events observed at the Molenaars study site

Year	Event Number	Date	Duration (hours)	Max Flow (m ³ /s)	Avg. Daily Flow (m ³ /s)	Volume (Mm ³)	DRIFT Class
2004	1	5 th June	28	7.27	2.08	0.40	I
	2	14 th June	44	84.51	32.58	3.48	IV
	3	26 th June	27	4.82	2.62	0.29	I
	4	3 rd July	24	11.74	5.68	0.44	II
	5	23 rd July	20	60.98	17.70	1.66	IV

Table 3.4: Flood events observed at the Berg study site

As mentioned previously, the highest water level for each flood event was recorded from the height of the mark left inside the pipe by the cork or grass. From the land survey, which included the leveling of the base of the pipes and from the measured height inside the pipes it was possible to calculate an average water level profile for each study reach. This was used to determine the water surface slope during the flood as well as the depth above each sampled stone. The water surface profiles for the observed flood events are given in Figures 3.12, 3.13 and 3.14.

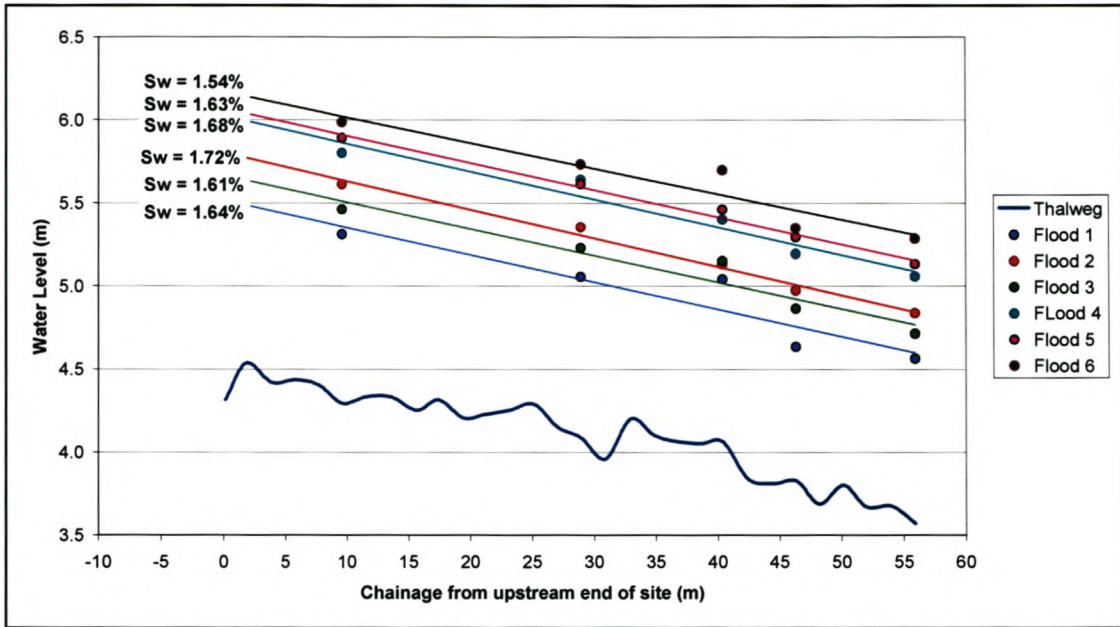


Figure 3.12: Water level profiles for the Molenaars study site in 2003

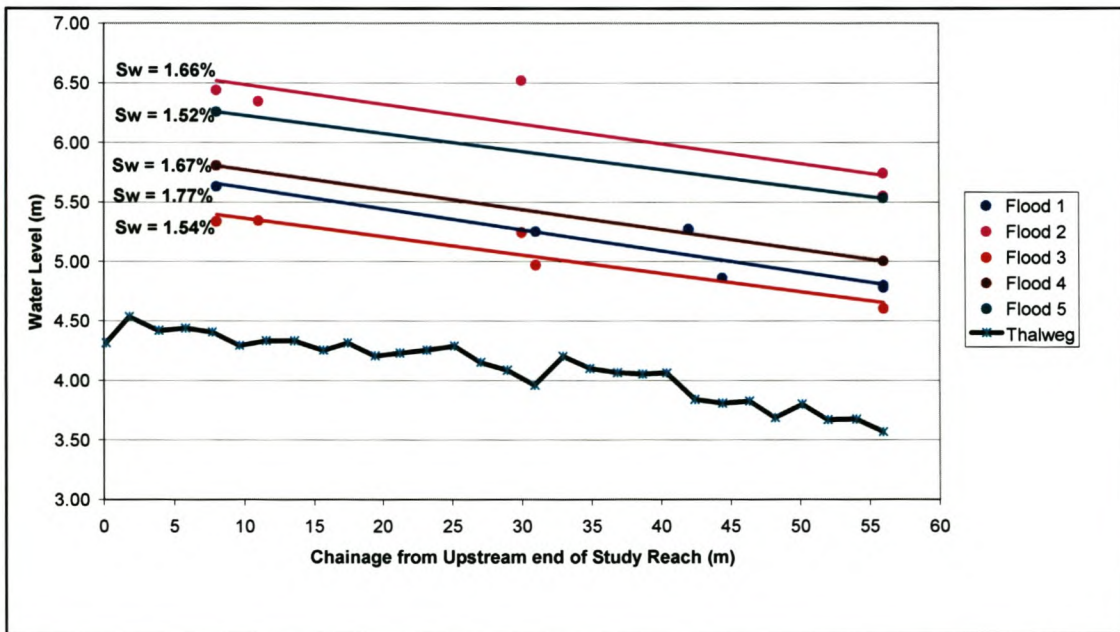


Figure 3.13: Water level profiles for the Molenaars study site in 2004

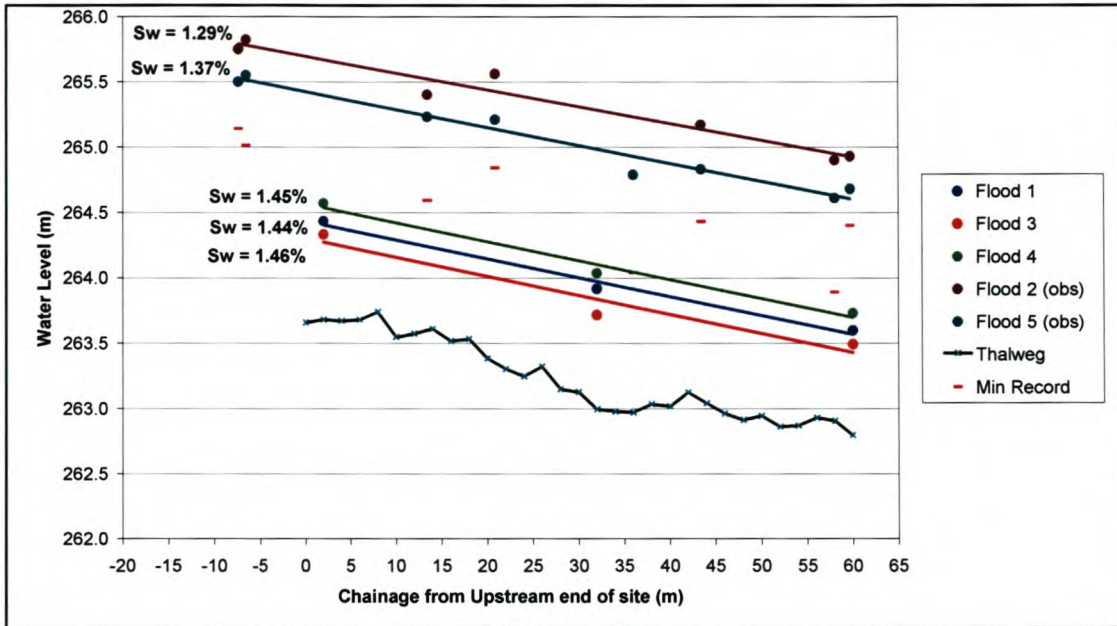


Figure 3.14: Water level profiles for the Berg study site in 2004

It has to be noted that the original water levels used for Flood 6 in 2003 on the Molenaars was considered to be inaccurate. This was based on a comparison with the profile for Flood 2 in 2004 on the same river, which was of similar magnitude (140.8 and 140.97 m³/s respectively). The reason for this is that the cork inside the pipes was washed off during Flood 6 of 2003 and the levels had been estimated visually. Flood 2 in 2004 did however leave clear cork marks and these heights were used to determine the average water slope and depths for Flood 6 in 2003. A problem also arose with the lower floods namely Floods 1, 3 and 4 on the Berg site. The minimum height that the pipes stationed on the banks could measure was too high for these particular floods. The levels of these floods were estimated using the following equation (3.1) (Jonker, 2002) for calculating the water depth in cobble/boulder bed rivers.

$$Q = A \sqrt{\frac{2gd_{50}s}{0.5285(R/d_{50})^{-2.166}}} \quad (3.1)$$

3.5 Collection of incipient motion data

After each flood event both study sites were revisited and the marked stones were located wherever possible. The movement of a stone was recorded as being removed out of its original position or simply turned over. In the case of a stone being removed out of its position the distance of the displacement was measured. In the case of the bigger floods some of the moved stones could not be relocated. It was assumed that these stones were washed out of the reach. They were replaced by equivalent size stones. The dimensions of the new stones were recorded and used in the analysis in subsequent floods. The field notes for the initial site setup and from each visit to locate moved stones are included in Appendix C and the locations of the stones that moved during each flood are given in Appendix D. A summary of the stone movements by stone class size is given in the Figures and Tables below.

Intensity of Movement: Molenaars 2003							
Stone Size Classification		Total	G	SC	LC	SB	LB
Max size in class (mm)			64	161	256	514	1000
Total Number of Stones		344	4	91	73	111	65
Flood 1	Moved Stones	0	0	0	0	0	0
	Movement %	0.0%	0.0%	0.0%	0.0%	0.0%	0.0%
Flood 2	Moved Stones	7	0	7	0	0	0
	Movement %	2.0%	0.0%	7.7%	0.0%	0.0%	0.0%
Flood 3	Moved Stones	2	0	1	1	0	0
	Movement %	0.6%	0.0%	1.1%	1.4%	0.0%	0.0%
Flood 4	Moved Stones	10	0	6	4	0	0
	Movement %	2.9%	0.0%	6.6%	5.5%	0.0%	0.0%
Flood 5	Moved Stones	26	1	18	4	3	0
	Movement %	7.6%	25.0%	19.8%	5.5%	2.7%	0.0%
Flood 6	Moved Stones	115	4	65	29	16	1
	Movement %	33.4%	100.0%	71.4%	39.7%	14.4%	1.5%

Table 3.5: Stone movement in the Molenaars River during 2003 flood events

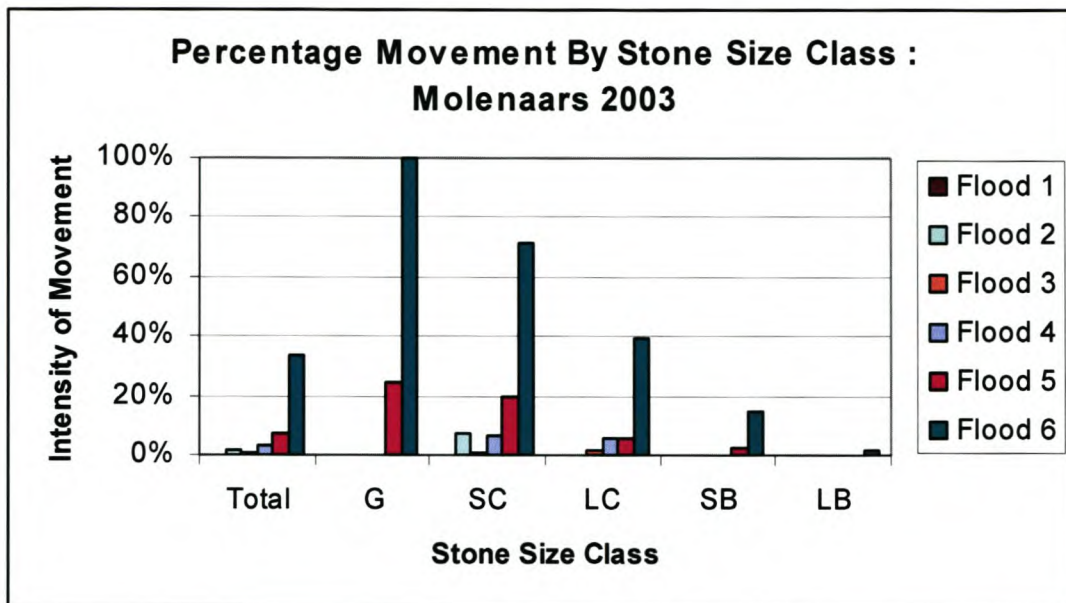


Figure 3.15: Level of disturbance in the Molenaars River during 2003 flood events

Intensity of Movement: Molenaars 2004							
Stone Size Classification		Total	G	SC	LC	SB	LB
Max size in class (mm)			64	161	256	514	1000
Total Number of Stones		343	5	60	73	136	69
Flood 1	Moved Stones	3	1	2	0	0	0
	Movement %	0.9%	20.0%	3.3%	0.0%	0.0%	0.0%
Flood 2	Moved Stones	78	4	41	20	13	0
	Movement %	22.7%	80.0%	68.3%	27.4%	9.6%	0.0%
Flood 3	Moved Stones	7	0	6	1	0	0
	Movement %	2.0%	0.0%	10.0%	1.4%	0.0%	0.0%
Flood 4	Moved Stones	15	1	7	2	5	0
	Movement %	4.4%	20.0%	11.7%	2.7%	3.7%	0.0%
Flood 5	Moved Stones	83	2	39	23	17	2
	Movement %	24.2%	40.0%	65.0%	31.5%	12.5%	2.9%

Table 3.6: Stone movement in the Molenaars River during 2004 flood events

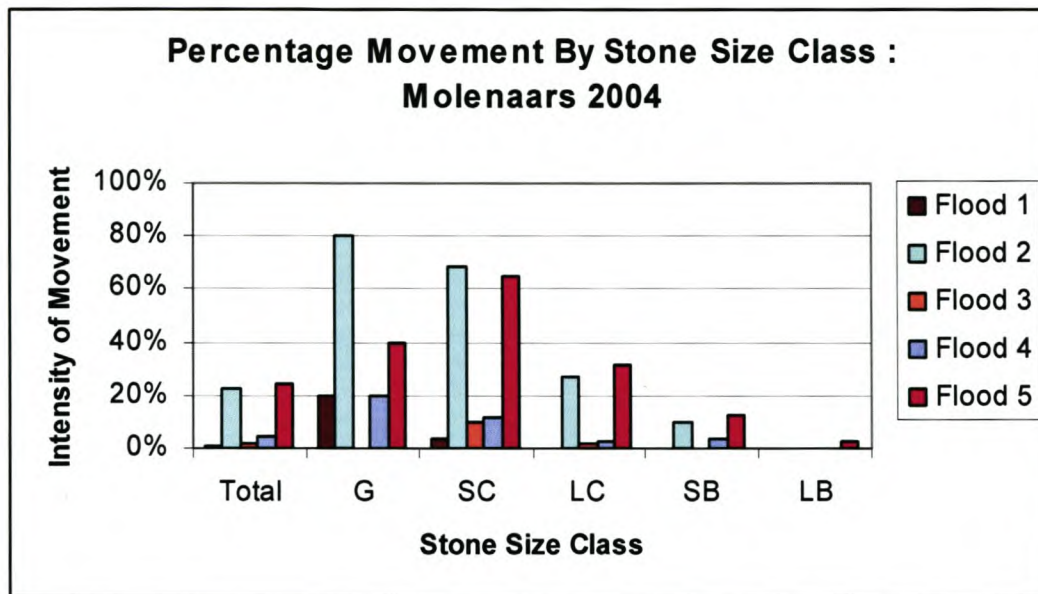


Figure 3.16: Levels of disturbance in the Molenaars River during 2004 flood events

Intensity of Movement: Berg 2004							
Stone Size Classification		Total	G	SC	LC	SB	LB
Max size in class (mm)			64	161	256	514	1000
Total Number of Stones		432	27	120	92	139	54
Flood 1	Moved Stones	1	1	0	0	0	0
	Movement %	0.2%	3.7%	0.0%	0.0%	0.0%	0.0%
Flood 2	Moved Stones	187	26	92	44	24	1
	Movement %	43.3%	96.3%	76.7%	47.8%	17.3%	1.9%
Flood 3	Moved Stones	10	2	3	3	2	0
	Movement %	2.3%	7.4%	2.5%	3.3%	1.4%	0.0%
Flood 4	Moved Stones	7	1	4	2	0	0
	Movement %	1.6%	3.7%	3.3%	2.2%	0.0%	0.0%
Flood 5	Moved Stones	111	10	58	28	14	1
	Movement %	25.7%	37.0%	48.3%	30.4%	10.1%	1.9%

Table 3.7: Stone movement in the Berg River during 2004 flood event

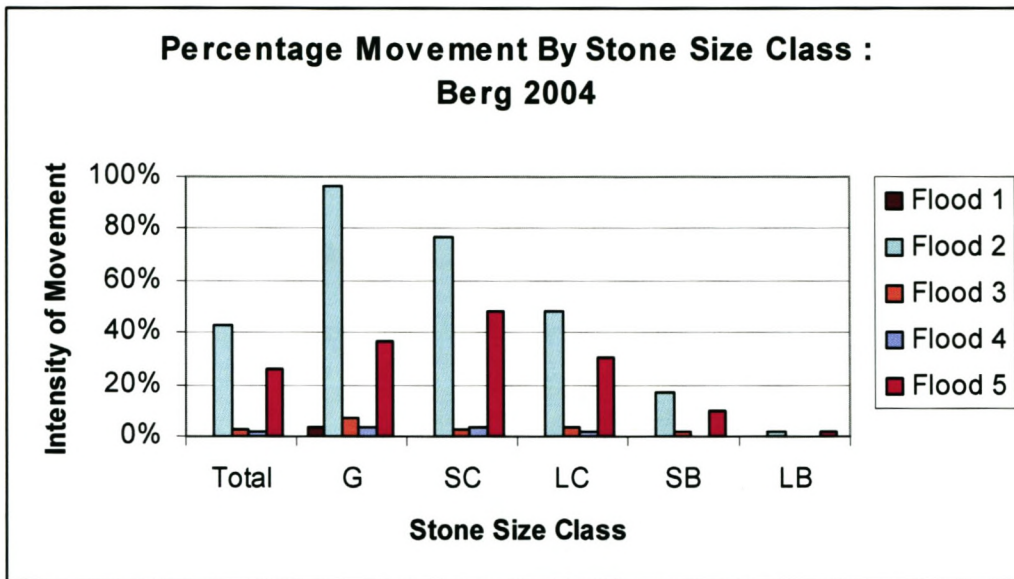


Figure 3.17: Level of disturbance in the Berg River during 2004 flood events

4 CRITICAL CONDITIONS

4.1 Original modified Liu-diagram

In order to test the applied stream power approach in describing the critical hydraulic relationships for each stone under flood conditions, all the measured data from the Molenaars and Berg Rivers have been plotted (Figures 4.2 – 4.4) in the original modified Liu diagrams (Rooseboom, 1992) as described in Chapter 2. The original modified Liu diagram shown in Chapter 2 is repeated (Figure 4.1). It should be noted that in original modified Liu diagram terms all observations can be expected to be in the rough turbulent zone, given the nature of the flow conditions during floods through cobble/boulder bed streams; i.e. the incipient motion line should have a constant value.

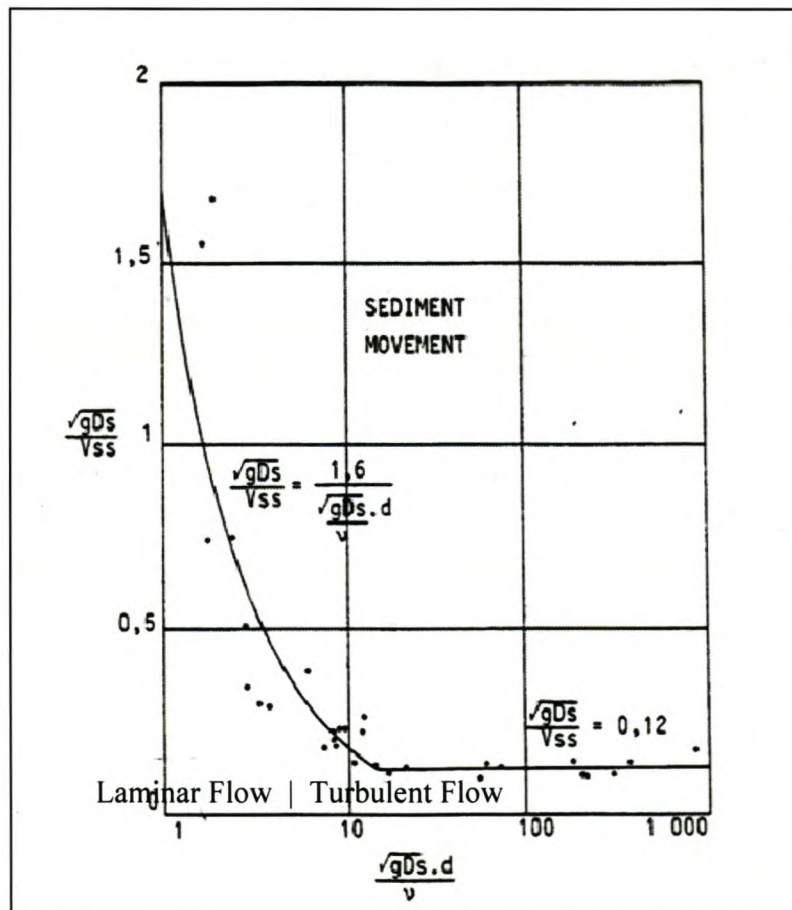


Figure 4.1: Original modified Liu diagram (Rooseboom, 1992)

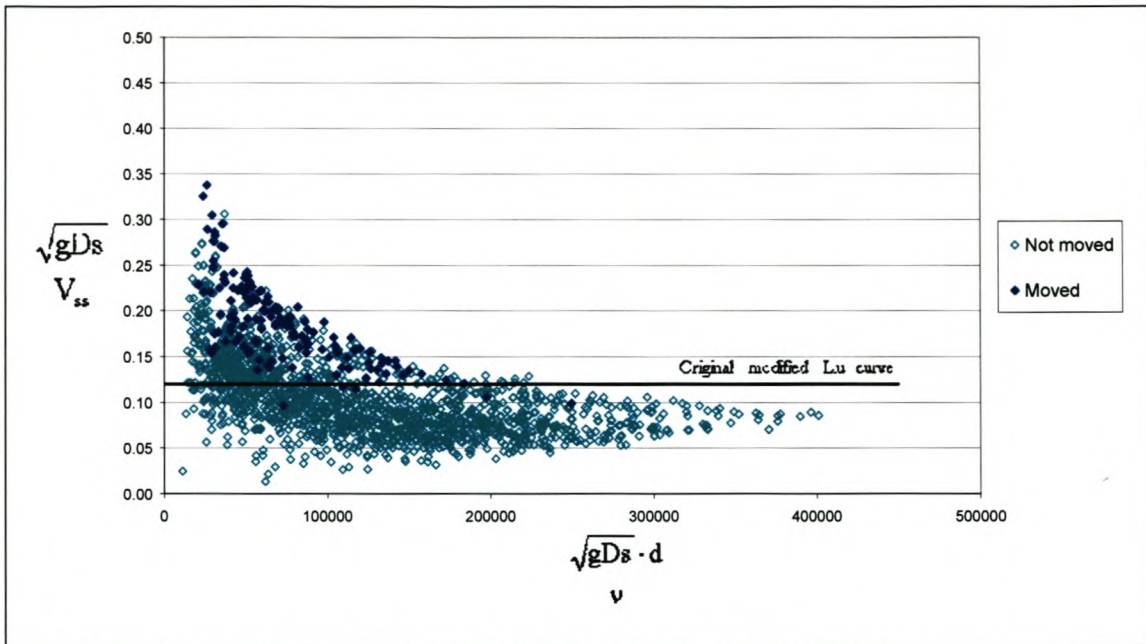


Figure 4.2: Molenaars 2003 data plotted in the original modified Liu diagram

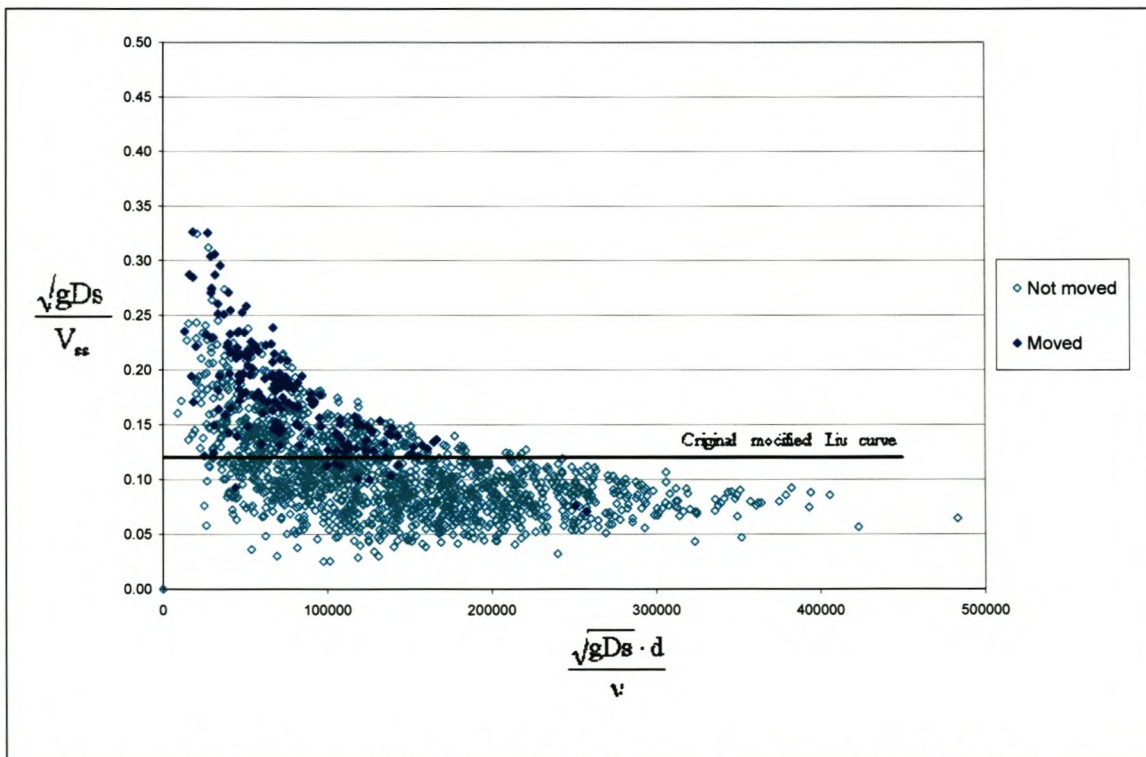


Figure 4.3: Molenaars 2004 data plotted in the original modified Liu diagram

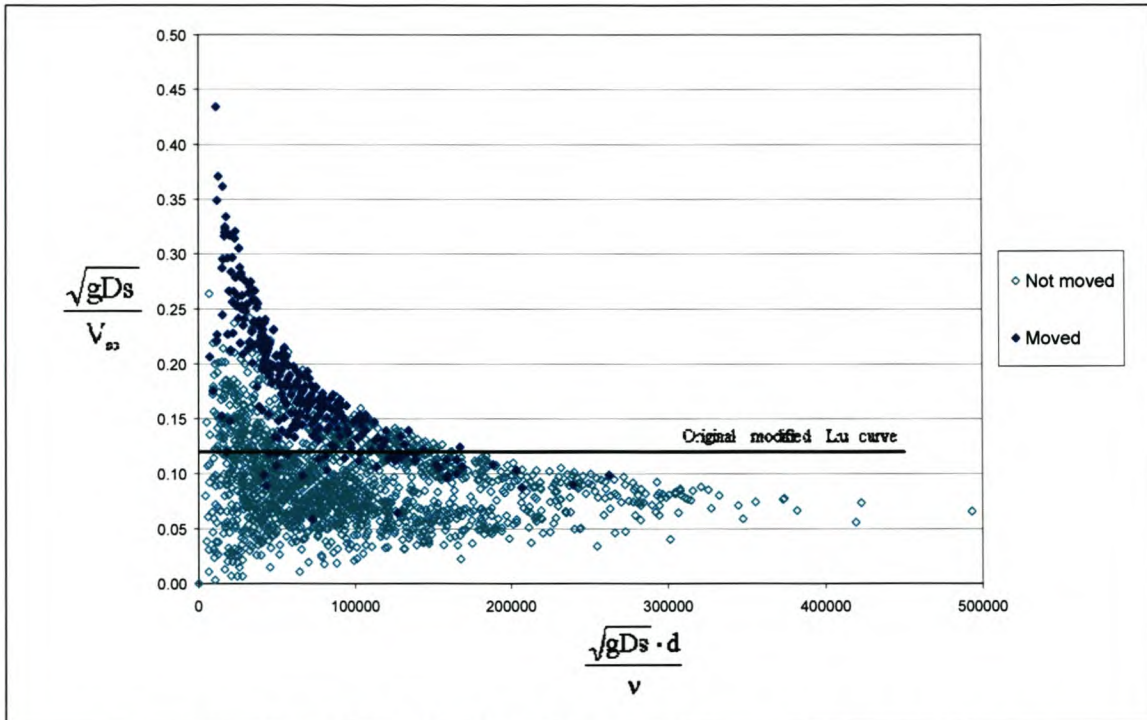


Figure 4.4: Berg 2004 data plotted in the original modified Liu diagram

The data points which represent stones that did move are not as reliable as those for stones that did not move due to the fact that movement did not necessarily take place at the peak measured discharge, as is implied. By using maximum recorded flood levels to represent incipient motion conditions, the upper points representing non-movement are more reliable as there is no doubt as to the maximum flow depths and applied power values that the non-moving stones had been subjected to. In other words, a stone that was moved might have moved early on in a flood at a lower level and discharge than those recorded and used in the data analysis. However, the deviating trend is evident for the stones that had moved as well as stones that had not moved.

It is noticeable from the above figures that the data for the Molenaars and Berg Rivers deviate from the expected constant value in the original modified Liu diagram, given the rough turbulent conditions in the Molenaars and Berg Rivers under flood conditions. It is only at an x-axis value smaller than 13 that any sort of deviation is expected as this is where laminar flow is prevalent (see Figures 4.1 and 4.17). Even though the data clearly fall within the turbulent boundary zones of the Liu diagram (i.e. x-axis values $\gg 13$),

most data of the stones that moved (dark data points in Figures 4.2 – 4.4) deviate from the expected constant value (0,12) for $\frac{\sqrt{gDs}}{V_{ss}}$ as derived in Chapter 2 for fully turbulent conditions. It is also evident that the deviation is much more pronounced for smaller stones (i.e. the data closest to the y-axis). The data points to the right, representing the larger stones, tend towards a constant value.

The deviation pattern noticed is strikingly similar to the pattern followed by the threshold of movement line in the original modified Liu diagram where laminar boundary conditions prevail (Figure 4.1). The boundary between points that represent movement and those that do not represent movement is equivalent to the incipient motion curve. In comparing the data with the original modified Liu curve it is necessary to consider the significance of the new data.

Three possible explanations exist as to why the Molenaars and Berg Rivers' data on incipient motion deviate from the expected horizontal line for the threshold of movement in the original modified Liu diagram for rough turbulent flow:

- The stones are embedded and the derivation of a constant value for the threshold of movement in the original modified Liu diagram does not account for such conditions.
- The original modified Liu diagram (Rooseboom, 1992) was derived for beds with uniform particle sizes, while the data for the Molenaars and Berg rivers represent beds which consist of non-uniform bed particles.
- The deviation noticed for the data from the Berg and Molenaars Rivers is due to laminar conditions playing a role in the entrainment process of the stones.

Each of these will be explored in turn.

4.2 Influence of embedded stones

No factor is included in the original theoretical derivation (Chapter 2) of the parameters in the original modified Liu diagram to correct for the level of embeddedness. Intuitively one expects the embedded stones to be more difficult to transport than non-embedded stones. They will therefore be able to withstand higher applied power values exerted on them than if they were not embedded. A stone in such a situation will typically plot above the theoretical threshold of movement line on the original modified Liu diagram (as shown in Chapter 2 the y-axis represents $\left[\frac{\text{Unit applied power along bed}}{\text{Unit power required to suspend particles}} \right]$) and this could possibly explain the deviation from the expected constant line.

During data collection, all the observed stones were classified as embedded or non-embedded depending on whether they could be removed from the bed by hand or not. Embedded stones would include stones that were covered by sediment as well as stones that were firmly lodged between other stones. The influence of embeddedness can be determined by excluding the data for these embedded stones from the data plotted in the original modified Liu diagram. Figures 4.5 – 4.7 depict the data from the Berg and Molenaars Rivers in the original modified Liu diagram, without the embedded stones data.

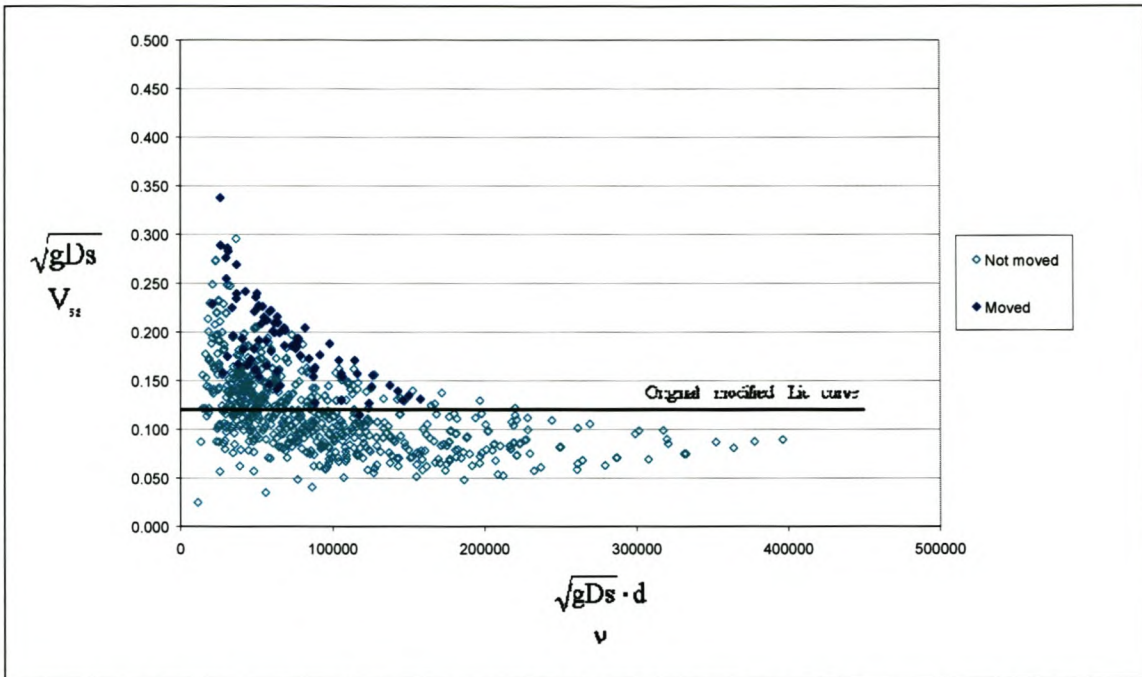


Figure 4.5: Molenaars 2003 data, excluding data for embedded stones, plotted on the original modified Liu diagram

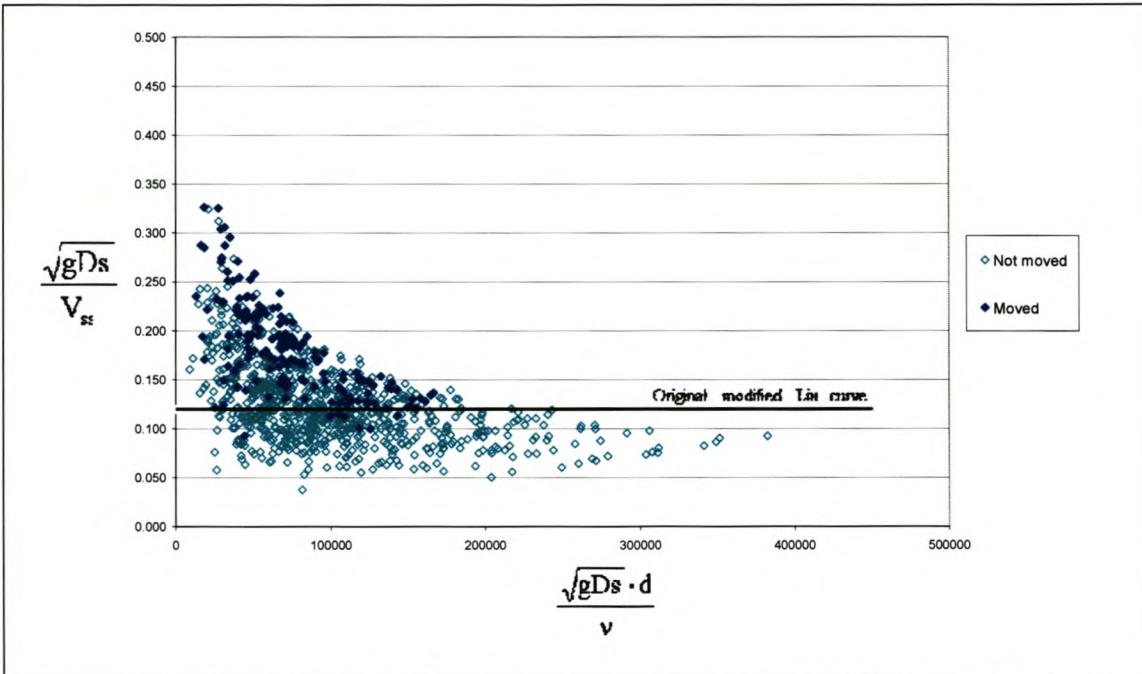


Figure 4.6: Molenaars 2004 data, excluding data for embedded stones, plotted on the original modified Liu diagram

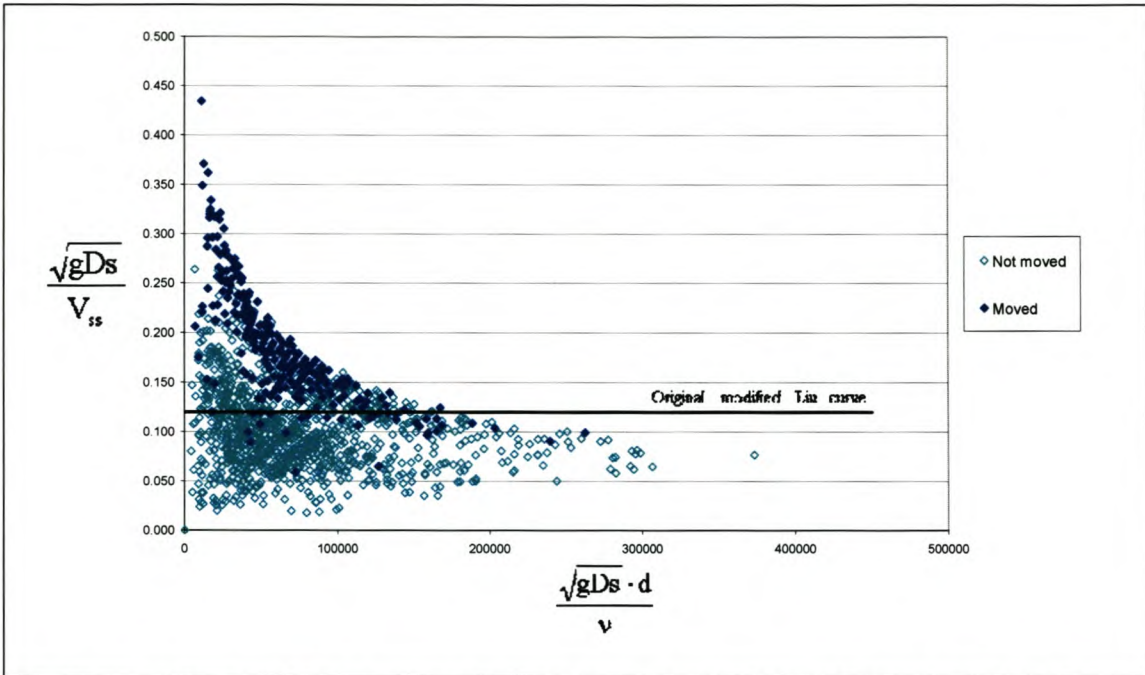


Figure 4.7: Berg 2004 data, excluding data on embedded stones, plotted on the original modified Liu diagram

Figures 4.5 - 4.7, show the same deviating patterns as seen in Figures 4.2 - 4.4. Even though embeddedness of stones could possibly play a role in the incipient motion criteria it does not account for the general deviation from the expected horizontal line when the data are plotted in the original modified Liu diagram.

4.3 Influence of non-uniformity under fully developed turbulent conditions

The Liu diagram shown in Chapter 2 was derived for beds with uniform particle sizes. In order to establish what should happen in the case of a non-uniform particle size bed, with varying roughness, the Liu parameters have to be derived anew to allow for the non-uniformity in the bed.

For rough turbulent flow, the unit stream power applied in maintaining motion along a bed consisting of particles with diameter d , as shown in Chapter 2, is proportional to

$$\frac{\rho g s D \sqrt{g D s}}{k} \quad (4.1)$$

with ρ : fluid density (kg/m^3)
 g : gravitational acceleration (m/s^2)
 s : energy gradient \approx channel gradient
 D : depth of water above stone (m)
 k : absolute bed roughness (m)

In terms of the concept of minimum applied power, the stream will begin to entrain particles when the power required to suspend the particles effectively becomes less than the unit power to maintain the status quo. At that stage

$$(\rho_s - \rho)gV_{ss} \propto \frac{\rho g s D \sqrt{g D s}}{k} \quad (4.2)$$

where $(\rho_s - \rho)gV_{ss}$ represents the unit applied power required to lift a particle.

According to the general equation for settling velocity (Graf, 1971)

$$V_{ss} \propto \sqrt{\frac{(\rho_s - \rho)gd}{\rho C_D}} \quad (4.3)$$

Thus when a particle is entrained,

$$(\rho_s - \rho)gV_{ss} = \frac{\rho C_D \cdot d (\rho_s - \rho)gV_{ss}}{\rho C_D \cdot d} \propto \frac{\rho g s D \sqrt{g D s}}{k} \quad (4.4)$$

From equation 4.3 it follows that

$$V_{ss}^2 = \frac{(\rho_s - \rho)gd}{\rho C_D} \quad (4.5)$$

Which, when substituted into equation 4.4, leads to

$$\frac{\rho C_D V_{ss}^3}{d} = \text{Constant} \cdot \frac{\rho g s D \sqrt{g D s}}{k} \quad (4.6)$$

This simplifies further to,

$$\frac{C_D V_{ss}^3}{d} = \text{Constant} \cdot \frac{(\sqrt{g D s})^3}{k} \quad (4.7)$$

and still further to,

$$C_D = \text{Constant} \cdot \frac{(\sqrt{g D s})^3}{V_{ss}^3} \cdot \frac{d}{k} \quad (4.8)$$

Assuming that C_D , the drag coefficient, is a constant, which is true for larger diameters, then from the above equation the condition of incipient motion under rough turbulent conditions for a non-uniform bed can be expressed as:

$$\frac{\sqrt{g D s}}{V_{ss}} \cdot \left(\frac{d}{k}\right)^{1/3} = \text{Constant} \quad (4.9)$$

This newly derived equation can be used to explain why the data in the original modified Liu diagram, for smaller stones, deviate from the expected horizontal line for the threshold of movement. The difference between equation 2.19 which was derived for uniform particle size beds and equation 4.9 which was derived for non-uniform particle

size beds (derivation shown in Chapter 2) is the extra factor $\left(\frac{d}{k}\right)^{1/3}$. This factor indicates that on a non-uniform particle size bed the power required, for a given value of \sqrt{gDs} , to entrain a particle of size d will increase as the overall absolute hydraulic roughness (k) increases. In order to determine the relationship between k and d , one will have to look closely at the eddy formation process at bed level.

The development of eddies, on any bed, is a three-dimensional process. The bed configuration (in all directions) in the vicinity of a stone in the bed will determine the local eddy size. In the case of a bed with uniform size particles the eddy size would be of the same order as the particle diameter. The reason for this is that on a uniform particle size bed the bed shape will generate eddies similar in size as the particles. This is shown in Figure 4.8.

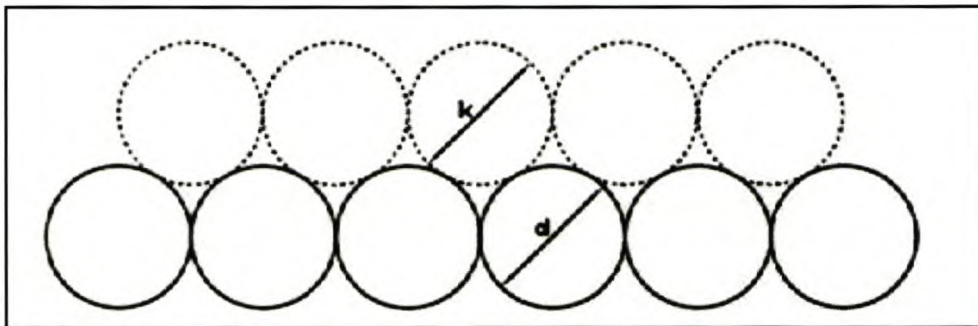


Figure 4.8: Two-dimensional representation of the eddy formation process in a uniform particle size bed

For this reason k can be substituted for d on a uniform bed. It is not possible to accurately predict the exact size of the eddies that will form in a non-uniform particle size bed due to the complexity and variability of such a bed configuration. However, in a non-uniform particle size bed the average bed roughness will be largely determined by the larger stones in the bed. Because flow resistance across the bed is not a localized phenomenon it may be assumed that the applied power and hence the eddy size across a non-uniform bed will tend towards uniformity, with the average eddy size of the same order as that of the

larger stones that dominate in determining the average absolute roughness of the bed. Figure 4.9 depicts a two-dimensional representation of the eddy formation process in a non-uniform particle size bed.

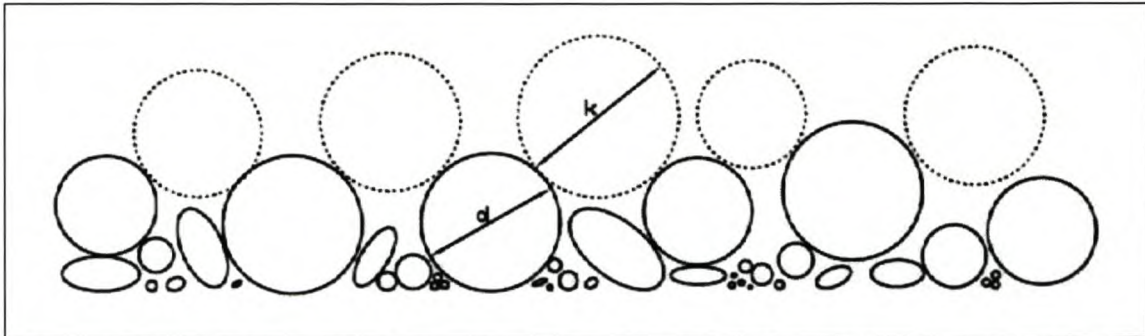


Figure 4.9: Two-dimensional representation of the eddy formation process in a non-uniform particle size bed

It is clear from Figure 4.9 that the bigger eddies will play a dominant role in the eddy formation process in a non-uniform particle size bed. Figure 4.9 not only depicts a two-dimensional representation of the eddy formation process in a non-uniform particle size bed but also the relative positions of different size stones. In a non-uniform particle size bed smaller particles will generally be found in lower positions i.e. in the sheltered hollows between the larger stones.

As indicated in Figure 4.9 in a non-uniform particle size bed, the average roughness and hence the average eddy size is largely determined by the larger stones in the bed. The smaller a stone the smaller the $\left(\frac{d}{k}\right)^{1/3}$ value will be for that stone since the general eddy size (k) will be of the same order of magnitude as the size of the larger stones in the bed.

As the stone size increases the value of the term $\left(\frac{d}{k}\right)^{1/3}$ will increase accordingly as the size difference between a stone and the average eddy diminishes.

The above observation helps to explain, mathematically, why a deviation is noticed in the plot of the Molenaars and Berg River data in the original modified Liu diagram (Figures 4.2 - 4.4). In these diagrams a uniform bed was assumed (i.e. k was set equal to d for every stone). It is thus apparent, when looking at Figure 4.9, that if k is set equal to d it underestimates the size of the average eddy forming over the smaller stones. This underestimation of eddy size increases as the stone size becomes smaller. Alternatively the bigger the stone size the more accurate the assumption that k equals d due to the fact that the average eddy size, which is being formed by the biggest stones, is much closer to the size of the bigger stones. This explains why the bigger stones on the graphs (i.e. furthest from the y -axis) plot close to the theoretical constant value (0,12) on the y -axis. It also clarifies why there is a deviation in the data plots of the smaller stones but does not yet explain the pattern of the deviation (i.e. an upward curve towards the y -axis). Mathematically this upward deviation in the Liu diagram for smaller stones (i.e. those closest to the y -axis) can be explained in terms of the function that represents

$$\left[\frac{\text{Unit applied power along bed}}{\text{Unit power required to suspend particles}} \right] \text{ for non-uniform beds, namely } \frac{\sqrt{gDs} \cdot \left(\frac{d}{k}\right)^{1/3}}{V_{ss}}.$$

For a certain size stone in a non-uniform particle size bed the applied power, represented by the numerator in the above term, will depend on the average eddy size (k) and the value of \sqrt{gDs} . A smaller k would indicate an increase in the applied power and vice versa. Also a smaller value of \sqrt{gDs} would indicate a decrease in the applied power and vice versa. As stated above, eddy sizes for the smaller stones (where the deviating trend is noticed) were underestimated by equating k to d and thus the k values that were used were too big. A bigger k value will thus cause the unit applied power value over the stone to decrease. When the applied power has decreased over a stone it will only increase with a bigger value of \sqrt{gDs} . A stone of a certain diameter will thus start to move at a higher value of \sqrt{gDs} than would have been the case for that stone in a uniform particle size bed due to the fact it underlies a bigger eddy. Several studies (Andrews 1983, Bathurst 1987, Egiazaroff 1965, Wiberg & Smith 1987, Wilcock 1993) found that in bed materials

with non-uniform size distributions, particles smaller than a particle reference size are relatively difficult to move while particles larger are relatively easy to move. The smaller the stone in a non-uniform particle size bed, the smaller the term $\left(\frac{d}{k}\right)^{\frac{1}{3}}$ will become and the higher the value of \sqrt{gDs} must become to move the stone. Figures 4.10 – 4.12 explain this situation graphically.

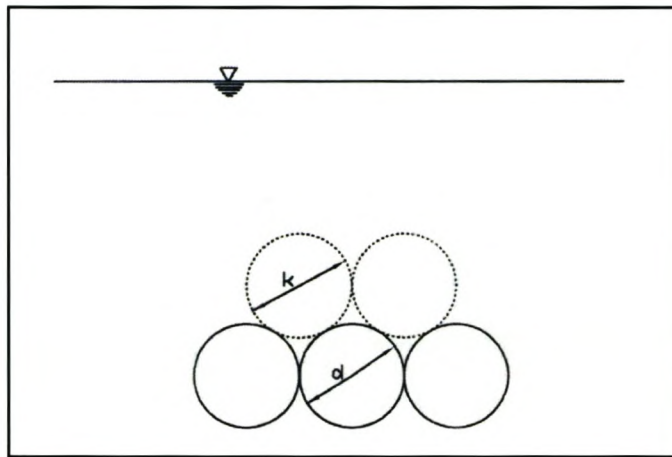


Figure 4.10: Stone d in a uniform particle size bed with a fixed \sqrt{gDs}

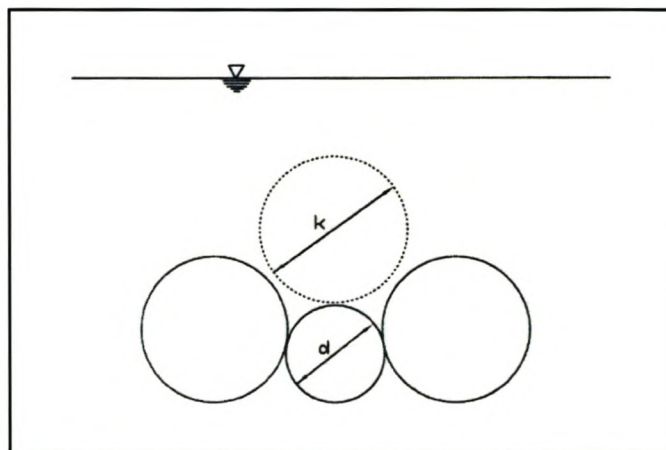


Figure 4.11: Stone d in a non-uniform particle size bed with a fixed \sqrt{gDs}

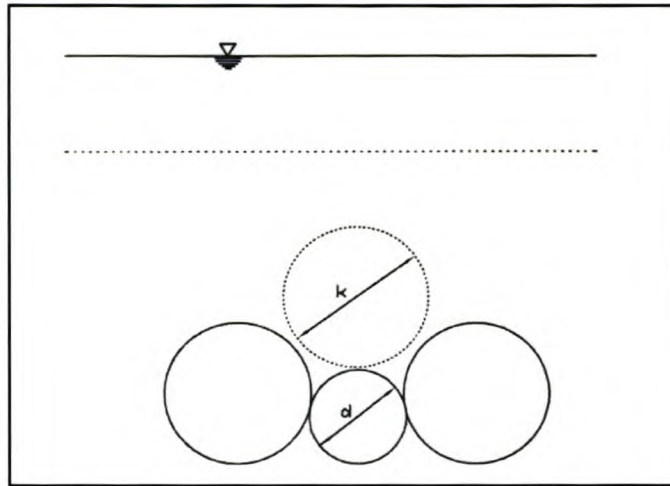


Figure 4.12: Stone d in a non-uniform particle size bed with an increased \sqrt{gDs}

Figure 4.10 depicts a stone of size d at the threshold of movement in a uniform particle size bed. In Figure 4.11 the same stone d is shown in a non-uniform particle size bed with the same \sqrt{gDs} as in Figure 4.10. This change in bed topography causes the eddy over stone d to increase in size. As shown in the previous paragraph this causes the applied power to decrease and hence the stone will be at rest and not be at threshold conditions anymore. The only way for the stone to approach threshold conditions again is through an increase in \sqrt{gDs} which will cause an increase in the applied power. This is shown in Figure 4.12 where the difference is shown between the level of water needed to move stone of diameter d in a uniform particle size bed (dashed line) and the water level required to move stone of diameter d in a non-uniform particle size bed. This difference in water level represents the increase of \sqrt{gDs} in order to reach threshold conditions between a stone in a uniform particle size bed and in a non-uniform particle size bed.

Figures 4.2 - 4.4, which were derived for uniform particle beds (equation 4.9), do make provision for this change in \sqrt{gDs} to be accommodated in the plotting of the data but not a change in eddy size. This deviation thus reflects the increase in \sqrt{gDs} needed to overcome the decrease in applied power over a stone due to increased eddy size.

The Liu diagram, as adapted for non-uniform particle size beds to make provision for this change in k , is shown in Figures 4.13 – 4.15 for the Molenaars and Berg River data respectively. The average eddy value (k) has been set equal to d_{84} . This is justified by the explanation given above that the average eddy size would be determined by the size of the larger stones in the bed. Stones in the size range d_{50} to d_{100} should play a determinant role in the eddy formation process. These are stones that protrude above the bed and will typically not be as sheltered as the stones smaller than d_{50} . Stones smaller than d_{50} , as mentioned before, fall in between and hide behind bigger stones and thus play a much smaller role (if indeed any for the smallest stones) in determining the average eddy size. Setting the average roughness equal to d_{84} is also justified through the fact that it provides the closest approximation for the data against a y-axis value of 0,12 compared to setting k equal to other values

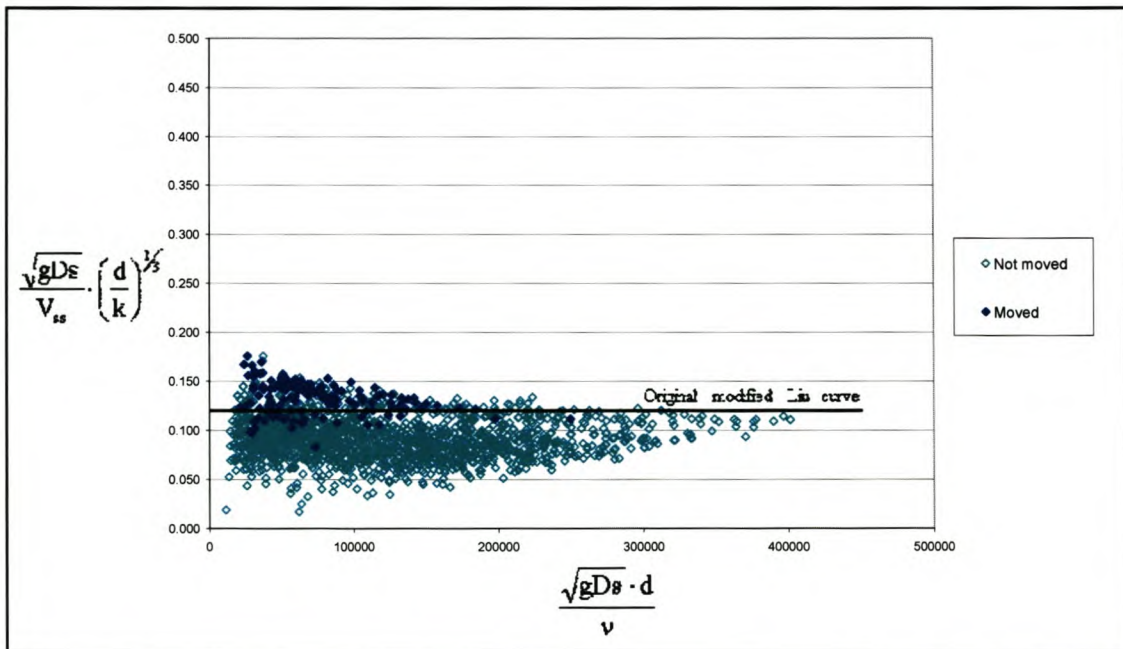


Figure 4.13: Liu diagram, adapted for non-uniformity, $k=d_{84}$ Molenaars 2003

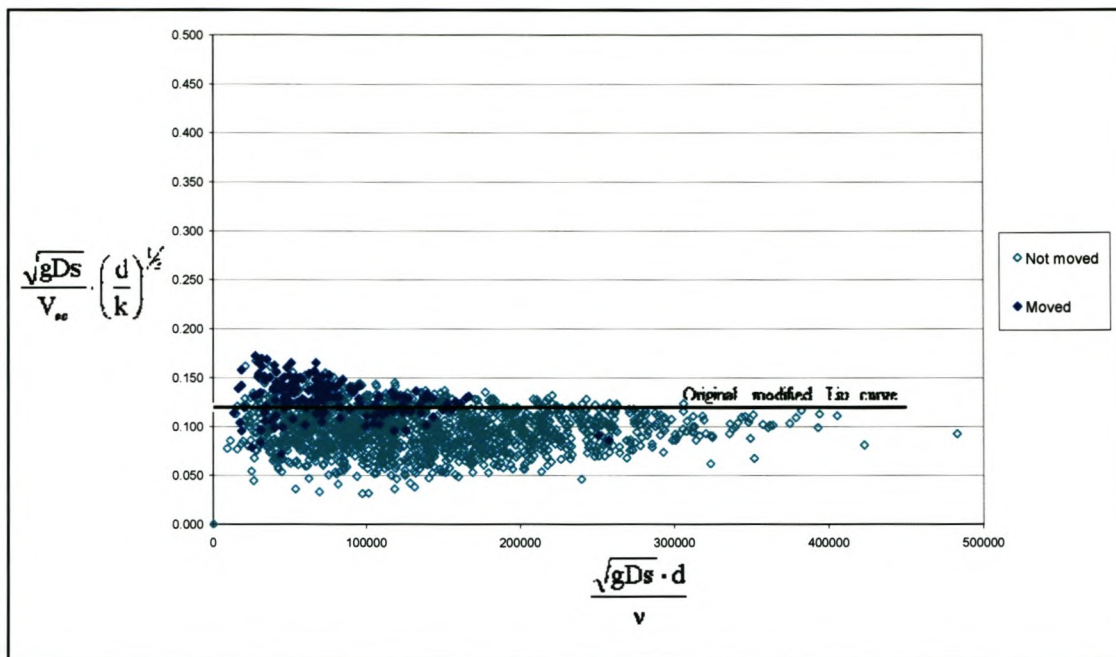


Figure 4.14: Liu diagram, adapted for non-uniformity, k=d84, Molenaars 2004

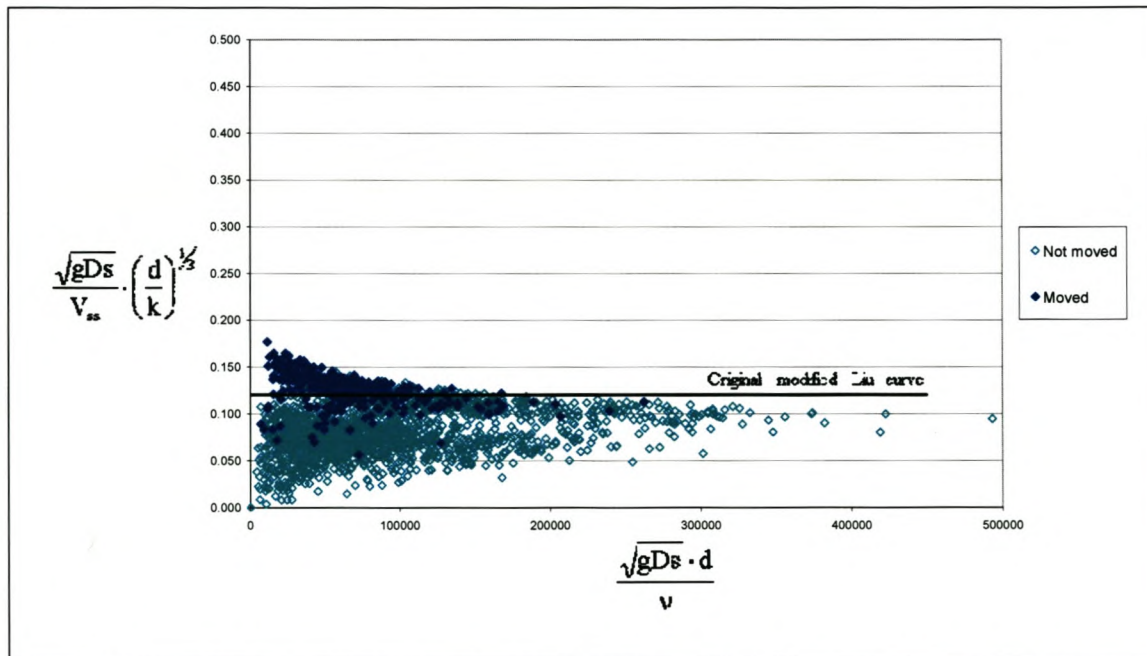


Figure 4.15: Liu diagram, adapted for non-uniformity, k=d84, Berg 2004

From the above figures it is clear that the data deviates much less from the theoretical horizontal line than in Figures 4.2 - 4.4, although there are still small but definite deviations noticeable. These small deviations can be attributed to the fact that even though provision has been made in terms of the average k value of the bed being used, transition effects in the hashed areas in Figure 4.16, were not modelled. These transition effects are highly complex and are thus impossible to model.

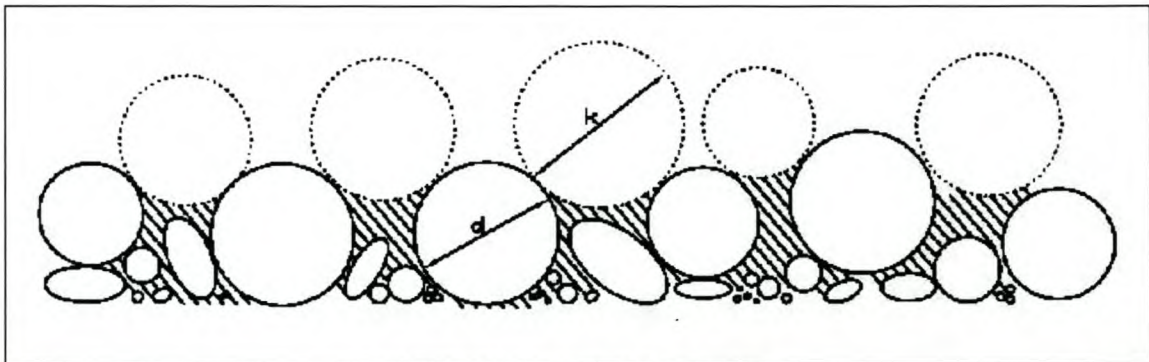


Figure 4.16: Transition zones

The smaller a stone, the deeper it will tend to lie in the bed (i.e. it won't protrude into the flow as much as bigger stones), and the further away from the prevailing turbulent eddies it will be located. Secondary effects will thus be greater for smaller stones and could explain why the biggest remaining variations in the Liu diagram, adapted for non-uniformity (Figures 4.13 – 4.15), are found for the smallest stones.

The deviation of the Molenaars and Berg Rivers data from the expected horizontal line for threshold of movement in the original modified Liu diagram (Figures 4.2 – 4.4) can thus be explained in terms of non-uniformity of bed materials.

4.4 Influence of laminar zones on incipient motion

As mentioned in Chapter 4.1 the deviations of the Molenaars and Berg Rivers data from the expected horizontal line for threshold of movement, when plotted in the original modified Liu diagram, show a striking resemblance to the deviation of the data on the left

in the original modified Liu diagram where laminar flow is dominant. Could laminar conditions thus also play a role in the incipient motion process in cobble stone river beds?

On plotting incipient motion data from sand bed rivers with large bedforms, Rooseboom and Le Grange (1994) found a dependency of the threshold of movement of particles on viscosity well into the turbulent boundary range. This can be seen in Figure 4.17.

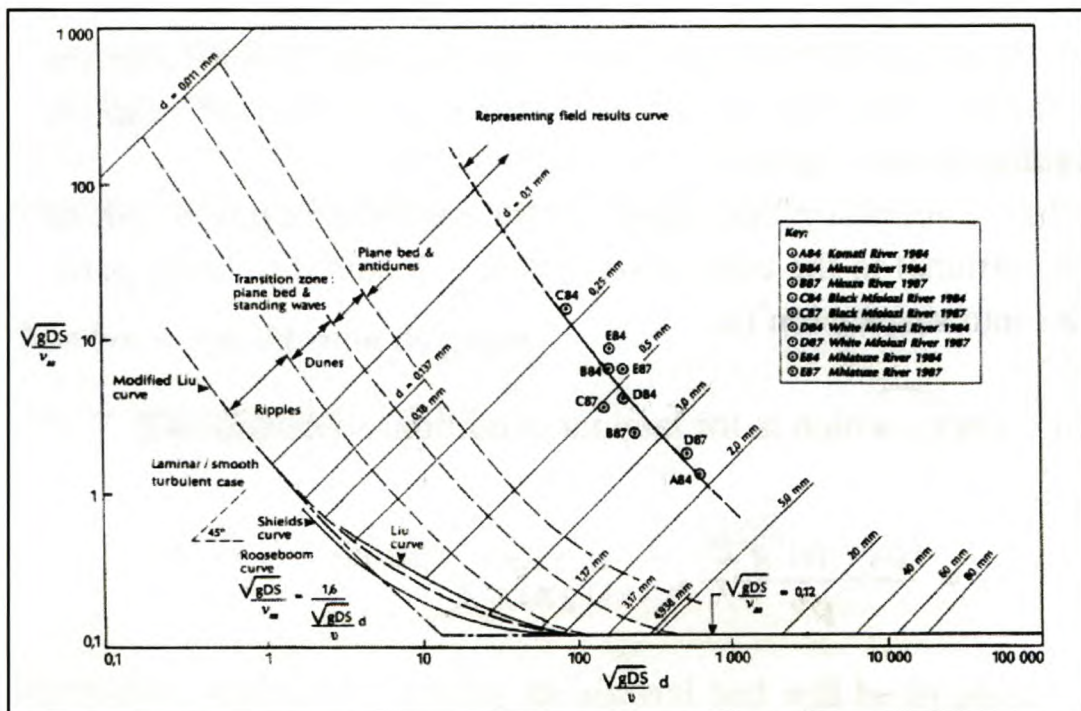


Figure 4.17: Critical conditions for sediment particles (Liu diagram) with river flood data and bedforms added (Rooseboom and Le Grange, 2000)

This observation led to the following statement:

“The only conceivable way in which viscosity can play a role is through the development of a laminar boundary layer beneath the turbulent flow zone. It is generally accepted that laminar boundary conditions develop along even beds and there is no reason why this should not happen in the sheltered hollows between bedforms” (Rooseboom and Le Grange, 2000).

It has also been shown (Rooseboom 1974, 1992) that whenever alternative modes of flow exist, that mode which requires the least amount of applied unit power will be followed. Flow will therefore be either laminar or turbulent depending on which mode requires the least amount of power to generate the equilibrium stresses. It also follows that fluid flowing over transportable material will not transport such material unless this would result in less power being applied than without sediment transport.

Using the equations (Chapter 2) for applied unit power,

$$\frac{30\rho g s D \sqrt{2\pi g D s}}{k} \quad (2.17)$$

and applied laminar power,

$$\frac{(\rho g S D)^2}{\rho \nu} \quad (2.13)$$

the values for unit applied power under turbulent and laminar conditions were determined. For both the Berg and Molenaars Rivers floods the value of unit applied laminar power exceeded that of unit applied turbulent power by orders of approximately a thousand times. According to the above statement that whenever alternative modes of flow exist, that mode which requires the least amount of applied unit power will be followed (Rooseboom 1974, 1992), turbulent power will prevail at bed level for the Molenaars and Berg Rivers.

4.5 Conclusions

In the first part of this chapter the data from the Molenaars (2003 and 2004) and Berg (2004) Rivers were plotted in the original modified Liu diagram (Rooseboom, 1992). The data sharply deviated from the expected constant horizontal line (y-axis value = 0,12). Three possible reasons were identified that could mathematically explain this deviation:

- The stones are embedded and the derivation of a constant value for the threshold of movement in the modified Liu diagram does not account for such conditions.
- The original modified Liu diagram (Rooseboom, 1992) was derived for beds with uniform particle sizes, while the data for the Molenaars and Berg rivers represent beds which consist of non-uniform bed particles.
- The deviation noticed for the data from the Berg and Molenaars Rivers is due to laminar conditions playing a role in the entrainment process of the stones.

It was found that the only reason that could account for the deviation from the expected horizontal line in the original modified Liu diagram was the fact the original modified Liu diagram was derived for uniform particle size beds whereas the data of the Molenaars and Berg Rivers represented non-uniform particle size beds. When the derivation for the y-axis in the original modified Liu diagram, which depicts

$$\frac{\sqrt{gDs}}{V_{ss}} \text{ or } \left[\frac{\text{Unit applied power along bed}}{\text{Unit power required to suspend particles}} \right],$$

was modified to provide for non-uniform bed particle sizes, an extra factor was obtained and the function on the y-axis changed to:

$$\frac{\sqrt{gDs}}{V_{ss}} \cdot \left(\frac{d}{k} \right)^{1/3}$$

An analysis of the observed flow data showed that the absolute roughness (k) of a non-uniform bed is reasonably well approximated by a value of d_{84} . This is due to the fact that the bigger stones in the bed (d_{50} to d_{100}) play the dominant role in determining the eddy size. When the Liu diagram was re-plotted with the newly derived y-axis function and the k -value for each stone set equal to the average roughness of the bed ($k=d_{84}$) the data plotted close to the expected horizontal line. The much smaller remaining deviation

from a horizontal line relationship is attributed to secondary effects which are not accounted for in the theory.

5 INTENSITY OF MOVEMENT GRAPHS

5.1 Introduction

In terms of the objectives set out in Chapter 1 of this thesis a graph or set of graphs were to be produced. These graphs would aid environmentalists and other interested parties who do not necessarily have a technical background in hydraulics to make management decisions e.g. on how much water must be released from dams to satisfy the ecological needs in terms of bed material transport.

5.2 Intensity of movement

(i) Original modified Liu-diagram

As shown in Chapter 4 the main reason for the deviation from the expected horizontal line (y-axis) when data from the Molenaars and Berg Rivers are plotted in the original modified Liu diagram is the fact that the original modified Liu diagram does not make provision for non-uniform bed particles. Due to the difficulty (also mentioned in Chapter 4) in predicting the roughness (k) accurately the graphs (Figures 4.2 – 4.4) are used in providing design curves for sediment movement. Rivers with similar bed roughness (even if the exact value of the roughness of every stone cannot be determined) will show similar deviation from the expected horizontal line when plotted in the original modified Liu diagram. Thus, even though the deviation is explained through the inclusion of the average roughness of the non-uniform particle size beds, the graphs (Figures 4.2 – 4.4) can be used to produce design curves for defining intensity movement.

As explained in Chapter 4.1, the boundary between data points that represent movement and those that represent non-movement in the original modified Liu diagram (Figures 4.2 – 4.4) is equivalent to the incipient motion curve. Also mentioned is the fact that the data on movement are not as accurate as those that depict non-movement. It is thus not possible to draw an exact incipient motion curve from the boundary between data points that represent movement and those that represent non-movement based on the observed

data from this study. However, the data plotted in the original modified Liu diagram reveal more than the location of the incipient motion curve. It also shows the maximum value of $\left[\frac{\text{Unit applied power along bed}}{\text{Unit power required to suspend particles}} \right]$ or $\frac{\sqrt{gDs}}{V_{ss}}$ for every stone size observed during a particular flood. Figure 5.1 depicts the Molenaars 2003 Flood No. 6 as an example of a single flood, with a curve drawn where the maximum $\frac{\sqrt{gDs}}{V_{ss}}$ value for every stone size class is located. Straight lines have been added to indicate stones with equivalent diameters. In this particular figure (5.1) lines have been assigned to only a few of the stone size classes to indicate the pattern stone sizes follow in the Liu diagram.

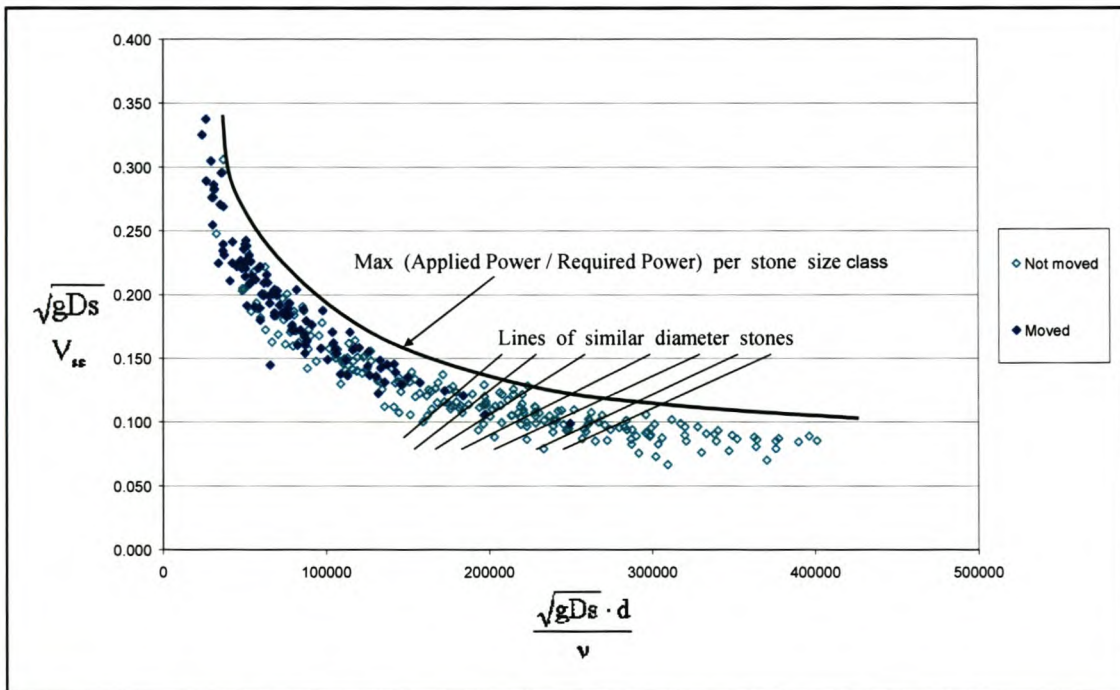


Figure 5.1: Max Applied Power/Required Power per stone size class for Molenaars 2003 Flood 6

From Figure 5.1 it can be appreciated that an upper envelope curve for the data of a specific flood represents the maximum $\frac{\sqrt{gDs}}{V_{ss}}$ value, for that flood, for every stone size class.

Although the data on movement in the Liu diagram (Figures 4.2 – 4.4) is not completely accurate, the number of stones that were moved during a flood is correct. When this data on the number of stones that moved during each flood is super-imposed on the curve (Figure 5.1) that represents the maximum $\frac{\sqrt{gDs}}{V_{ss}}$ value for every stone size, it reveals a curve that represents the number of stones that were moved by a certain size flood.

Figures 5.2 -5.4 contain data from the Molenaars and Berg Rivers plotted in the original modified Liu diagram. The data have been plotted for each flood. The amount of bed movement in each flood is indicated in the legend. The amount of movement has been defined as the percentage of stones that were moved.

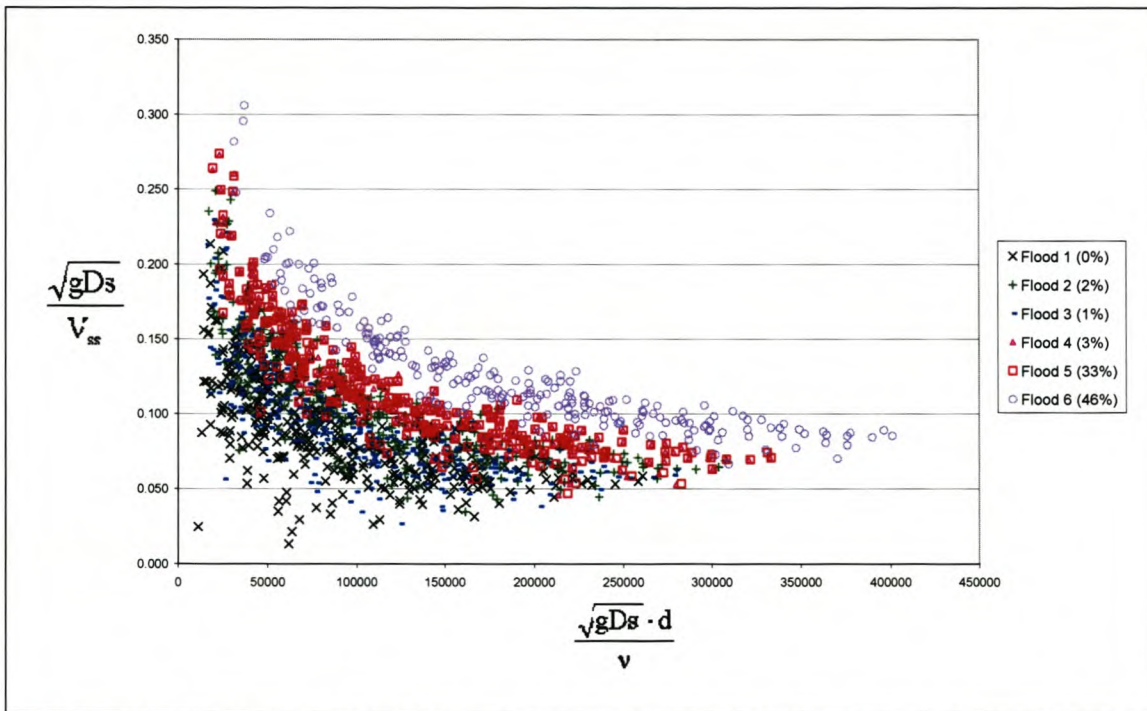


Figure 5.2: Molenaars 2003 data, floods separated, plotted in the original modified Liu diagram

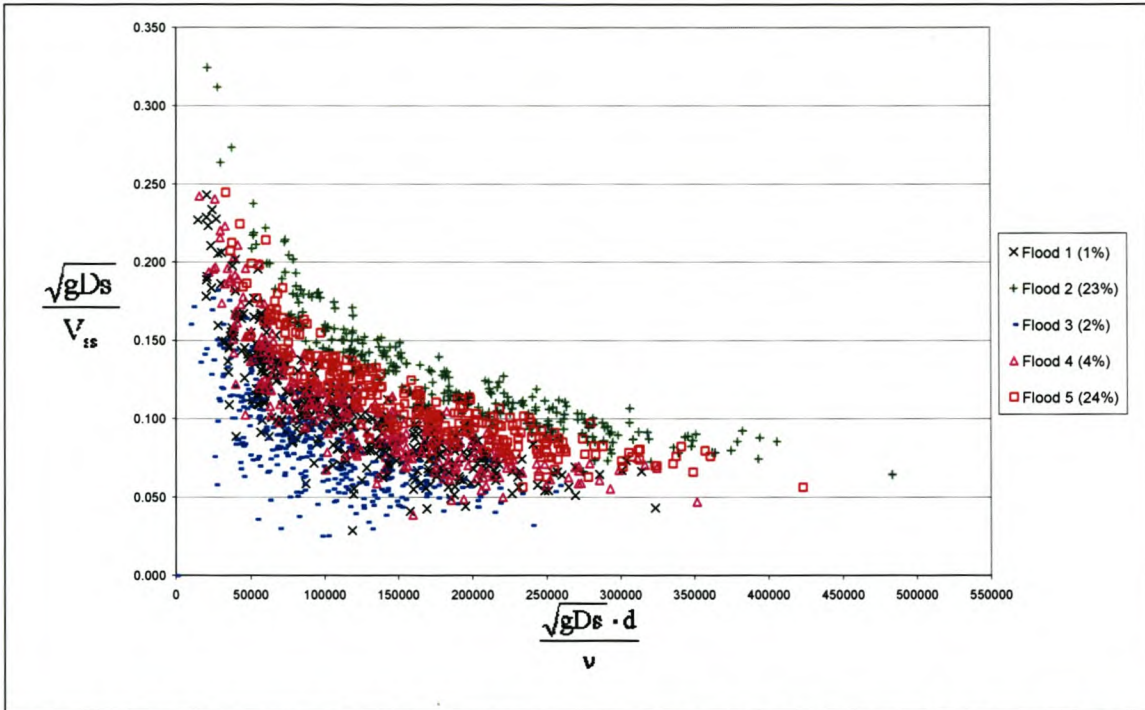


Figure 5.3: Molenaars 2004 data, floods separated, plotted in the original modified Liu diagram

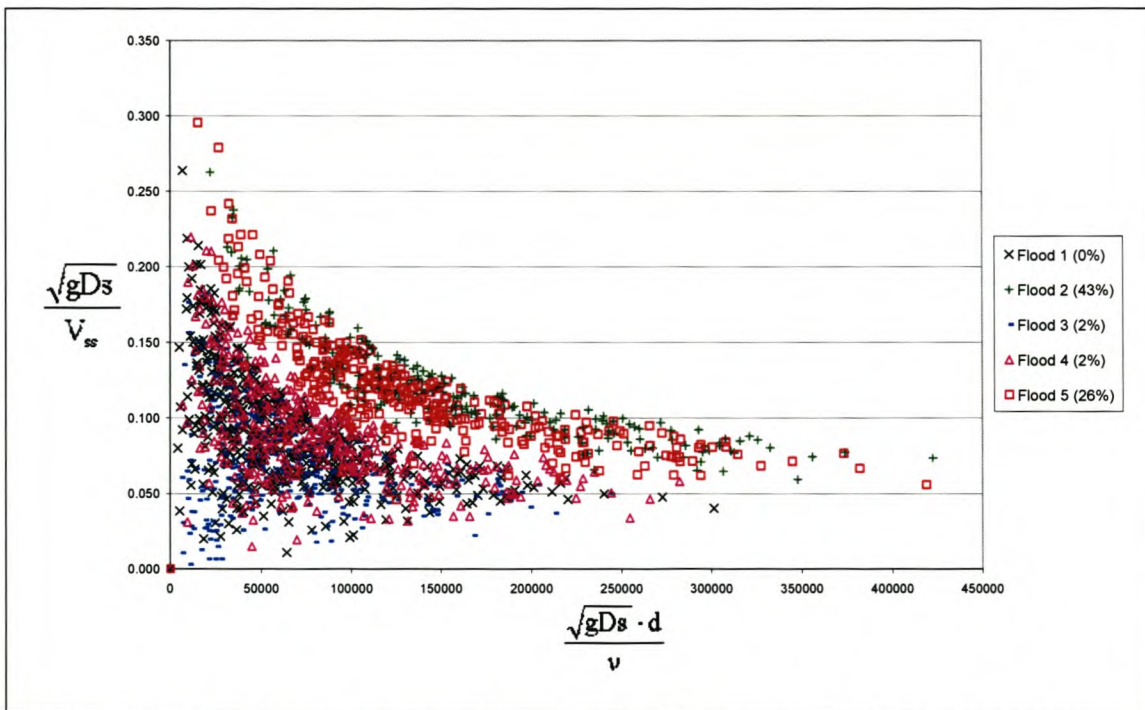


Figure 5.4: Berg 2004 data, floods separated, plotted in the original modified Liu diagram

Considering Figures 5.2 – 5.4 a general trend is revealed. Comparing the upper data points for every flood (through which the topmost envelope curve for every flood is drawn) and the intensity of movement, it is seen that as the $\frac{\sqrt{gDs}}{V_{ss}}$ value increases more stones are transported. Figures 5.5 – 5.7 provide a clearer picture of these envelope curves. All the data in Figures 5.5 – 5.7 have been provided with envelope curves for every flood (the data points have been removed to provide clearer graphs)

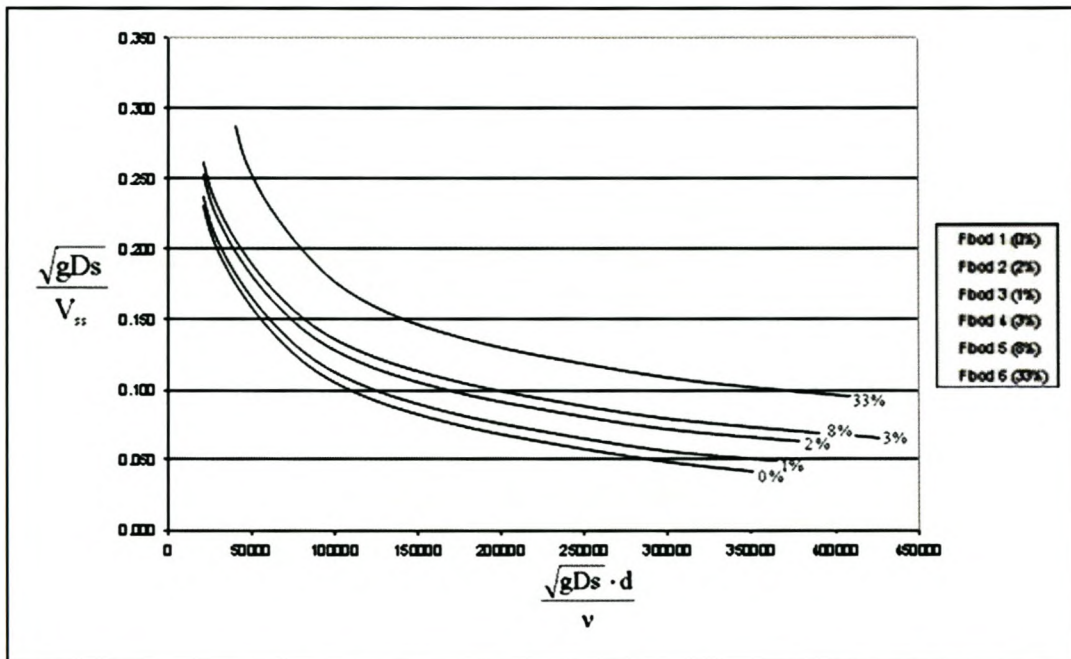


Figure 5.5: Envelope curves for intensity of movement, Molenaars 2003

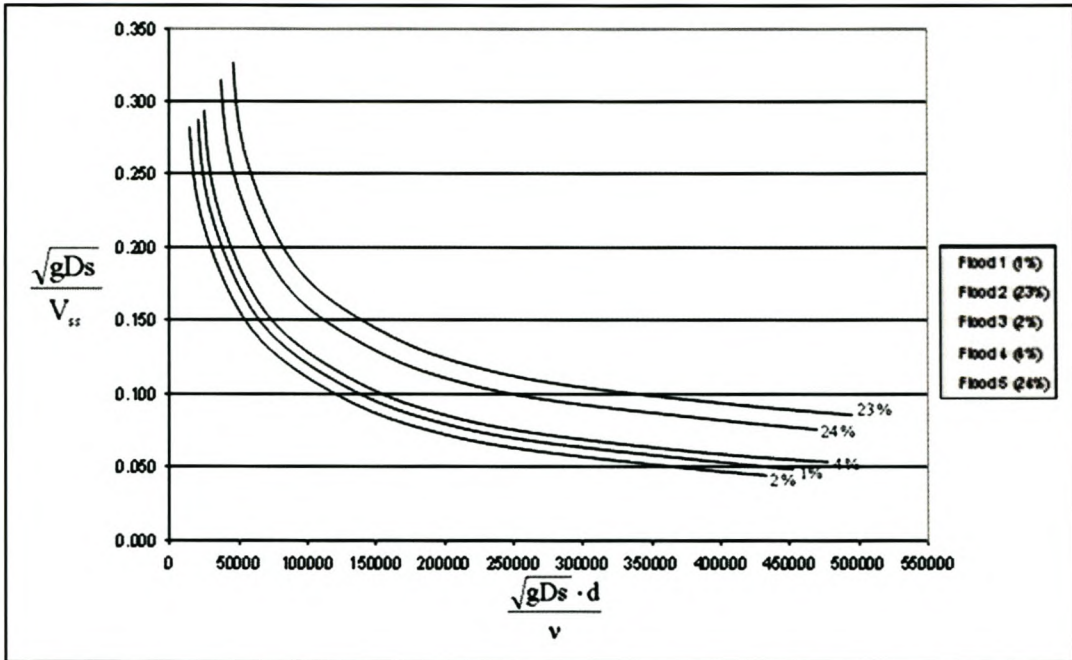


Figure 5.6: Envelope curves for intensity of movement, Molenaars 2004

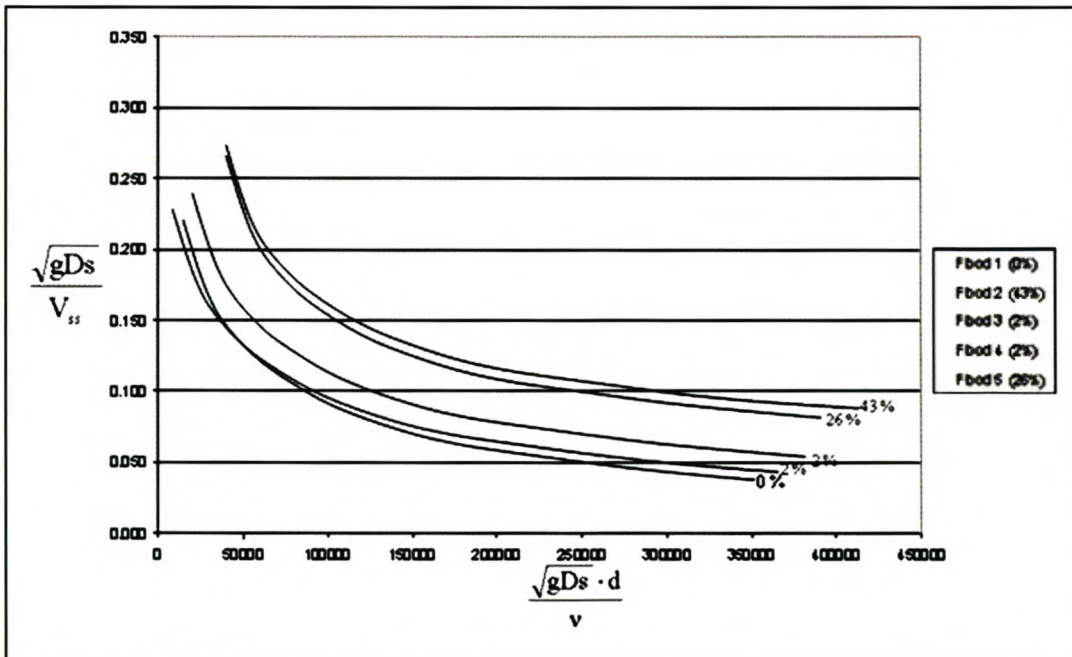


Figure 5.7: Envelope curves for intensity of movement, Berg 2004

Analysis of Figures 5.5 – 5.7 reveals the following:

- Although, the overall trend of the curves indicates that the intensity of movement increases as the curves plot higher it is not necessarily the case that a higher plot will yield a bigger intensity of movement. For example in Figure 5.6 the curve that is associated with 2% movement plots lower than the curve associated with 1% movement.
- The intensity of movement does not increase linearly with $\frac{\sqrt{gDs}}{V_{ss}}$. The lower curves are associated with relatively small values of intensity of movement. From there a point is reached where a relatively small increase in $\frac{\sqrt{gDs}}{V_{ss}}$ is associated with a rapid increase in the intensity of movement.

The above Figures 5.5 – 5.7 do not distinguish between floods of different durations and thus the first of these remarks can possibly be explained in terms of the durations of floods. Tables 3.3 and 3.4 contain the particulars of every flood (which include the durations) and are repeated here as Tables 5.1 and 5.2 for the purpose of comparison.

Year	Event Number	Date	Duration (hours)	Max Flow (m ³ /s)	Avg. Daily Flow (m ³ /s)	Volume (Mm ³)	DRIFT Class
2003	1	10 th July	33	5.56	3.72	0.41	I
	2	18 th July	21	15.23	5.41	0.49	I
	3	25 th July	14	8.60	4.20	0.28	I
	4	1 st August	26	28.76	7.98	0.95	I
	5	8 th August	26	36.46	14.45	1.74	II
	6	18 th August	32	140.80	30.29	4.15	III
2004	1	6 th June	29	20.20	10.02	1.04	I
	2	14 th June	33	140.97	37.21	3.82	III
	3	26 th June	31	8.87	5.13	0.66	I
	4	3 rd July	21	46.38	16.08	1.35	II
	5	23 rd July	18	113.93	29.17	2.67	III

Table 5.1: Flood events observed at the Molenaars study site

Year	Event Number	Date	Duration (hours)	Max Flow (m ³ /s)	Avg. Daily Flow (m ³ /s)	Volume (Mm ³)	DRIFT Class
2004	1	5 th June	28	7.27	2.08	0.40	I
	2	14 th June	44	84.51	32.58	3.48	IV
	3	26 th June	27	4.82	2.62	0.29	I
	4	3 rd July	24	11.74	5.68	0.44	II
	5	23 rd July	20	60.98	17.70	1.66	IV

Table 5.2: Flood events observed at the Berg study site

When comparing the positions of the curves relative to each other (Figures 5.5 -5.7) with the duration of every flood (Tables 5.1 and 5.2) no explanation is evident in terms of the durations of the floods that would describe all the discrepancies.

Although it is not possible to read off accurate values of movement values (to within 1%) directly from these curves, it should be possible to use judgement and deduce accurate enough volumes in practical situations since management decisions on the amount of water to be released will typically indicate small, medium or large movements and not a singular percentage value of movement.

(ii) Incipient motion in terms of DRIFT classification

When plotting the intensity of movement for every flood against the DRIFT classifications of these floods, a clearer picture is obtained of when (in terms of DRIFT classification) stones start to move (incipient motion) and how the intensity of movement varies with flood size.

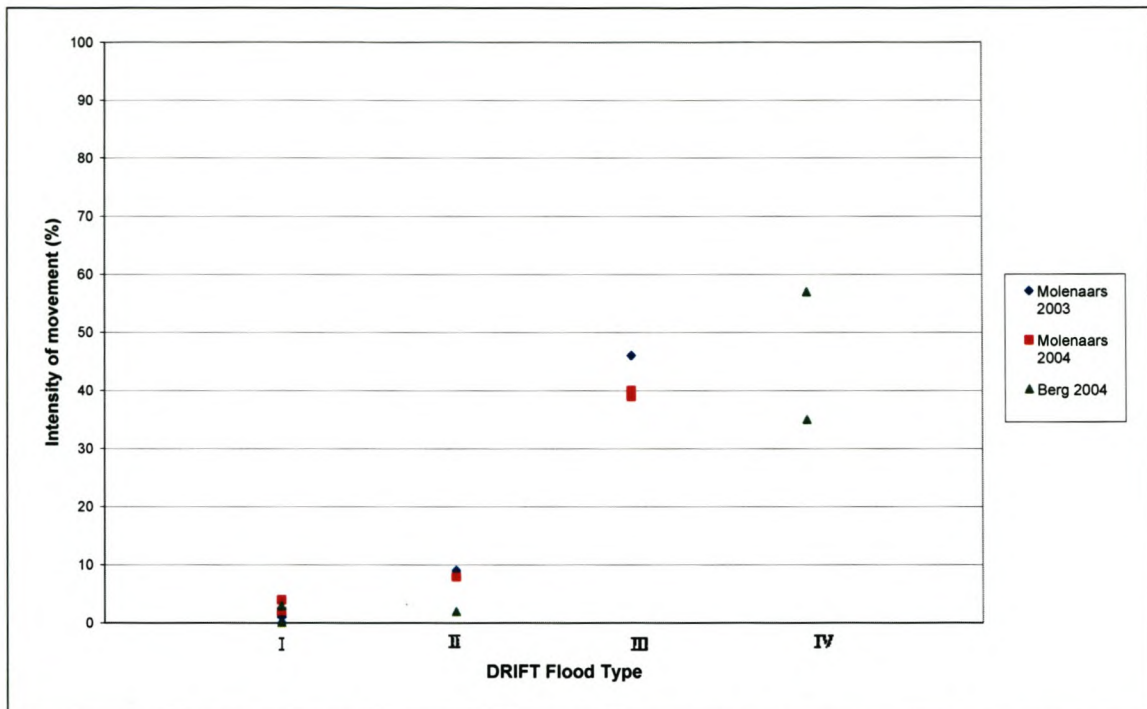


Figure 5.8: DRIFT flood classification vs. Intensity of movement (excluding non-embedded stones)

Figure 5.8 shows that very little movement is noticed with DRIFT Class I and II floods. The intensity of movement might in some cases be even less for a class II flood than for a class I flood. However, there is a definite increase in the intensity of motion between a class II and a class III flood. It is also noticed that class IV floods in some cases have smaller values of intensity of motion than class III floods. This indicates that in terms of incipient motion movement starts somewhere before the DRIFT class II floods are reached

When Figure 5.8 is adapted to include data on embedded stones the effect of embeddedness on incipient motion can be detected. This is shown in Figure 5.9.

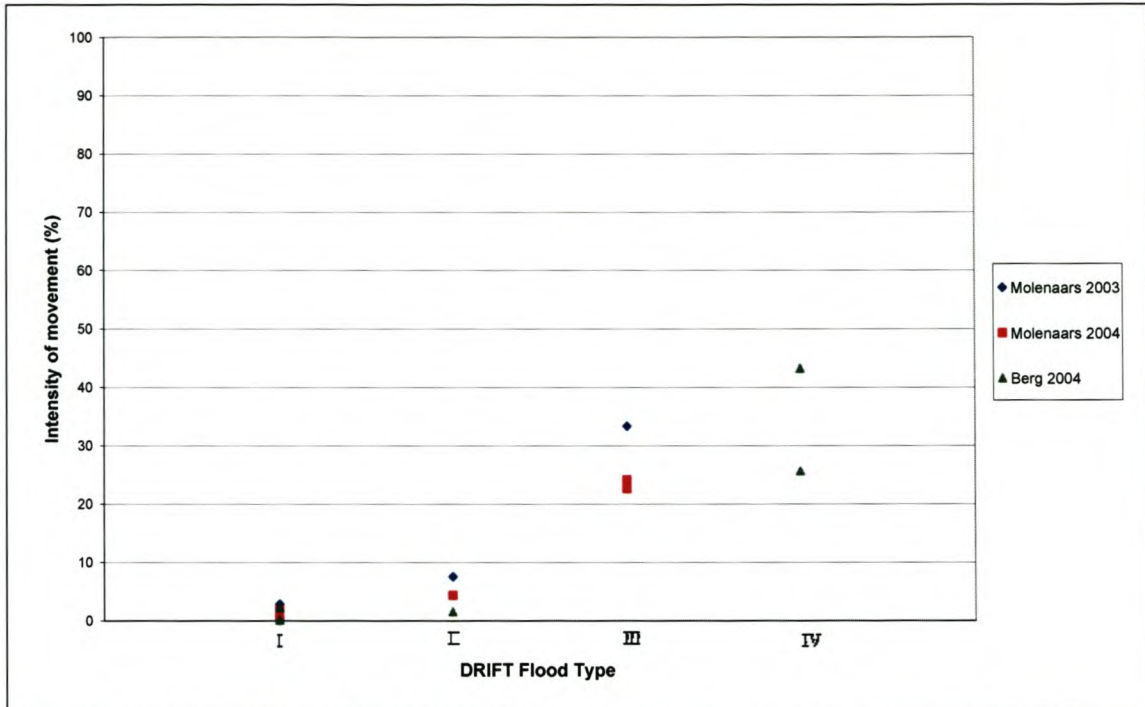


Figure 5.9: DRIFT flood classification vs. Intensity of movement (all stones)

Figure 5.9 depicts the same trend as is noticed in Figure 5.8 namely that a rapid increase in intensity of motion is noticed between a class II and a class III flood. Although in Figure 5.9 (for all the stones) the shift is smaller than in Figure 5.8 (non-embedded stones only).

5.3 Conclusions

From the information in this chapter it can be concluded that a curve through those data points in the original modified Liu diagram that represent the maximum $\frac{\sqrt{gD_s}}{V_{ss}}$ value for every stone size, forms an upper envelope curve for the data of every flood. This curve represents the intensity of motion for this flood. Unfortunately when separate curves were drawn for the Molenaars and Berg Rivers, it was found that no singular pattern is revealed that would allow these curves to be used as accurate design curves for practical use. However, they did reveal a trend with the higher plotting lines representing higher intensities of motion and vice versa. Although it is not possible to read off accurate

values of movement values (to within 1%) directly from these curves, it should be possible to use judgement and deduce accurate enough volumes in practical situations since management decisions on the amount of water to be released will typically indicate small, medium or large movements and not a singular percentage value of movement. The intensity of motion also does not increase linearly with flood size but there is a sudden increase in the number of stones that move after a certain flood size is reached. When plotting the DRIFT classes of the floods against their respective intensity of movements it is seen this sudden increase in the number of stones that move is at a point between a DRIFT class II and class III flood. It also indicated that a DRIFT class II flood does not necessarily go with a higher value of intensity of movement than a DRIFT class I flood. The same is noticed at the higher floods where a DRIFT class IV flood does not necessarily mean a higher value of intensity of movement than a DRIFT class III flood. In terms of intensity of motion it indicates that incipient motion takes place some point before the DRIFT class II floods are reached. When the data on non-embedded stones are included (Figure 5.9) the same trend as explained above is noticed with the one difference being that the increase in intensity of movement between DRIFT class II and class III flood is not as rapid when the data on embedded stones is included (Figure 5.9).

6 COMBINED CONCLUSIONS AND RECOMMENDATIONS

6.1 Combined conclusions

The objectives which were defined at the start of this research, have been met through describing the incipient motion process in terms of the applied power approach and producing graphs which provide a clearer picture of incipient motion in cobble/boulder bed rivers.

The main conclusions that have been reached are:

- Data which represent incipient motion on non-uniform particle size beds deviate from the expected horizontal line (y-axis value = 0,12) when plotted in the original modified Liu diagram. It was found that the only reason that can account for this deviation is the fact that the original modified Liu diagram does not make provision for non-uniform particle size beds.
- When the derivation of the parameters the original Liu diagram was redeveloped to provide for non-uniform particle beds an extra factor was obtained and the function on the y-axis changed to: $\frac{\sqrt{gDs}}{V_{ss}} \cdot \left(\frac{d}{k}\right)^{1/3}$. When the absolute roughness (k) was set equal to d84 for every stone the data plotted close to the expected horizontal line. Using d84 as a value for the absolute roughness of the bed is justified through the fact that the bigger stones in the bed (d50-d100) play the dominant role in determining eddy size. The much smaller remaining deviation from a horizontal line relationship is attributed to secondary effects which are not accounted for in the theory.
- Intensity of motion curves were obtained by drawing upper envelope curves through the data of every flood in the original modified Liu diagram and super-imposing this curves on the number of stones that were moved during the flood. Although it is not possible to read off accurate percentages of movement values directly from these curves, it should be possible to use judgement and deduce accurate enough values in practical situations.

- In terms of DRIFT class flood classification incipient motion of sediment takes place at a size flood smaller or equal to a DRIFT class II flood. There is a rapid increase in the intensity of movement between DRIFT class II and class II floods.

6.2 Recommendations

- The curves shown in Figure 5.5 – 5.7, which depict intensity of movement, should be calibrated with more data sets. This would allow more accurate design curves to be produced for predicting stone movement. These data sets used for further calibration should typically be of rivers with different particle size distributions in order to see what effect size distribution has on incipient motion.
- Embeddedness should be recorded in as much detail as possible in future data collections. This will aid in making provision for embeddedness in the Liu diagram.
- The impact of the duration of floods should be included in further development of design curves for intensity of movement.
- The benefits of introducing extra physical variables into the theory (e.g. particle shape, hydraulic sheltering etc.) should be investigated.
- The intensity of movement curves should be linked to some physical river characteristic/s. This will avoid gathering of large data sets (as was done for this study) in order to calibrate design curves.

7 REFERENCES

- ALLEN J.R.L. (1970). *Physical processes of sedimentation: an introduction*. Allen and Unwin, London, UK.
- ANDREWS E.D. (1983). *Entrainment of gravel from naturally sorted riverbed material*, Geological Society of America Bulletin, Vol, 94, 1225-1231.
- ANDREWS E.D. (1984). *Bed material entrainment and hydraulic geometry of gravel bed rivers in Colorado*, Geological Society of America Bulletin, Vol, 95, 371-378.
- AGUIREE-PE J., OLIVERO M.L., MONCADA A.T. (2003). *Particle densimetric froude number for estimating sediment transport*, ASCE J. of Hydr. Eng, Vol 129, No 6, 428-437.
- ARMITAGE N.P and McGAHEY C. (2003). *A unit stream power model for the prediction of local scour in rivers* : Report to the Water Research Commission.
- ASHWORTH P.J. and FERGUSON R.I. (1989). *Size-selective entrainment of bedload in gravel-bed streams*, Water Resources Research, Volume 25, Issue 4, p. 627-634.
- ASHWORTH P.J., FERGUSON R.I., ASHMORE P.E., PAOLA C., POWELL D.M. and PRESTEGAARD K.J. (1992). *Measurements in a braided river chute and lobe (2). Sorting of bed load during entrainment, transport and deposition*, Water Resources Research, 28, 1887 – 1896.
- BAGNOLD R.A. (1966). *An approach to the sediment transport problem from general physics*. U.S. Geological Survey Professional Paper 422 – I. U.S Government Printing Office, Washington, DC.

BATHURST J.C. (1987). *Critical conditions for bed material movement in steep, boulder-bed streams*, Erosion and Sedimentation in the Pacific Rim (Proceedings of the Corvallis Symposium. IAHS Publ. no. 165, 309-318.

BROWN C. and KING J. (2002). *DRIFT application*. Report prepared as part of the Breede River Basin Study, Unpublished. Southern Waters Report for Department of Water Affairs and Forestry, and Water Research Commission. Available on www.southernwaters.co.za.

BROWN C. and KING J. (2000). *Environmental flow assessment: Concepts and methodologies*, World Bank Water Resources and Environmental management Guideline Series, Guideline No. 6.

CARLING P.A. (1983). *Threshold of coarse sediment transport in broad and narrow streams*, Earth Surfaces Processes and Landforms, Vol. 8, 1-18.

D'AGOSTINO V., GREGORETTI C., LENZI M.A. (1999)(a). *Initiation of motion and dimensionless critical shear stress in a steep mountain stream*, Graz proceedings 1999.

D'AGOSTINO V., GREGORETTI C., LENZI M.A. (1999)(b). *Transport distances of marked cobbles in a steep mountain stream*, Graz proceedings 1999.

DAY T.J. (1980). *A study of the transport of graded sediments*, Rep. IT 190, Hydraul. Res. Stat., Wallingford, England.

DHAMOTHARAN S., WOOD A., PARKER G., STEFAN H. (1980). *Bedload transport in a model gravel stream*, Proj. Rep. 190, St. Anthony Falls Hydraul. Lab., Univ. of Minn., Minneapolis.

EGIAZAROFF I.V. (1965). *Calculation of non-uniform sediment concentrations*. ASCE J. Hydr. Div., 91(4), 225 – 247.

EINSTEIN H.A. (1942). *Formulae for transportation of bed load*. Trans. Am. Soc. Civ. Eng., 107(2140), 251 – 573.

FERGUSON R.I., PRESTEGAARD K.L. and ASHWORTH P.J. (1989). *Influence of sand on gravel transport in a braided bed river*, Water Resources Research, 25, 635 – 643.

GORDON N.D., McMAHON T.A., FINLAYSON B.L., *Stream hydrology, an introduction for ecologists*, John Wiley and sons, England, 330-331.

GRAF W.H. (1971). *Hydraulics of Sediment Transport*, McGraw-Hill, New York.

GRASS A.J. (1970). *Initial instability of fine bed-sand*. Journal Hydraulic Division, ASCE Proceedings, Vol. 96, No. HY3, Paper 7139, 619 - 632

HAMMOND F.D.C., HEATHERSHAW A.D., LANGHORNE D.N. (1984). *A comparison between Shields' threshold criterion and the movement of loosely packed gravel in a tidal channel*, Sedimentology, 31, 51 – 62.

HJULSTROM F. (1939). *Transportation of detritus by moving water*. In recent Marine Sediments, Edited by Trask P.D., Dover, NY.

HOWARD H. (2004). *Hydrology*, Report prepared as part of the Berg River Baseline Monitoring Study.

HUGUES R.M., WHITTLER T.R., ROHM C.M., LARSEN D.P. (1990). *A regional framework for establishing recovery criteria*, Environmental Management 14, 673 – 683.

JONKER V.J. (2002). *Environmentally significant morphological and hydraulic characteristics of cobble and boulder bed rivers in the Western Cape*, PhD Thesis, University of Stellenbosch.

KING J.M., BROWN C.A. and SABET H. (2003). *A scenario-based holistic approach to environmental flow assessments for regulated rivers*. *Rivers Research and Applications* 19 (5-6), 619-640.

KOMAR P.D. (1987). *Selective grain entrainment by a current from a bed of mixed sizes: a reanalysis*, *Journal Sedimentary Petrology*, 57, 203 – 211.

KOMAR P.D. and CARLING P.A. (1991) *Grain sorting in gravel bed streams and the choice of particle sizes for flow-competence evaluations*. *Sedimentology* 38, 489 – 502.

LAMOUREUX N., SOUCON Y., HEROUIN E. (1995). *Predicting velocity frequency distributions in stream reaches*, *Water Resources Research*, Vol. 31, No. 9.

LOPEZ J. L. and FALCON M.A. (1999). *Calculation of bed changes in mountain streams*, *ASCE J. Hydr. Eng.* Vol. 125, No. 3, 263-270.

LORANG M.S. and HAUER F.R. (2003). *Flow competence and streambed stability: an evaluation of technique and application*, *J. N. Am. Benthol. Soc.*, 22, 475-491.

LI Z. and KOMAR P.D. (1986). *Laboratory measurements of pivoting angles for applications to selective entrainment of gravel in a current*, *Sedimentology*, 33, 413 – 423.

LIU H.K. (1957). *Mechanics of sediment-ripple formation*, *Proc. Am. Soc. Civil Engrs.*, Vol. 83, No. HY2.

MILHOUS R.T. (1973). *Sediment transport in a gravel-bottomed stream*, PhD Thesis, Oreg. State Univ., Corvallis.

MISRI R.L., GARDE R.J., RANGA RAJU K.G. (1984). *Bed load transport of coarse non-uniform sediment*, J. Hydraul. Eng., 110(3), 312 – 328.

PARKER G., KLINGEMAN P.C. and McLean D.G. (1982). *On why gravel bed streams are paved*, Water Resources Research, 18, 1409 – 1423.

PETIT F. (1994). *Dimensionless critical shear stress evaluation from flume experiments using different gravel beds*, Earth Surface Processes and Landforms, Vol. 19, 565-576.

PICKET S.T.A and WHITE P.S. (1985). *The ecology of natural disturbance and patch dynamics*. Academic.

ROOSEBOOM A. (1974). *Open channel fluid mechanics*, Technical Report No. 62, Department of Water Affairs, Pretoria, SA.

ROOSEBOOM A. (1992). *Sediment transport in rivers and reservoirs – a South African perspective*, WRC Report No. 297/1/92.

ROOSEBOOM A. (1998). *The cinderella of hydraulics – the law of conservation of power*. Proc. 3rd International conference on Hydroscience and Engineering. Cottbus, Germany.

ROOSEBOOM A. and LE GRANGE A. (1994). *Equilibrium scour in rivers with sandbeds*, 2nd Int. conference on River Flood Hydraulics, Vol 38, No. 1.

ROOSEBOOM A. and LE GRANGE A. (2000). *The hydraulic resistance of sand streambeds under steady flow conditions*, J. of Hydraulic Research, Vol. 38, No 1, 27-35.

ROUSE H. (1950). *Engineering Hydraulics*, Proceedings of Iowa Institute of Hydraulic Research, 1039.

SCHOKLITSCH A. (1962). *Handbuch des Wasserbaus*, 3rd Ed., Springer-Verlag, Vienna, Austria.

SHIELDS A. (1936). *Anwendung der Ahnlichkeitsmechanik und Turbulenzforschung auf die Geschiebebewegung*, Mitteil, Preuss. Versuchsanst. Wasser, Erd. Schiffsbau, Berlin, No. 26.

WIBERG P.L. and SMITH J.D. (1987). *Calculations of the critical shear stress for motion of uniform and heterogeneous sediments*, Water Resources Research, Vol. 23, No. 8, 1471-1480.

WILCOCK P.R. (1993). *Critical shear stress of natural sediments*, ASCE J. Hydr. Eng Vol 119, No. 4, 491-505.

WILCOCK P. R. and SOUTHARD J.B. (1988). *Experimental study on incipient motion in mixed-sized sediment*, Water Resources Research, Vol. 24, No. 7, 1137-1151.

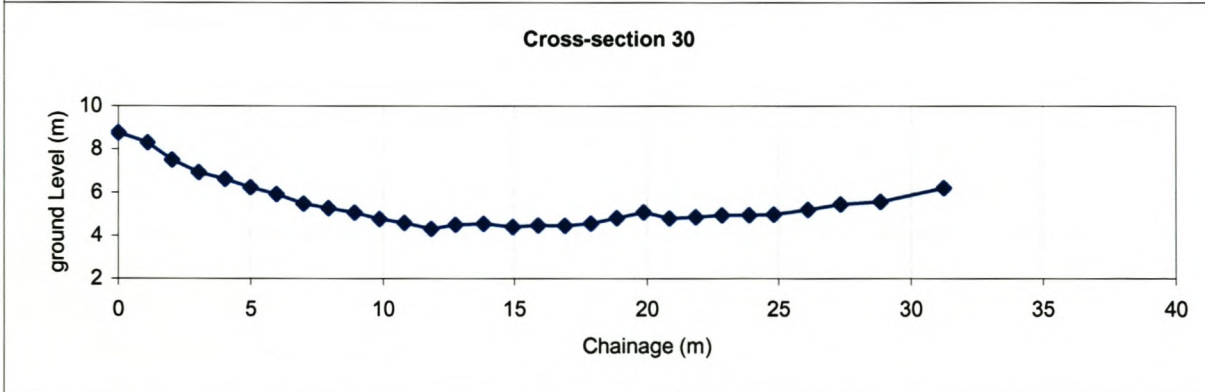
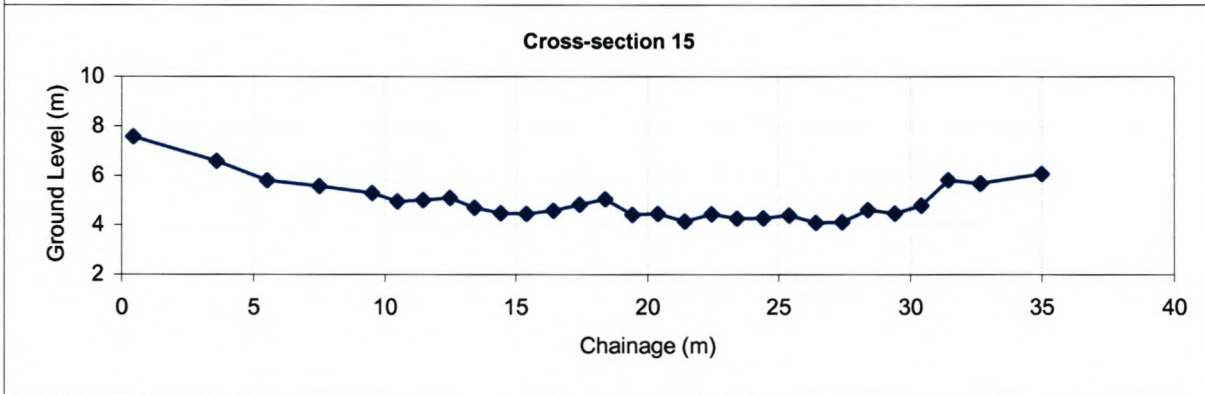
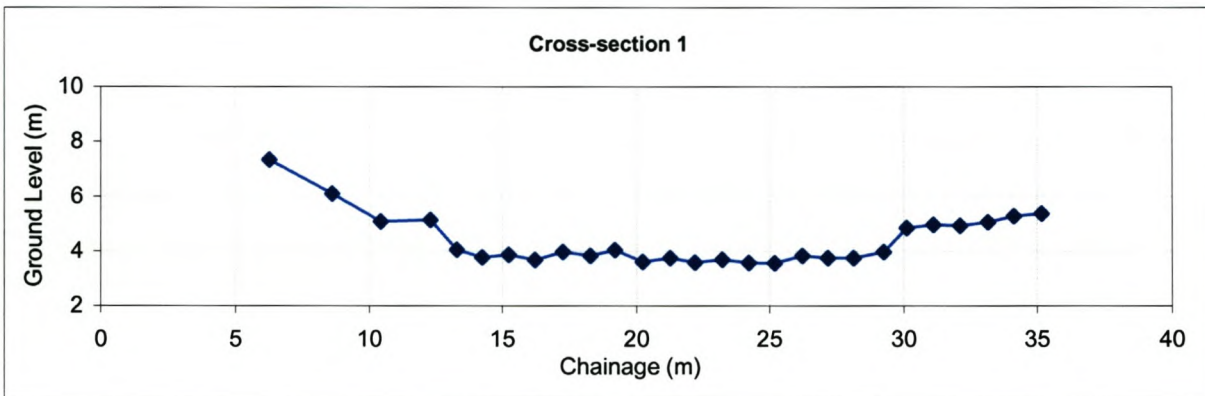
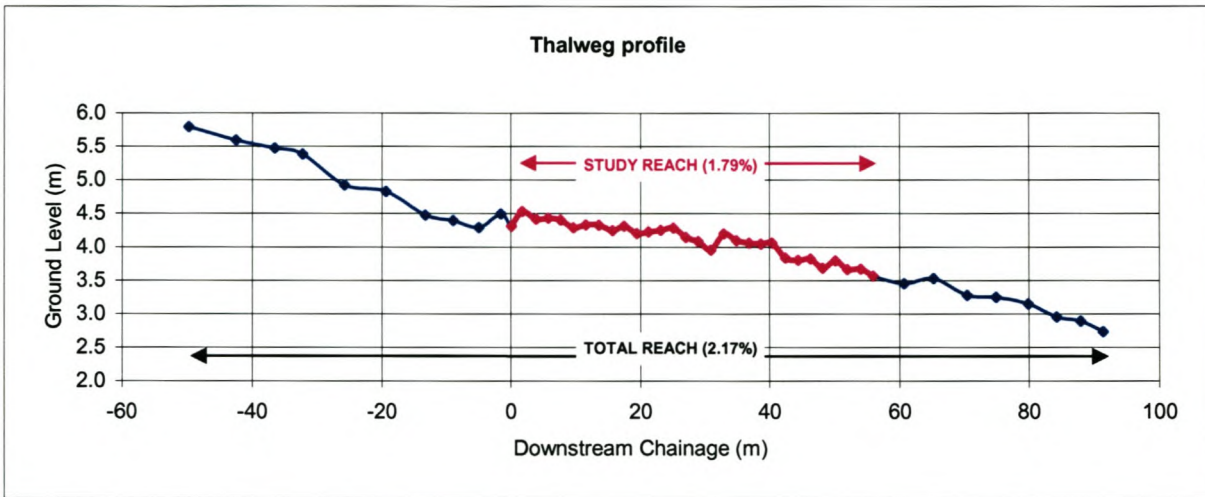
WOOLMAN M.G. (1955). *A method of sampling coarse river-bed material*, Trans. American Geophysical Union, Vol.35 No.6.

WILCOCK P. R. and SOUTHARD J.B. (1988). *Experimental study on incipient motion in mixed-sized sediment*, Water Resources Research, Vol. 24, No. 7, 1137-1151.

YANG C.T. (1973). *Incipient Motion and Sediment Transport*. Journal of Hydraulic Engineering. Vol. 99, no. 10, 1679-1704.

Appendix A: Details of Study Sites

Figure A1a: Molenaars Study Site: Thalweg and Sample Cross-sections



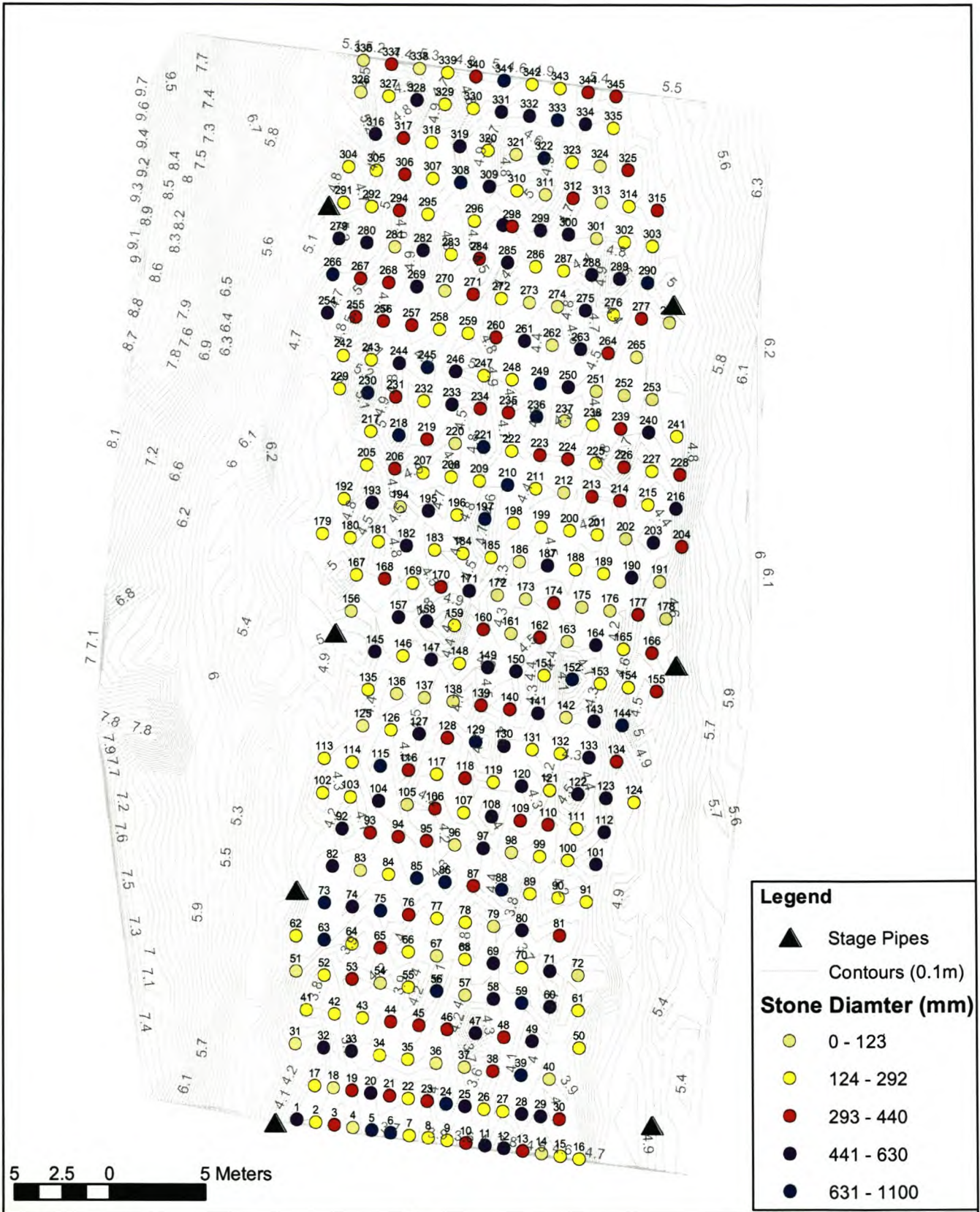


Figure A1b
Study Site Set Up
Molenaars River

WRC K5/1411
The Determination of Substrata
Maintenance Flows in Cobble
and Boulder Bed Rivers:
Ecological and Hydraulic
Considerations

Legend

- ▲ Stage Pipes
- Contours (0.1m)

Stone Diameter (mm)

- 0 - 123
- 124 - 292
- 293 - 440
- 441 - 630
- 631 - 1100



Figure A1c: Molenaars Study Site: Partical Size Distribution

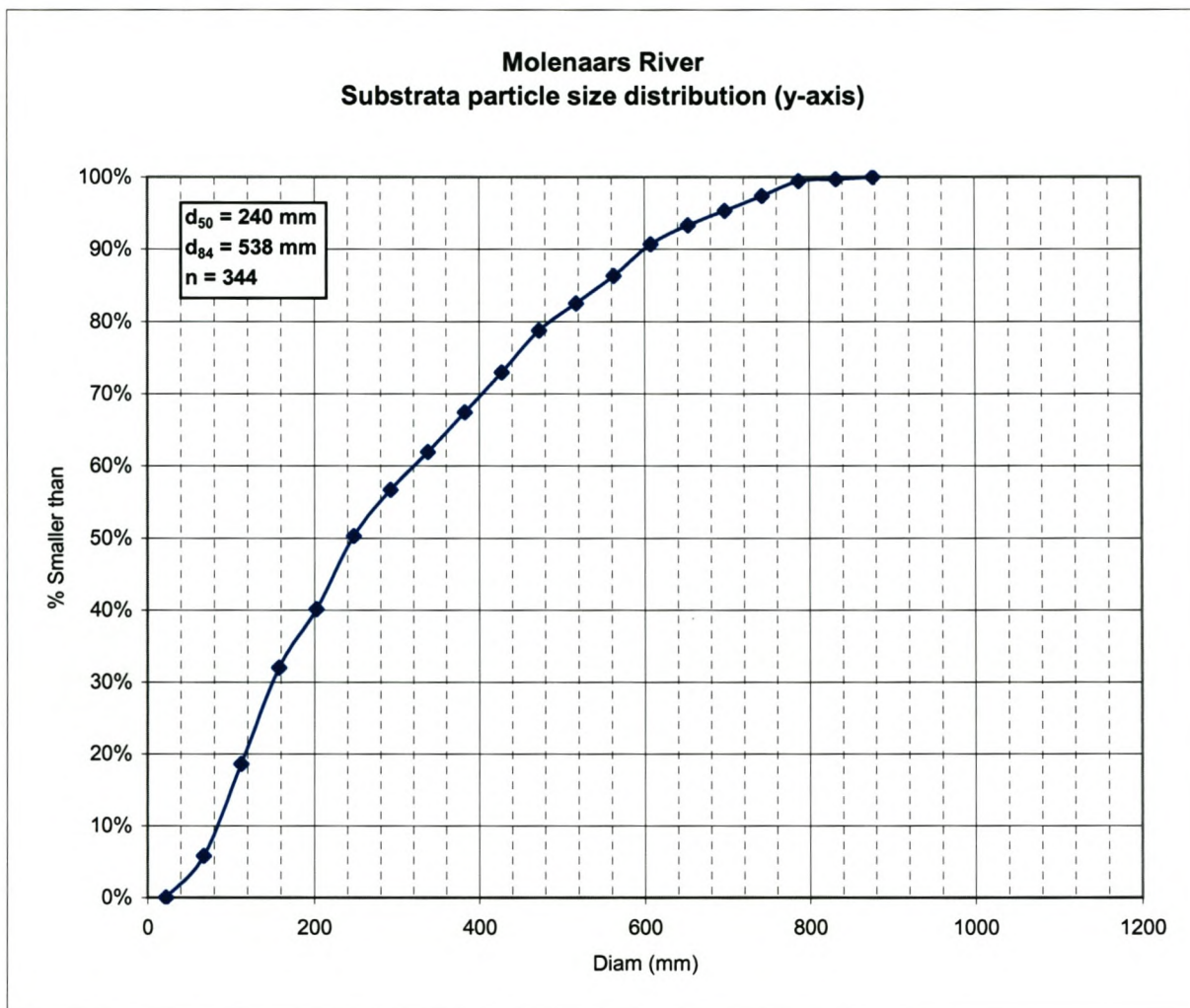
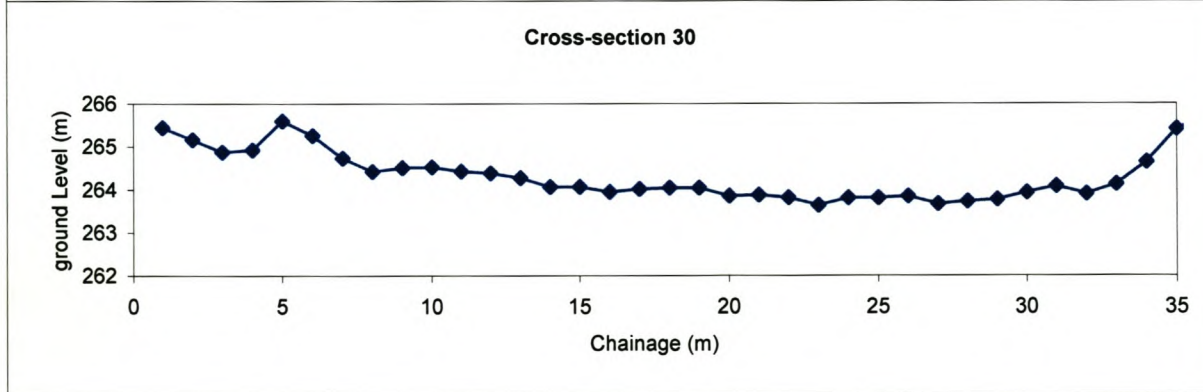
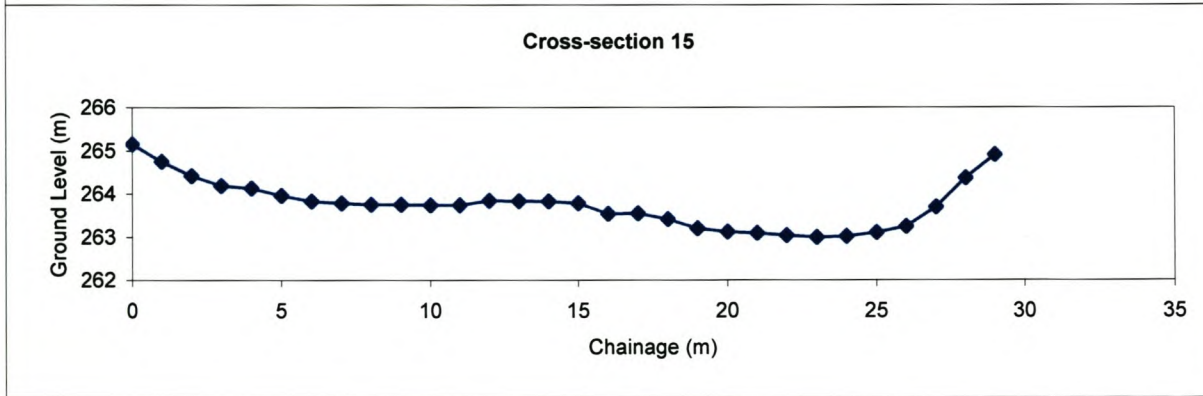
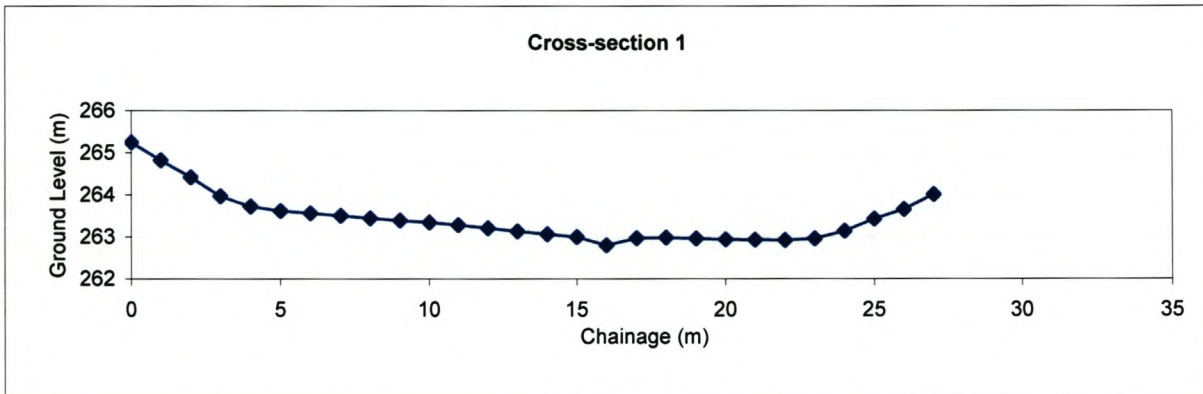
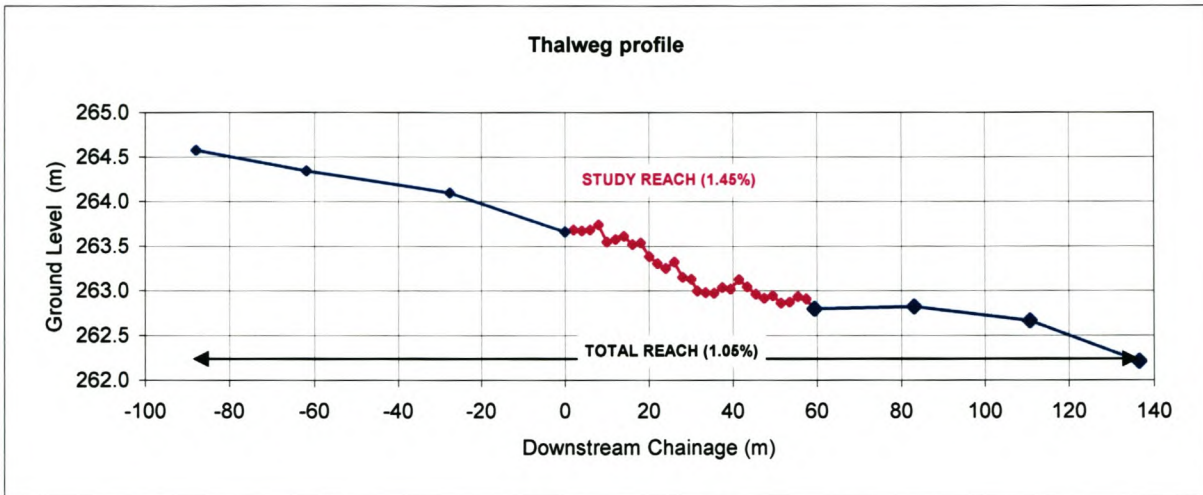


Figure A2a: Berg River Study Site: Thalweg and Sample Cross-sections



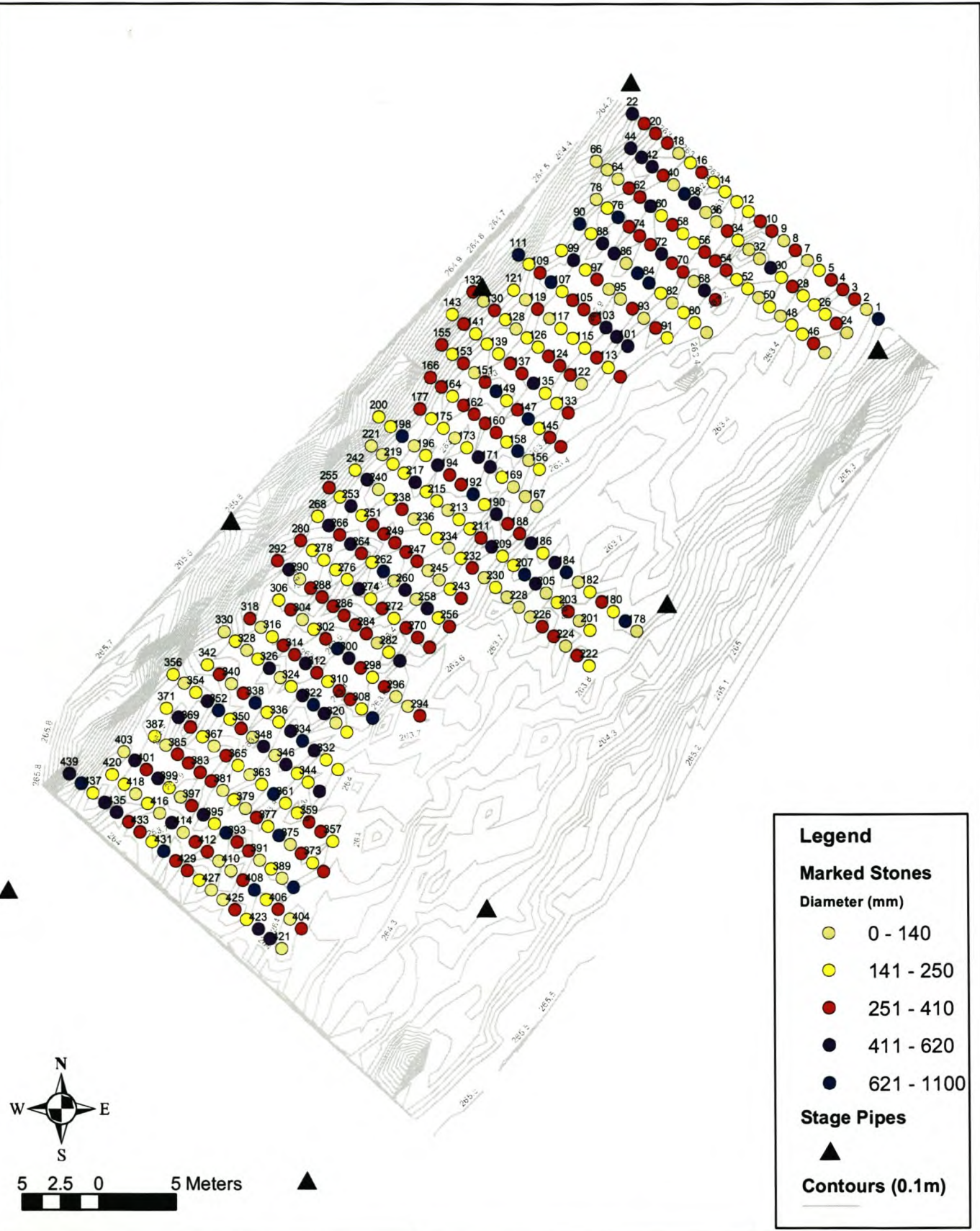
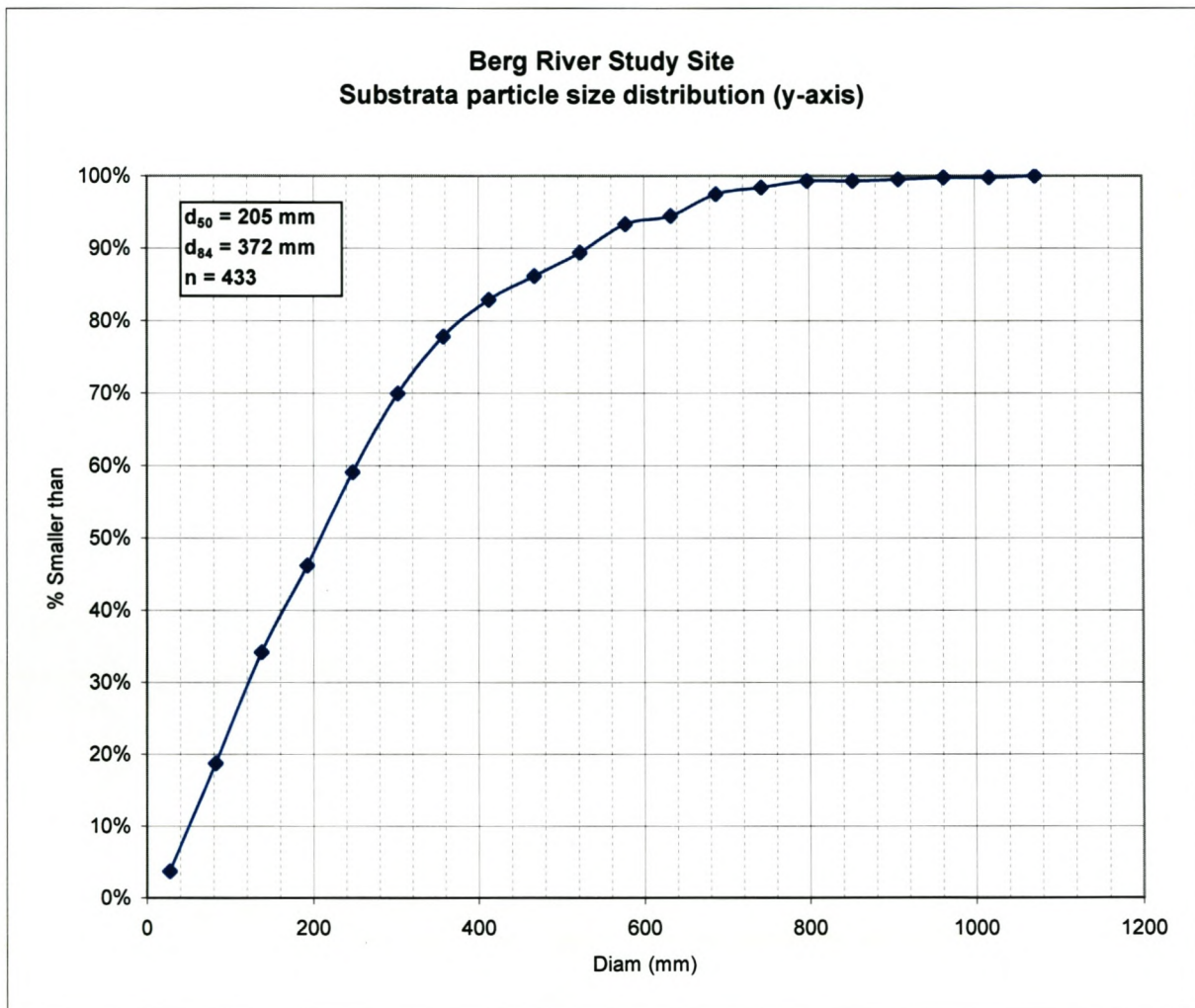


Figure A2b
Study Site Set Up
Berg River

WRC K5/1411
The Determination of Substrata
Maintenance Flows in Cobble
and Boulder Bed Rivers:
Ecological and Hydraulic
Considerations

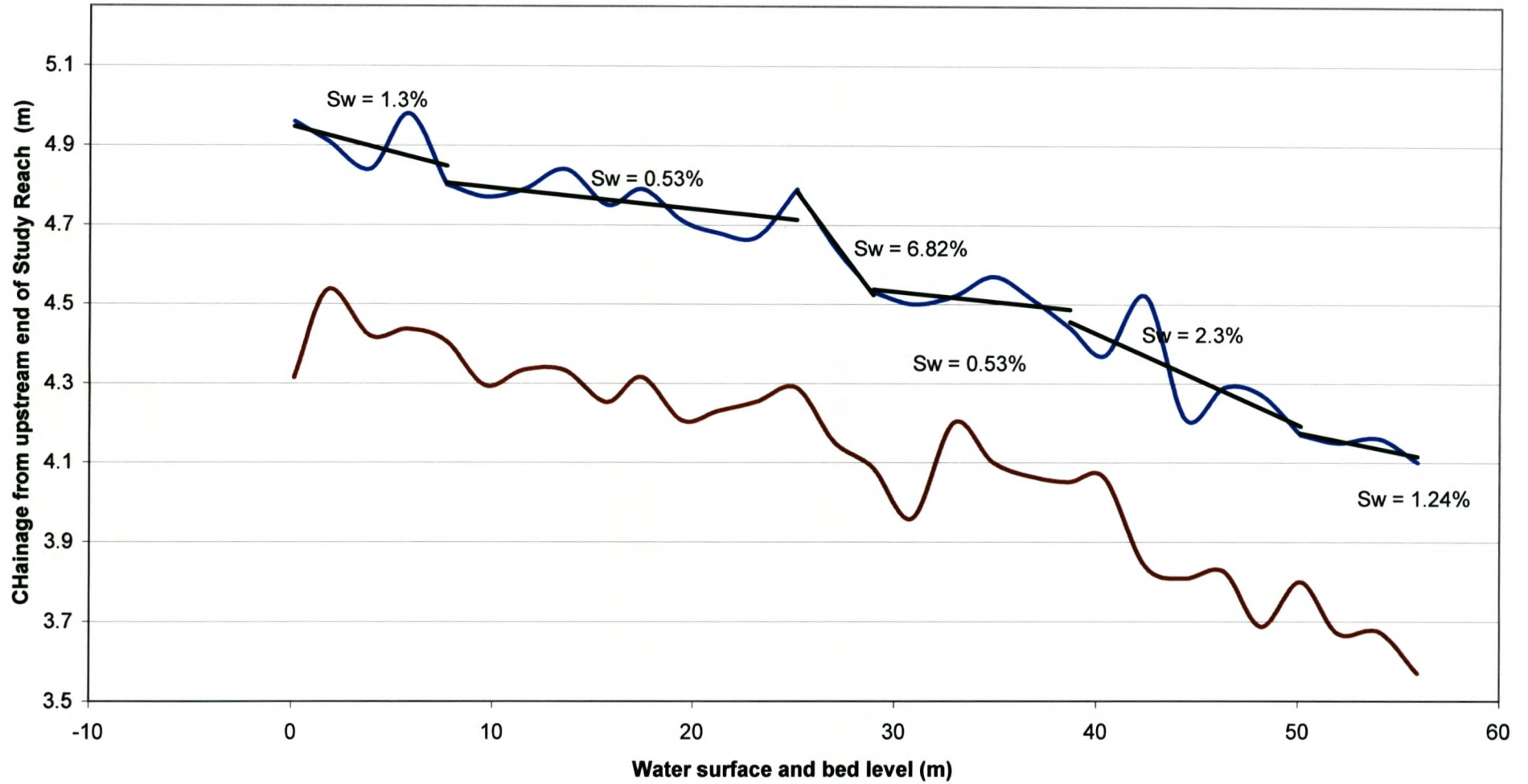


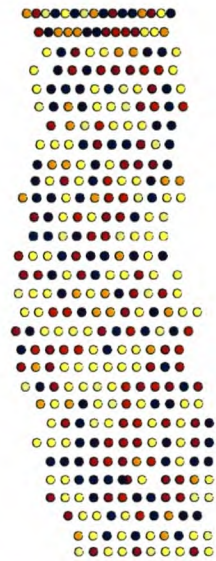
Figure A2c: Berg River Study Site: Partical Size Distribution



Appendix B: Base Flow Conditions

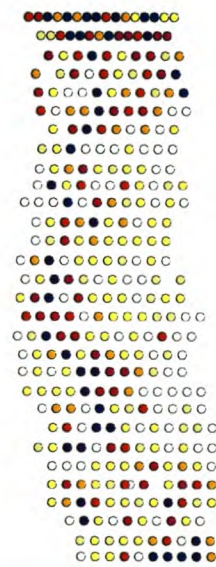
Figure B1a: Base Flow Water Surface Profiles Molenaars River Study Stie Initial Set up 2003
Low flow water surface profile





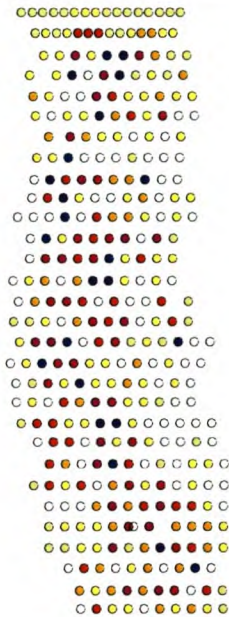
Diameter (mm) <http://scholar.sun.ac.za>

- 0 - 85
- 86 - 142
- 143 - 197
- 198 - 246
- 247 - 294
- 295 - 365
- 366 - 450
- 451 - 560
- 561 - 690
- 691 - 870



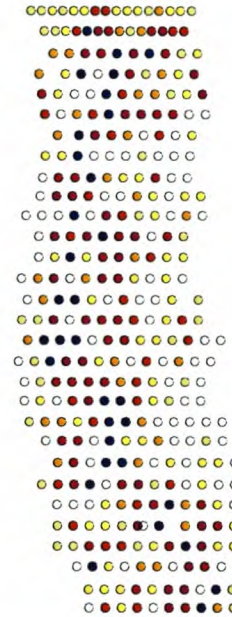
Depth (cm)

- 0 - 4
- 5 - 9
- 10 - 15
- 16 - 21
- 22 - 26
- 27 - 30
- 31 - 34
- 35 - 41
- 42 - 48
- 49 - 60



Velocity (m/s)

- 0.00 - 0.06
- 0.07 - 0.14
- 0.15 - 0.21
- 0.22 - 0.29
- 0.30 - 0.37
- 0.38 - 0.45
- 0.46 - 0.54
- 0.55 - 0.67
- 0.68 - 0.92
- 0.93 - 1.16



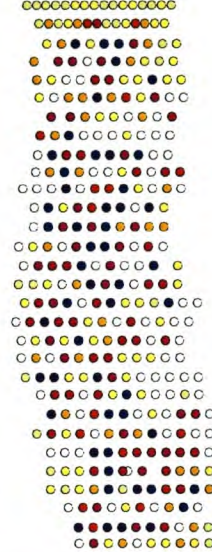
Depth x Vel (m2/s)

- 0.0000 - 0.0051
- 0.0052 - 0.0113
- 0.0114 - 0.0200
- 0.0201 - 0.0333
- 0.0334 - 0.0505
- 0.0506 - 0.0773
- 0.0774 - 0.1168
- 0.1169 - 0.1668
- 0.1669 - 0.2398
- 0.2399 - 0.5300

Figure B1b
Base Flow Conditions
Molenaars Study Site
2003

WRC K5/1411
 The Determination of Substrata Maintenance Flows
 in Cobble and Boulder Bed Rivers:
 Ecological and Hydraulic Considerations

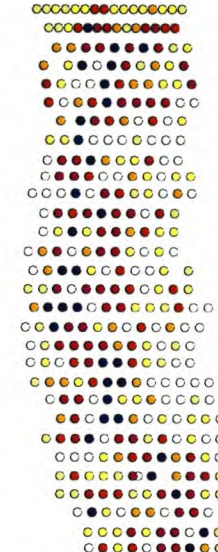




Froude No.

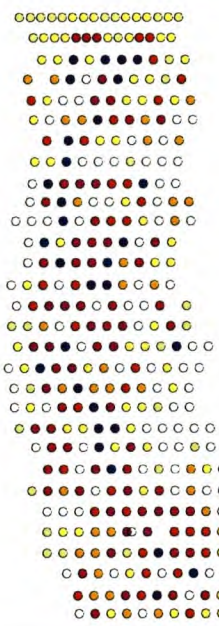
Stellenbosch University <http://scholar.sun.ac.za>

- 0.0000 - 0.0301
- 0.0302 - 0.0718
- 0.0719 - 0.1158
- 0.1159 - 0.1668
- 0.1669 - 0.2216
- 0.2217 - 0.2770
- 0.2771 - 0.3355
- 0.3356 - 0.4358
- 0.4359 - 0.7804
- 0.7805 - 1.4735



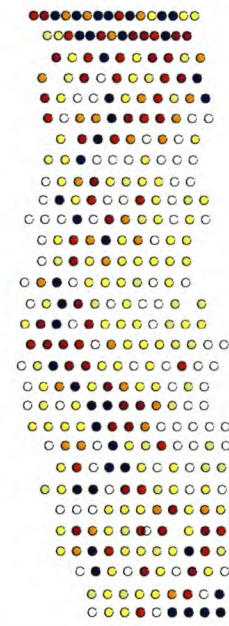
Keyhole No.

- 0 - 4323
- 4324 - 9947
- 9948 - 17500
- 17501 - 29193
- 29194 - 44289
- 44290 - 67807
- 67808 - 102421
- 102422 - 146316
- 146317 - 210316
- 210317 - 464912



Stream Power

- 0.0000 - 5.2307
- 5.2308 - 12.5293
- 12.5294 - 19.0981
- 19.0982 - 27.0050
- 27.0051 - 35.6417
- 35.6418 - 47.4412
- 47.4413 - 60.9376
- 60.9377 - 81.0149
- 81.0150 - 112.2774
- 112.2775 - 141.1070



Bed Shear Stress

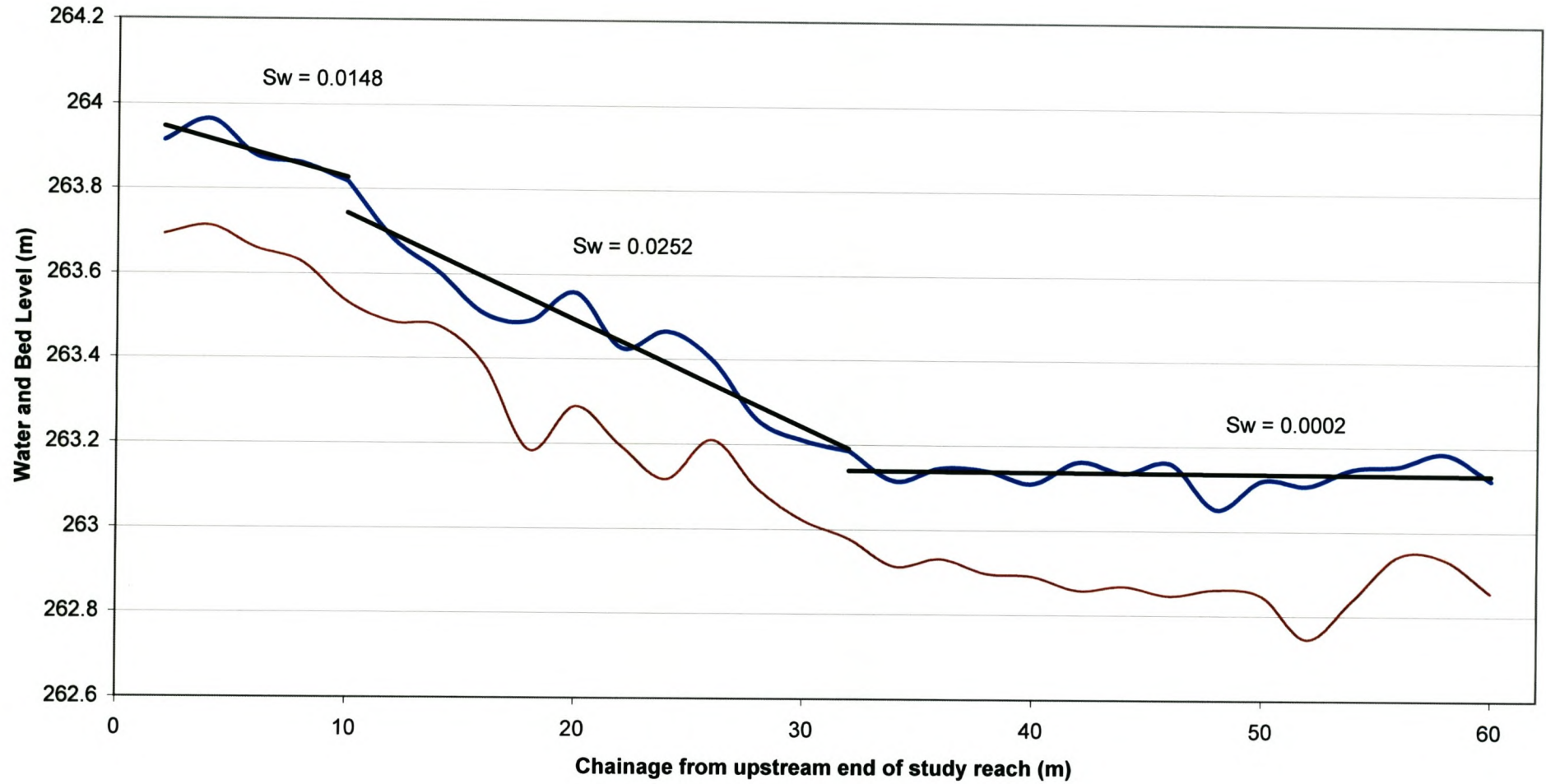
- 0.0000 - 0.4960
- 0.4961 - 1.1160
- 1.1161 - 1.8600
- 1.8601 - 2.6040
- 2.6041 - 3.2240
- 3.2241 - 3.7200
- 3.7201 - 4.2160
- 4.2161 - 5.0840
- 5.0841 - 5.9520
- 5.9521 - 7.4400

Figure B1c
Base Flow Conditions
Molenaars Study Site
2003

WRC K5/1411
 The Determination of Substrata Maintenance Flows
 in Cobble and Boulder Bed Rivers:
 Ecological and Hydraulic Considerations



**Figure B2a: Average Base Flow Water Level
Berg River Study Site
Initial Set Up**

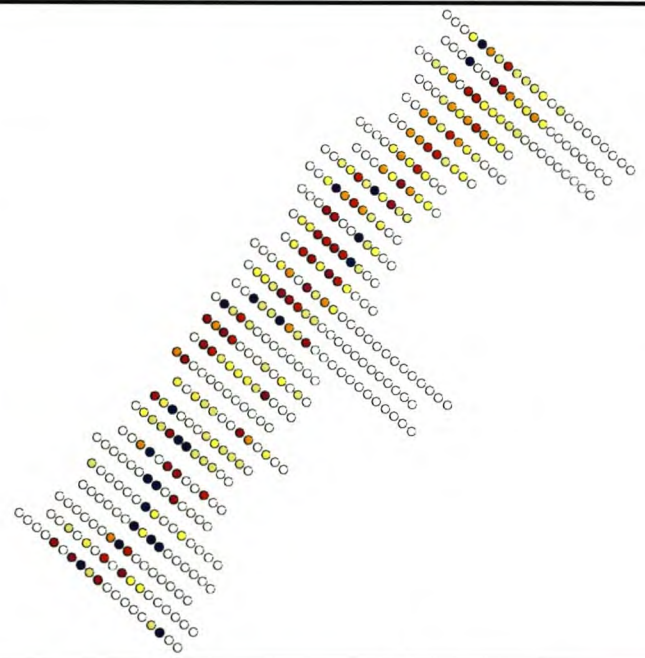




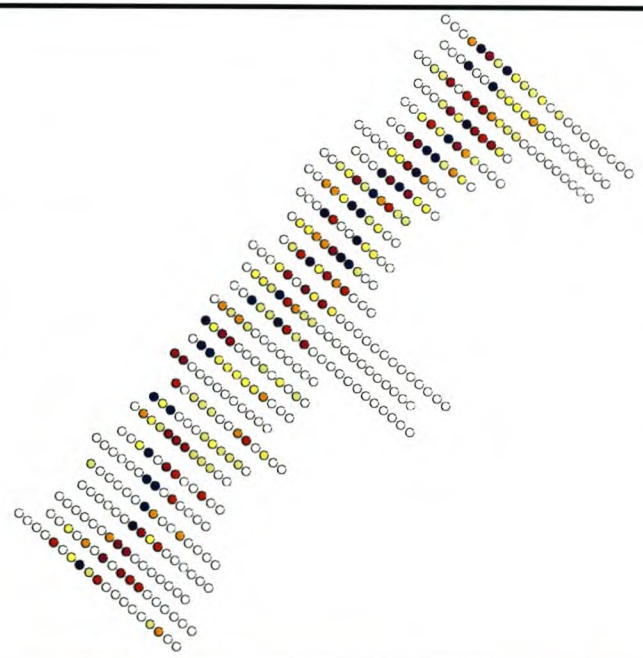
- Diameter (mm)**
- 0 - 75
 - 76 - 130
 - 131 - 190
 - 191 - 250
 - 251 - 315
 - 316 - 385
 - 386 - 485
 - 486 - 600
 - 601 - 780
 - 781 - 1100



- Depth (cm)**
- 0 - 3
 - 4 - 6
 - 7 - 9
 - 10 - 12
 - 13 - 16
 - 17 - 20
 - 21 - 25
 - 26 - 30
 - 31 - 36
 - 37 - 50



- Velocity (m/s)**
- 0.00 - 0.03
 - 0.04 - 0.08
 - 0.09 - 0.14
 - 0.15 - 0.19
 - 0.20 - 0.25
 - 0.26 - 0.33
 - 0.34 - 0.40
 - 0.41 - 0.50
 - 0.51 - 0.60
 - 0.61 - 0.78



- Depth x Vel (m²/s)**
- 0.000 - 0.002
 - 0.003 - 0.006
 - 0.007 - 0.012
 - 0.013 - 0.018
 - 0.019 - 0.026
 - 0.027 - 0.036
 - 0.037 - 0.050
 - 0.051 - 0.073
 - 0.074 - 0.101
 - 0.102 - 0.161

Figure B2b
Base Flow Conditions
Berg River Site
2004

WRC K5/1411
 The Determination of Substrata Maintenance Flows
 in Cobble and Boulder Bed Rivers:
 Ecological and Hydraulic Considerations



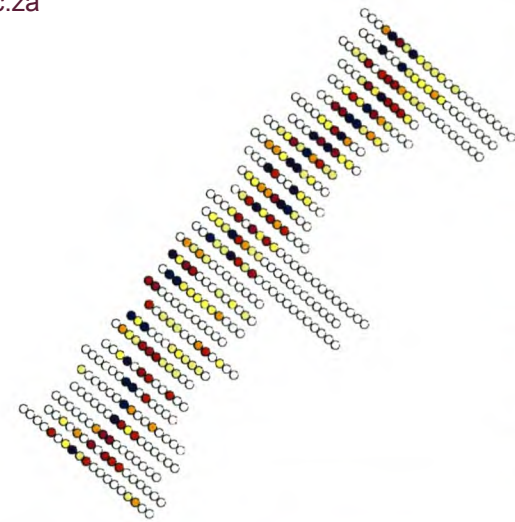
Froude No.

Stellenbosch University <http://scholar.sun.ac.za>



- 0.0000 - 0.0171
- 0.0172 - 0.0531
- 0.0532 - 0.0939
- 0.0940 - 0.1440
- 0.1441 - 0.1999
- 0.2000 - 0.2737
- 0.2738 - 0.3725
- 0.3726 - 0.5268
- 0.5269 - 0.7024
- 0.7025 - 1.2452

Reynolds No.



- 0 - 2105
- 2106 - 5614
- 5615 - 10526
- 10527 - 16140
- 16141 - 23158
- 23159 - 31579
- 31580 - 43860
- 43861 - 63860
- 63861 - 88421
- 88422 - 141228

Stream Power



- 0.00 - 0.21
- 0.22 - 0.68
- 0.69 - 2.47
- 2.48 - 7.40
- 7.41 - 12.34
- 12.35 - 24.67
- 24.68 - 52.43
- 52.44 - 81.42
- 81.43 - 115.96
- 115.97 - 192.45

Bed Shear



- 0.000 - 0.015
- 0.016 - 0.036
- 0.037 - 0.061
- 0.062 - 0.089
- 0.090 - 0.742
- 0.743 - 1.761
- 1.762 - 2.767
- 2.768 - 4.527
- 4.528 - 8.048
- 8.049 - 12.576

Figure B2c
Base Flow Conditions
Berg River Study Site
2004

WRC K5/1411
 The Determination of Substrata Maintenance Flows
 in Cobble and Boulder Bed Rivers:
 Ecological and Hydraulic Considerations



Appendix C: Field Notes from Flood Event Data Collection

Table with columns: Offset from 0, stone no., invert sample, Putty Magn Koki, description, hydraulic shelter, flow type, Stone Category, Stone x (mm), Stone y (mm), Stone z (mm), revs / 60 sec, depth (cm), Velocity (m/s) From rating tables, movement post flood of July 9-10, July, movement post flood of July 18-19, July, movement post flood of July 24-25, July, movement post flood of July 30-Aug 1, Aug, movement post flood of Aug 8-10, field visit 16 Aug, movement post flood of Aug 17-25 (to peaks), field visit 31 Aug. The table contains detailed field observations for each stone, including its location, size, shape, color, and the velocity of water flow over it during various flood events.

original set-up stone data - 9-14 June 2003

														none	7 moved	2 moved	10 moved	26 moved	115 moved
Offset from 0	stone no.	invert sample	Putty Magn t (Koki)	description	hydraulic shelter	flow type	Stone Categories	Stone x (mm)	Stone y (mm)	Stone z (mm)	rvs / 60 sec (mini)	depth (cm)	Velocity (m/s) From rating tables	movement post flood of July 9-10, field visit 13 July	movement post flood of July 18-19, field visit 24 July	movement post flood of July 24-25, field visit 27 July	movement post flood of July 30-Aug 1, field visit 3 + 6 Aug	movement post flood of Aug 8-10, field visit 16 Aug	movement post flood of Aug 17-25 (to peaks), field visit 31 Aug
21	215	236 (24 Jul 3 Aug)	full samp	M	flat orange squarish mc, narrowside facing up immed u/str of large flatish, whrey golden submerged b.	hs = d/str b	LC	250	155	121	119	39	0.601						
21	23	237	full samp	M	angular reddish sc, narrowside up but <-d toward d/str	hs = d/str lc	LC	162	138	54	19	39	0.103						
21	24.5	238	full samp	PM	dark brown oval sc, flat face upward, d/str of large long B with orange X	u/str B = hs	SC	149	105	71	15	15	0.083						
21	26	239	no	P	orange oval lc, pinned by adjacent white emergent B with lichen	pinned on side + d/str B = hs	SB		414		69	9	0.350						
21	27.5	240	inv = sa net	P	flat white submerged with crevice-lines, another flat SB on top of part of the stone, rem = visible, long emerg B on LHS	pinned by B on top = hs	MB		542		64	7	0.325						
21	29	241	full samp	PM	light pink angular flat LG/sc just u/str of large white B	hs = white B in bank	SC	83	69	46	1	7	0.013						
2	11	242	full samp	M	white with deep red teeth/triangle shapes, angular, just d/str of large irregular red raggedy B in b/w	hs = u/str red B	LC	327	172	102	0	dry	0.000						
2	12.5	243	full samp	M	pretty brown oval flat face s-mc, grey fine lines over long - b/w	hs = u/str +d/str B, but not immed. Adjacent	LC	164	139	84	0	2	0.000						
2	14	244	no	K	irreg-oval shaped brown B in lichen B	hs = u/str series of lc -sb in line	MB		560		0	dry	0.000						
2	15.5	246	no	K	large creamy oval B, flatish side facing u/str	no immed hs	MB		644		0	dry	0.000						
2	17	248	full samp	M	square cream + orange mc on gr bed set between 2 submerged B's	in hollow between larger elements = hs	LC	202	196	109	16	26	0.086						
2	18.5	247	full samp	M	white irregular planar surfaces facing flow which comes sideways between u/str + d/str B's	hs between 2 emergent u & d/str B's	SB	311	257	145	86	2	0.435						
2	20	248	inv = upper 1/2 sa stone	P	large white log like sb/lc with brown splotches + small crevices	2 d/str submerged b's =hs	SB		7250		25	15	0.133						
2	21.5	249	full samp	M	brown round cobble	in hollow between 5 B's =hs	LC	238	172	140	105	43	0.531						
2	23	260	no	K	white-orange round emergent B	d/str B sort of hs but not adjacent	MB		524		0	dry	0.000						
2	24.5	261	full samp	M	brown rectangle-ish flat faced lc arround flatish bed elements	no hs	LC	295	244	178	62	17	0.315						
2	26	262	full samp	M	whitish red flat square sc, angled upward at d/str end against large grey embedded B	no hs	LC	161	178	82	65	16	0.330						
2	27.5	263	full samp	M	whitish + bits of fawn mc, flat face up, a bit under emergent sc that sits on it	hs = flat u/str B-not much	LC	247	207	156	0	<1 cm	0.000						
3	10	264	no	K	brown, flatish tri angularish b.	hs = u/str boulder clump	SB		460		0	dry	0.000						
3	11.5	266	inv = 1/2 tot stone area - top and 1/2 sides	P	squarish golden sb., with round top, crags+crevices	d/str emergent b. = hs	SB	439	369	210	27	4	0.143						
3	13	266	full samp	M	red, rectangularish sc, 1/2 under lichen b. on left	d/str lc = hs	SC	151	107	103	39	4	0.202						
3	14.5	267	no	K	oval white sb emergent, d/str + to right of red blockish LB	u/str LB	SB		313		0	dry	0.000						
3	16	268	full samp	M	greenish brown rectangular mc, where water = slow in "hollow" from u/str+d/str larger elements	in hollow, but no immed larger overlaps etc.	LC	233	148	127	6	14	0.038						
3	17.5	269	no	K	rectangular white lc/sb with scratchy + irregular top - lying perpendicular to current	u+d/str B + lc clumps	SB		251		0	dry	0.000						
3	19	260	no	P	pear-shaped lc, pointy side facing u/str	u/str B = a bit further d/str = lichen B = hs	SB		346		71	6	0.361						
3	20.5	261	full samp	M	grey mc in bubbly bsw d/str of 2 adjacent B's	hs = u/str B's	LC	210	190	68	232	41	1.160						
3	22	262	full samp	PM	small (actually whitish) grey sc just next to pear shaped golden B, flatish submerged	lc u/str on RHS = partial hs no hs	CG	106	60	60	93	46	0.471						
3	23.5	263	no	K	large emergent darkish brown B, whitey-brown on emergent bit	no hs	MB		567		0	dry	0.000						
3	25	264	no	P	golden pear shaped, point d/str, deeply submerged overlapping mc at top end, d/str of lichen B-just submerged	lichen B upstream = hs	SB		315		50	25	0.257						
3	26.5	266	full samp	M	diamond orange, pinned by lichen B, with scribble - irregular surface, white B on other side	lichen B = hs	SC	252	115	115	60	8	0.305						
3	28	266	no	K	large irregular red boulder with lichen spots	smaller B u/str + d.str =hs(part)	MB		640		0	dry	0.000						
3	11.5	267	no	K	flat oval sb, with narrow side facing up at angle	pinned by stacked lc on u/str and + big red sandstone B above this	SB		400		0	dry	0.000						
3	13	268	full samp	PM	grey rectangular box like with sharp side facing up, inserted betw jin of 2 other stones	in hollow formed by u/str +d/str white emergent b's	SC	119	96	75	32	9	0.167						
3	14.5	269	no	K	golden sB with ring of lichen above water level	dry, rsf around	SB		465		0	dry	0.000						
3	16	270	full samp	PM	irregular, white +red blotchy, set with narrow side facing up 1/2 under white lc, pointy side sticking up	hs = u/str +d/str white emergent b.'s	SC	166	115	66	77	12	0.390						
3	17.5	271	full samp	M	oval, flatish brown lc	u/str, d/str sds = hs	SB	408	308	164	14	3	0.078						
3	19	272	full samp	M	flat greenish white round 2 "eyebrows" d/str ridges, smile ridges, big forehead	no hs	SB	369	333	125	82	22	0.415						
3	20.5	273	full samp	PM	large round blotchy brown B. ball shaped, 2 white eyes u/str and one deep notch = funny mouth	hs = sortof u/str lc (not bigger, but higher of brb)	SB	381	357	177	45	28	0.232						
3	22	274	no		orange white(white where dry) emergent b. spots of lichen around waters edge round top w crevice	no hs	MB		552		0	dry	0.000						
3	23.5	276	inv = sa net	PM	large, flat, orange b. pinned down by emergent, purple-ish brownish	pinned down by purple boulder	MB		640		73	36	0.370						
3	25	276	full samp	M	orange angular sc just right of white +fawn sB in line with 3 white emergent b's just d/str	no hs (d/str b's too far away)	SC	166	101	66	39	37	0.202						
3	26.5	277	full samp	M	squarish cream+orange sc, just under pointy edge of pink lc, with emergent tip	not really (pink lc=sort of hs d/str mc/slightly overlapping sc)	LC	180	147	90	58	12	0.268						
3	28	278	full samp	PM	tiny grey sc b/w of small bed elements	no hs	SC	116	109	62	0	1	0.000						
3	10	279	no	K	large rectangular sandstone b. one of a stack	dry, in b/w, upwell from under, prob frf under B	SB		500		0	dry	0.000						
3	11.5	280	no	P	orange, bullet-shaped b., with flat surface, submerged	d/str of a ridge of large s/stone Bs	MB		624		41	6	0.212						
3	13	281	full samp	M	round mc, red on 1 side orange on the other, on top of 2 sc. in V made by orange b.'s, in hole	2 u/str B + d/str emergent B ridge	LC	155	142	91	65	20	0.330						

Initial set-up stone data - 9-14 June 2003										none	7 moved	2 moved	10 moved	26 moved	115 moved				
Offset from 0	stone no.	invert sample	Putty Magn Koki	description	hydraulic shelter	flow type	Stone Catalogue	Stone x (mm)	Stone y (mm)	Stone z (mm)	revs / 60 sec	depth (cm)	Velocity (m/s) From rating tables	movement post flood of July 9-10, field visit 13 July	movement post flood of July 18-19, field visit 24 July	movement post flood of July 24-25, field visit 27 July	movement post flood of July 30-Aug 1, field visit 3 + 6 Aug	movement post flood of Aug 8-10, field visit 16 Aug	movement post flood of Aug 17-25 (to peaks), field visit 31 Aug
14.5	282	inv = sa net	P	submerged flat orange oval B, pinned down by huge s/stone ridged B	d/str huge B ridge	rsf going into bsw	MB		566		64	10	0.325						
16	283	full samp	M	irregular red stone -mc - narrow side upwards, lying next to smooth orange rectangular lc/sb	not much d/str sb++hs	fast rsf	SB	315	275	74	90	30	0.456						OUT
17.5	284	no	P	white LC pinned down by emergent s/stone B, red white irregular	hs = sandstone pinning B	deep fast frf	LC		246		70	20	0.355						
19	286	no	P	another flat orange rectangular B, submerged	hs u/str = lichen B	frf+abt	SB		426		49	14	0.252						
20.5	286	full samp	PM	round pinkish orange mc-ic, between 2 white lc, but d/str end open	u/str ic =hs	deep frf	SB	336	260	152	96	6	0.501						
22	287	no	P	brown rounded - rectangle, lying perpendicular to flow	no real hs	rsf	SB		358		50	5	0.257						
23.5	288	no	K	large but submerged white B, d/str of even larger white emergent lichen B	u/str lichen B = hs	rsf	SB		462		0	< 1cm	0.000						
25	289	no	K	creamy lichen B		dry, rsf around	MB		548		0	dry	0.000						
26.5	290	no	K	creamy lichen B		dry, rf around; in b/w	MB		658		0	dry	0.000						
10	291	full samp	PM	red irregular sc set among mc just beyond isolepis bank	no real hs	bpf	SC	130	106	79	16	18	0.088						OUT
11.5	292	full samp	M	white, semi diamond irregular surface, on sand between embedded B's	hs=lc lichen B d/str	bpf	LC	268	214	128	44	24	0.227						OUT
13	294	no	PM	deep embedded orange lc, pinned by emergent white B with one angular side	B pinning =hs	?	SB		340		50	32	0.257						
14.5	296	inv = 1/2 tot stone area	PM	whitish fawn lc on gravel with 3 emergent B's upstream	u/str B's =hs	rsf	SB	414	399	187	51	12	0.263						
17	296	full samp	M	orange, slightly triang mc, long side at lower edge facing up, just to RHS of emergent orange B	hs = sort of d/str lc but only a bit	sbt out of deep riffle	LC	216	170	170	93	28	0.471						OUT
18.5	297	no	K	emergent orange B with pointed top	hs=-: if packed against d/str sb=lichen B	dry, chute around	SB		444		0	dry	0.000						
19	298	no	P	grey flat circular, with 2 white spots downstream tip(in addit to putty)	some what embedded between lc++hs	frf	SB		458		79	22	0.400						
20.5	299	inv = sa net	P	large fawn B with scratchy tip just submerged	hs=part-other emergent u/str B's	rsf to almost frf	MB		762		43	2	0.222						
22	300	no	P	large orange B, embedded	hs = emergent u/d/str white B(bigger d/str)	shall rsf	MB		605		39	6	0.202						
23.5	301	inv = 1/2 tot stone area - samp discarded	P	embedded ???7?elongated dark brown sc, just next to 2 greenish submerged SB's	hs = u/str green B	bpf	MB	1092	776	398	21	16	0.113						
25	302	full samp	M	whitish sc with red bluish on RHS + crack out of LHS; set below sc + mc	no hs	bpf	LC	161	148	109	25	29	0.133						
26.5	303	full samp	M	red + grey mc just d/str of submerged lc/sb	hs=u/str	rf, b/w formed by Bs at Tr 27	LC	229	160	120	0	12	0.000						
10	304	full samp	P	lg-angular fawn, in V between 2 B's, with mc just d/str -suspect it will go	u/str + d/str mc's plus B's on either side =part hs	rsf	SC	97	82	55	28	12	0.148						OUT
11.5	306	full samp	P	oval brown sc in almost middle of 2 lichen B's, one with orange X		shallow slow rsf	SC	112	81	85	54	3	0.278						OUT
13	306	full samp	P	oblong with flatter side d/str perpendicular to current, partially pinned by dark red scraggly B, emergent with tiny salix shoot	u/str white/yellow sb on hs + emergent B =hs; also d/str hs = subimg Golden B	fast rsf	SB	529	309	164	73	24	0.370						
14.5	307	no		deeply submerged greenish sb, oval with patch of red +2 white spots pinned both sides d/str by lc+sb	pinned by 2B + 1 lc (d/str) = hs	fast rsf to nearly sbt	SB		430		74	36	0.375						
16	308	inv = sa net		large oval flattish top, subimg golden B w fissures	pinned slightly on edge by sb (not bigger)	usw to bsw over B	MB		762		121	10	0.611						
17.5	309	inv = sa net		reddish gold B with tip just submerged under sheet flow to bsw	series of u/str B's = hs	frf	SB		482		47	4	0.242						
19	310	full samp	M	semi triangular golden brown mc, set among others, just below flat/round B causing riffle, stone long side // to B, at 7 O clock d/str =hs of lichen B	u/str round flat B with ++simulidae	frf	SB	297	255	185	40	6	0.021						
20.5	311	inv = 2/3 tot stone area		gold lc with ++ black lichen, altho submerged (flow at angle to channel)	wedged b/w d/str emergent + 2 on sides	deep frf	SB	462	435	233	94	8	0.476						?OUT OR LOST LABEL
22	312	no		submerged greenish orange round flattish top, next to larger oblong B which is just emergent tip	embedded = hs	rsf	MB		536		36	24	0.187						
23.5	313	full samp	M	brown round flattish mc, in hollowish part of channel = deep run	no hs	rsf	LC	198	157	71	33	40	0.172						OUT
25	314	full samp	PM	rectangular, flattish sides sc set with a whole bunch just below large lc + an embedded ic to hs	u/str lc but no real hs at top flow	rf	SC	134	103	64	0	19	0.000						OUT
26.5	316	inv = sa net	P	embedded oval very flat sb, in b/w water jaggedy lichen-topped (grey) red sand stone rock	embedded in clump of B's forming b/w	nf	SB		443		5	5	0.033						
28	316	no	K	oval orange sb with flat face, d/str of emergent brown B broken water over face of #317	pinned by u/str sand rock = hs	dry, rsf around	SB		472		0	dry	0.000						
28	317	inv = sa net	P	oval white-green mc/lc sitting pretty proud adjacent to sb's, on sc bed	u/str emergent B = HS	frf	SB		491		154	10	0.773						
28	318	full samp	M	white-fawn emergent B with few lichen spots on edge of the mid chann B clump	NO HS	rsf out of frf	LC	287	239	214	51	33	0.263						OUT
28	319	no	K	white-fawn emergent B with few lichen spots on edge of the mid chann B clump	nothing bigger immed, but in line of stacked lc+B	dry, swirling rsf around	MB		670		0	dry	0.000						
28	320	inv = sa top + 1/2 sides	P	small white flattish sc u/str of emergent fawn-orange B in same clump, #320 is deep, in hollow formed by surround B's	(++ hs = surround B's)	frf	SB	306	252	145	46	14	0.237						
28	321	full samp	M	small orange oval sc flat sides, in hole formed by surrounding lc+B's	(++ hs = surround lc+B's)	rsf	LC	148	138	67	17	29	0.083						OUT
28	322	no	K	large white -brown B emergent with orange X	nothing larger ,but clump u/d/str to RHS	dry, rsf around	MB		610		0	dry	0.000						
28	323	full samp	M	white grey oval sc/mc just d/str of emergent brownish oblong sb - creating riffle area	B u/str = hs	frf	LC	198	154	114	43	5	0.222						OUT
28	324	full samp	M	greyish triangular immed. U/str of lichen B, just to left of the apex of the lichen B	d/str lichen B = hs	rsf out of riffle area	SC	167	101	96	67	40	0.340						OUT
28	326	no	K	oblong, rounded top, embedded white-gold B, tip just emerg., with "eye"	embedded + d/str B(not immed)=hs	dry, rsf around	SB		410		0	dry	0.000						
29	326	full samp	P	very small piece of gravel on sand in b/w formed by u/str sandstone rock (just u/str of TR30)	hs=lc + embedded rock/surround, but small stone	nf	SC	85	76	69	0	20	0.000						OUT

original set-up stone data - 9-14 June 2003

Offset from 0	stone no.	invert sample	Putty Magn t Koki	description	hydraulic shelter	flow type	Stone Category	Stone x (mm)	Stone y (mm)	Stone z (mm)	revs / 60 sec (min)	depth (cm)	Velocity (m/s) From rating tables	none	7 moved	2 moved	10 moved	26 moved	115 moved	
														movement post flood of July 9-10; field visit 13 July	movement post flood of July 18-19; field visit 24 July	movement post flood of July 24-25; field visit 27 July	movement post flood of July 30-Aug 1; field visit 3 + 6 Aug	movement post flood of Aug 8-10; field visit 16 Aug	movement post flood of Aug 17 25 (to peaks); field visit 31 Aug	
11.5	327	full samp	M	dark brown oval wedge- z-axis = flat band facing d/str. Hole in centre of upper surface, with pebble-looks like eye	stone = in hole > d/str row of B's = hs	bpf	LC	337	171	230	82	40	0.315							
13	328	no	K	sandstone ragged oblong red rock lying perpendicular to flow, lichen +moss	d/str golden B d/str not really hs	deep rsf u/str - frf	MB		625		0	dry	0.000							
14.5	329	full samp	MP	greenish white lc just u/str of chute formed by #328+ lichen B on either side	d/str submerged B = hs	deep rsf (nearly sb) going to chute	LC	322	227	186	76	25	0.385							
16	330	full samp	M	angular red brown mc. long axis perpendicular to direction of flow = chute formed by upstream B + lichen B the LHS of #330	just below point of meeting of B's; B = hs at high flow	chute	LC	298	141	133	105	20	0.531							OUT
17.5	331	inv = sa net	P	flat round orange B. submerged + embedded, d/str of clump of emergent B's	u/str B clump = hs	rsf/frf	MB		615		46	6	0.237							
19	332	full samp	M	oval, flat mc, narrow side facing upwards, d/str of oblong brown B, tip just emerging	u.stream B = hs	rsf just out of frf	LC	247	178	128	92	14	0.466				TS			OUT
20.5	333	no	P	large golden submerged B, well set into river bed	hs = emdedded + emergent B's u/str	?rsf	MB		730		42	4	0.217							
22	334	full samp	M	whitish grey sc just to left of brown B (emergent) - backing up water to form chutes	d/str row B's lc's = hs	rsf u/str going into chutes around	LC	184	129	144	33	10	0.172				TS	TS		OUT
23.5	336	inv = 1/2 lot stone area	P	pinkish, white splotches mc, flat face tilted up at back, small spot of lichen on d/str end	+ - hs = slight overlapping stone of same size	shallow frf	LC	275	235	130	53	4	0.273							
10	336	full samp	P	flat white round sc in b/w formed by s/stone + lichen SB's	hs = u/str B's	rf, in b/w	SC	118	107	53	0	16	0.000				TS			OUT
11.5	337	no	P	deep - lying flat, square-ish sb, crack line, immovable	overlapped by u/str B = hs	bpf in b/w	SB		415		14	38	0.078							
13	338	full samp	M	blotchy red+white round mc mostly exposed a little d/str of flattish oval deep, gold B	no real hs	deep run rsf	LC	170	156	133	54	51	0.278							OUT
14.5	339	full samp	M	angular triangularish mc, gold/green, set among other mc	u/str+d/str hs = sB+B respect	deep run rsf	LC	247	186	164	30	44	0.157							OUT
16	340	full samp	P	oval brown sc, triangle wedge broke out of stone facing d/str. Below golden B	check stone details!!!!	slow run bpf	SC	195	70	86	42	52	0.217							
17.5	341	no	K	oval light brown, dull sB, facing d/str but propped against d/str stacked B's		dry; bpf around	SB		410		0	dry	0.000							
19	342	full samp	P	narrow, oval sc, whitish brown, narrow side up, wedged between B u/str +lc d/str		bpf	SC	128	119	58	40	22	0.207				TS			OUT
20.5	343	full samp	P	flat white irregular sc just left of embedded white B with tip out of water - lichen		rsf	LC	159	131	69	23	14	0.123							
22	344	no	P	golden brown with whitish patches flat top sb, overlain by white lc + sc		frf to rsf	SB		426		62	11	0.315							
23.5	346	full samp	M	white sc/mc set between 2 white sB's, rectangular/round, angled surface up long axis perpendicular to channel /flow		trickle thro B + cobble	LC		??129		0	dry	0.000							

MOLENAARS RIVER STUDY SITE : FIELD OBSERVATIONS DATABASE 2004

Second season set-up stone data - May 2004 green shading indicates stones that were lost in 2003 and replaced during setup 2004

red = corrected measurements for 2003 stones

2004 FLOODS blue = moved; pink = OUT;

green shading = stones lost in 2003, replaced at setup in 2004

old stone size incl, followed by NEW stone size where replaced

Table with columns: stone no., invert sample, Putty (P) Paint (PT), description, hydraulic shelter, Stone Catego, Stone z (mm), Stone y (mm), Stone x (mm), revs / 60 sec, Velocity (m/s), FLOOD 1-10, FLOOD 2-25 Jun, FLOOD 3-1 JULY SEARCH, FLOOD 4-16 JULY SEARCH, FLOOD 5-8 August Search, stone no., potential for invert sample, Putty (P) Paint (PT), Description: original (setup) description, followed by NEW description where stones have been lost, Stone z (mm), Stone y (mm), Stone x (mm).

Table with columns: Stone no., invert sample, Putty (P) Paint (PT), description, hydraulic shelter, Stone Category, Stone x (mm), Stone y (mm), Stone z (mm), rvs / 60 sec (bucket), Velocity (m/s), FLOOD 1-10 Jan, BIG FLOOD 2-25 Jun, FLOOD 3-7 JULY SEARCH, FLOOD 4-18 JULY SEARCH, FLOOD 5-8 August Search, stone no., potential for invert sample, Putty (P) Paint (PT), Description: original (setup) description, followed by NEW: description where stones have been lost, Stone x (mm), Stone y (mm), Stone z (mm). Rows 1-139.

Second set-up stone data - May 2004 green shading indicates stones that were lost in 2003 and replaced during setup 2004

Table with columns: stone no., invert sample, Pully (P) Paint (PT), description, hydraulic shelter, Stone Category, Stone X (mm), Stone Y (mm), Stone Z (mm), revs / 60 sec (bucket), depth (cm), Velocity (m/s) From rating tables, FLOOD 1-10 Jun, FLOOD 2-15 Jun, FLOOD 3-1 JULY SEARCH, FLOOD 4-16 JULY SEARCH, FLOOD 5-8 August Search, stone no., potential for invert sample, Pully (P) Paint (PT), description, Stone X (mm), Stone Y (mm), Stone Z (mm). Includes detailed field notes and observations for various stones.

MOLENAARS RIVER STUDY SITE : FIELD OBSERVATIONS DATABASE 2004

Second season set-up stone data - May 2004 green shading indicates stones that were lost in 2003 and replaced during setup 2004

2004 FLOODS blue = moved; pink = OUT;

green shading = stones lost in 2003; replaced at setup in 2004

OLD stone size incl. followed by NEW stone size where replaced

stone no.	invert sample	invert	Paint (PT)	description	hydraulic shelter	Stone Catalogue	Stone X (mm)	Stone Y (mm)	Stone Z (mm)	revs / 60 sec (bucket)	depth (cm)	Velocity (m/s) from rising tables	2004 FLOODS				potential for invert sample	Paint (PT)	Description: original (setup) description, followed by NEW: description where stones have been lost	Stone X (mm)	Stone Y (mm)	Stone Z (mm)				
													FLOOD 1-10 Jun	FLOOD 2-25 Jun	FLOOD 3-1 JULY SEARCH	FLOOD 4-16 JULY SEARCH							FLOOD 5-8 August Search			
TR18	195	no	P Pt	immov lichen B hidden in B field	ha = boulder field	SB	612									196	no	P Pt	orange-red semi-sq. just to it of B field, ridges on upper flat surface							
TR18	196	X	P Pt	orange-red semi-sq. just to it of B field, ridges on upper flat surface	lg lichen B topped over last winter now + ha. plus white lichen B	SB	410	273	180							197	no	P Pt	large, protruding lichen B							
TR18	197	no	P Pt	large, protruding lichen B	no ha	SB	772									198	X	Pt	oblong, purple w green + white veins, v strong. dist. top points up but submerged on top of orange LC							
TR18	198	X	Pt	oblong, purple w green + white veins, v strong. dist. top points up but submerged on top of orange LC	no real ha	SB	375	191	104							199	X	Pt	squashy grey MC, narrow end up, mostly embed in gravel #189 + dist and rim of pink LC = orange stations B flow and mid of smaller pink MC = weaker stations							
TR18	199	X	Pt	squashy grey MC, narrow end up, mostly embed in gravel #189 + dist and rim of pink LC = orange stations B flow and mid of smaller pink MC = weaker stations	round grey flat mc w old magnet plug v distinct, immed dist of orange SB which is slightly embed and has tracks on the substrate	LC	295	210	204							200	X	Pt	round grey flat mc w old magnet plug v distinct, immed dist of orange SB which is slightly embed and has tracks on the substrate							
TR18	200	X	Pt	round grey flat mc w old magnet plug v distinct, immed dist of orange SB which is slightly embed and has tracks on the substrate	suboval, med brown, flatish top, immed dist whitened emergent post-44-B	SB	335	265	85							201	X	Pt	suboval, med brown, flatish top, immed dist whitened emergent post-44-B							
TR18	201	X	Pt	suboval, med brown, flatish top, immed dist whitened emergent post-44-B	red-black patchy sc in deep run, just dist of oblong green brown LC w long axis perp to flow	SC	125	104	82							202	X	Pt	red-black patchy sc in deep run, just dist of oblong green brown LC w long axis perp to flow							
TR18	202	X	Pt	red-black patchy sc in deep run, just dist of oblong green brown LC w long axis perp to flow	large irregular shape, flat faced grey lc with face angled	no ha	SB	479								203	no	P Pt	large irregular shape, flat faced grey lc with face angled							
TR18	203	no	P Pt	large irregular shape, flat faced grey lc with face angled	sb - embedded in bank	b = bank + ha	SB	374								204	no	P Pt	sb - embedded in bank							
TR18	204	no	P Pt	sb - embedded in bank	ha ulfr = B adj to bank	SB	214	249	155							205	X	Pt	semi oval, greyish mc surround by isopods							
TR18	205	X	Pt	semi oval, greyish mc surround by isopods	ulfr = also submerged B, but 0.5 m dist	SB	379	339	184							206	X	P Pt	round reddish mc with flat top + ridges, just slightly emergent							
TR18	206	X	P Pt	round reddish mc with flat top + ridges, just slightly emergent	emergent white cream, irregular shape at top of B field, wedged up to 2 embed Bs w lichen	dnB B held + ha	LC	410	227	195						207	7X	Pt	emergent white cream, irregular shape at top of B field, wedged up to 2 embed Bs w lichen							
TR18	207	7X	Pt	emergent white cream, irregular shape at top of B field, wedged up to 2 embed Bs w lichen	recoval flat dirty brown LC w whiter band on top, the dist ms = embed under olive brown/green LC. immed dist = pale grey SB just emergent and w stations B flow and holes on ms of B	dist B = ha	LC	315	229	100						208	X	Pt	recoval flat dirty brown LC w whiter band on top, the dist ms = embed under olive brown/green LC. immed dist = pale grey SB just emergent and w stations B flow and holes on ms of B							
TR18	208	X	Pt	recoval flat dirty brown LC w whiter band on top, the dist ms = embed under olive brown/green LC. immed dist = pale grey SB just emergent and w stations B flow and holes on ms of B	creamwith lots of dark brown mottle, sub-oval between 2 lichen B, pencil #	not really B at side but does not overlap	LC	446	174	122						209	X	Pt	creamwith lots of dark brown mottle, sub-oval between 2 lichen B, pencil #							
TR18	209	X	Pt	creamwith lots of dark brown mottle, sub-oval between 2 lichen B, pencil #	large round flat with ridges creamy colour	no ha	MB	862								210	no	P	large round flat with ridges creamy colour							
TR18	210	no	P	large round flat with ridges creamy colour	oval creamy green LC, on SCMC bed, immed dist of dirty brown creamy LC w large emble quartz eye	no ha	LC	306	230	164						211	7X	Pt	oval creamy green LC, on SCMC bed, immed dist of dirty brown creamy LC w large emble quartz eye							
TR18	211	7X	Pt	oval creamy green LC, on SCMC bed, immed dist of dirty brown creamy LC w large emble quartz eye	old stone #251 creamy brown oval flat faced to w stations, on LHS = orange station B w open hole on its surface and this B forms the eye of chule	no ha	LC	310	250	185						212	7X	Pt	old stone #251 creamy brown oval flat faced to w stations, on LHS = orange station B w open hole on its surface and this B forms the eye of chule. NEW 25 Jun emergent, 1 m dist of yellow SB							
TR18	212	7X	Pt	old stone #251 creamy brown oval flat faced to w stations, on LHS = orange station B w open hole on its surface and this B forms the eye of chule	immov embed submerged pinkgrey B w plane on upper its surface and eye on dist end w purly, surrounded by SC	no ha	LC	435	300	?						213	no	P	immov embed submerged pinkgrey B w plane on upper its surface and eye on dist end w purly, surrounded by SC							
TR18	213	no	P	immov embed submerged pinkgrey B w plane on upper its surface and eye on dist end w purly, surrounded by SC	long red ridged with patches, perpendicular to current, embed	ha = conc embed lower than dist stones	SB	369								214	no	P	long red ridged with patches, perpendicular to current, embed							
TR18	214	no	P	long red ridged with patches, perpendicular to current, embed	red, sub-oval, flat face, ulfr of emergent lichen B	ha = orange lichen B dist	SB	295	257	112						215	X	Pt	red, sub-oval, flat face, ulfr of emergent lichen B							
TR18	215	X	Pt	red, sub-oval, flat face, ulfr of emergent lichen B	immov large cream oval, B embedded in bank with lichen spots	ha = embedded in bank, B ulfr	MB	570								216	no	Pt	immov large cream oval, B embedded in bank with lichen spots							
TR18	216	no	Pt	immov large cream oval, B embedded in bank with lichen spots	small embedded but emergent, red ridged below lichen B, dist red ridged to ulfr	wedged between ulfr + dist B = ha	SB	305	190							217	no	P Pt	small embedded but emergent, red ridged below lichen B, dist red ridged to ulfr							
TR18	217	no	P Pt	small embedded but emergent, red ridged below lichen B, dist red ridged to ulfr	immov orange lichen boulder pinned by ulfr large white boulder	ulfr B pinned + ha	MB	600	695							218	no	P Pt	immov orange lichen boulder pinned by ulfr large white boulder							
TR18	218	no	P Pt	immov orange lichen boulder pinned by ulfr large white boulder	orange red triangle flat face, pointed end between 2 LC, dist top emergent	no ha	SB	490	320	190						219	X	P Pt	orange red triangle flat face, pointed end between 2 LC, dist top emergent							
TR18	219	X	P Pt	orange red triangle flat face, pointed end between 2 LC, dist top emergent	brown sc, in creek bed 2 emergent lichen B on right, dist of submerged flat sc in hole	b. dist & to right + ulfr lc = ha	SC	130	110	74						220	X	P Pt	brown sc, in creek bed 2 emergent lichen B on right, dist of submerged flat sc in hole							
TR18	220	X	P Pt	brown sc, in creek bed 2 emergent lichen B on right, dist of submerged flat sc in hole	immov, embed B, lichen, largest in vicinity	ha = smaller B dist which are also shaded by it	LC	1300	1100	?						221	no	P Pt	immov, embed B, lichen, largest in vicinity							
TR18	221	no	P Pt	immov, embed B, lichen, largest in vicinity	flat oval gold MC, pinned into by oval flattish orange-brown SB w crescent crease on top, the dist ms = embed under olive brown LC. immed dist = pale grey SB just emergent and w stations B flow and holes on ms of B	no ha	LC	470	270	?						222	no	P	flat oval gold MC, pinned into by oval flattish orange-brown SB w crescent crease on top, the dist ms = embed under olive brown LC. immed dist = pale grey SB just emergent and w stations B flow and holes on ms of B							
TR18	222	no	P	flat oval gold MC, pinned into by oval flattish orange-brown SB w crescent crease on top, the dist ms = embed under olive brown LC. immed dist = pale grey SB just emergent and w stations B flow and holes on ms of B	immov embed submerged pinkgrey B w plane on upper its surface and eye on dist end w purly, surrounded by SC	no ha	LC	435	300	?						223	X	Pt	immov embed submerged pinkgrey B w plane on upper its surface and eye on dist end w purly, surrounded by SC							
TR18	223	X	Pt	immov embed submerged pinkgrey B w plane on upper its surface and eye on dist end w purly, surrounded by SC	reddish round creamy grey green, on the grey brown submerged B w smooth top, #224 + dist of emergent SB w some cracks and dist angled up, on cobble bed	dist + ha = of B	LC	410	360	145						224	X	Pt	reddish round creamy grey green, on the grey brown submerged B w smooth top, #224 + dist of emergent SB w some cracks and dist angled up, on cobble bed							
TR18	224	X	Pt	reddish round creamy grey green, on the grey brown submerged B w smooth top, #224 + dist of emergent SB w some cracks and dist angled up, on cobble bed	red brown flat MC (prev displaced magnet rock), 30 cm dist of chule below embed lichen B, this one = situations B flow, LHS one orange w ridge	no ha, in chule below B	LC	220	182	90						225	X	Pt	red brown flat MC (prev displaced magnet rock), 30 cm dist of chule below embed lichen B, this one = situations B flow, LHS one orange w ridge							
TR18	225	X	Pt	red brown flat MC (prev displaced magnet rock), 30 cm dist of chule below embed lichen B, this one = situations B flow, LHS one orange w ridge	embedd, round flattish brown B, just dist of circle of emergent SB	ha = circle of B's ulfr B emerg	SB	475	367							226	no	P	embedd, round flattish brown B, just dist of circle of emergent SB							
TR18	226	no	P	embedd, round flattish brown B, just dist of circle of emergent SB	light brown MC, speckled 1/2 circle, flat face, ulfr of lichen B	ha = 2 B down stream on the none on this	LC	287	221	171						227	X	Pt	light brown MC, speckled 1/2 circle, flat face, ulfr of lichen B							
TR18	227	X	Pt	light brown MC, speckled 1/2 circle, flat face, ulfr of lichen B	immov flat cream brown LC embed into back, dist of oval flat lichen B	set in bank	LC	475	310							228	no	P Pt	immov flat cream brown LC embed into back, dist of oval flat lichen B							
TR18	228	no	P Pt	immov flat cream brown LC embed into back, dist of oval flat lichen B	lichen lc, dry at edge of channel immovable, set into bank	ha = ulfr + bank no larger stuff around	?	255	230							229	no	P Pt	lichen lc, dry at edge of channel immovable, set into bank							
TR18	229	no	P Pt	lichen lc, dry at edge of channel immovable, set into bank	dry brownish white sb, adjacent large smooth lichen B + ulfr another red lichen B rectangular flat faced, in shelter of 2 lichen B's	dist B's	SB	505	391							231	no	P Pt	dry brownish white sb, adjacent large smooth lichen B + ulfr another red lichen B rectangular flat faced, in shelter of 2 lichen B's							
TR18	231	no	P Pt	dry brownish white sb, adjacent large smooth lichen B + ulfr another red lichen B rectangular flat faced, in shelter of 2 lichen B's	emergent, light brown, sb with B's ulfr + dist	ha = ulfr B's	SB	362	286	149						232	X	P	emergent, light brown, sb with B's ulfr + dist							
TR18	232	X	P	emergent, light brown, sb with B's ulfr + dist	large ovalish, flat face orange + cream B, w concave reddish bit on dist side, long axis perpendicular to flow	ha = ulfr + dist B's ulfr + slightly overhanging	SB	500	475							233	no	P Pt	large ovalish, flat face orange + cream B, w concave reddish bit on dist side, long axis perpendicular to flow							
TR18	233	no	P Pt	large ovalish, flat face orange + cream B, w concave reddish bit on dist side, long axis perpendicular to flow	immov golden brown round MC, flat topped black spots on ulfr edge, pinned into by cream green rechteg LC w orange dist on the	immov	SB	370	305	150						235	no	P - 2 blocks	immov golden brown round MC, flat topped black spots on ulfr edge, pinned into by cream green rechteg LC w orange dist on the							
TR18	235	no	P - 2 blocks	immov golden brown round MC, flat topped black spots on ulfr edge, pinned into by cream green rechteg LC w orange dist on the	immov large, flattish wavy golden submerged B	no ha but big	LC	605	775	?						236	no	P	immov large, flattish wavy golden submerged B							
TR18	236	no	P	immov large, flattish wavy golden submerged B	old + round flat brown speckled SC immed ulfr grey pear shaped MC, point on dist end # 237 on LHS of flat round orange subm SB # 237 and m more deeply set. NEW 26 Jun truss beam, SC immed ulfr of round flat MC	no ha	LC	447	127	73						237	X	Pt	old + round flat brown speckled SC immed ulfr grey pear shaped MC, point on dist end # 237 on LHS of flat round orange subm SB # 237 and m more deeply set. NEW 26 Jun truss beam, SC immed ulfr of round flat MC							
TR18	237	X	Pt	old + round flat brown speckled SC immed ulfr grey pear shaped MC, point on dist end # 237 on LHS of flat round orange subm SB # 237 and m more deeply set. NEW 26 Jun truss beam, SC immed ulfr of round flat MC	immov - embed angular-rectang orange + pink at 45 deg to flow, ulfr and in grey, dist end in cobble. Slightly dist of track	ulfr orange X B + ha	LC	470	165	165							238	no	P - 2 blocks	immov - embed angular-rectang orange + pink at 45 deg to flow, ulfr and in grey, dist end in cobble. Slightly dist of track						
TR18	238	no	P - 2 blocks	immov - embed angular-rectang orange + pink at 45 deg to flow, ulfr and in grey, dist end in cobble. Slightly dist of track	orange oval lc, pinned by adjacent white emergent B with lichen, no on the putty + partially off-shouldered	pinned on side + dist B = ha	SB	474								239	no	P - 3 blocks	orange oval lc, pinned by adjacent white emergent B with lichen, no on the putty + partially off-shouldered							
TR18	239	no	P - 3 blocks	orange oval lc, pinned by adjacent white emergent B with lichen, no on the putty + partially off-shouldered	flat white + orange submerged with crevice lines, another flat SB on top of part of the stone, rem + visible, long emergent B on LHS	pinned by B on top + ha	MB	542								240	no	sv + sa net	flat white + orange submerged with crevice lines, another flat SB on top of part of the stone, rem + visible, long emergent B on LHS							
TR18	240	no	sv + sa net	flat white + orange submerged with crevice lines, another flat SB on top of part of the stone, rem + visible, long emergent B on LHS	angular brown + pink emergent, beta 2 embed white lichen spotted B's, both embed in bank	ha = white B in bank	SB	235	200	120						241	X	Pt	angular brown + pink emergent, beta 2 embed white lichen spotted B's, both embed in bank							
TR18	241	X	Pt	angular brown + pink emergent, beta 2 embed white lichen spotted B's, both embed in bank	emergent white with deep red tooth/triangle shapes, angular, just top of large irregular red irregular B in low	ha ulfr red B	LC	327	172	102						242	X	Pt	emergent white with deep red tooth/triangle shapes, angular, just top of large irregular red irregular B in low							
TR18	242	X	Pt	emergent white with deep red tooth/triangle shapes, angular, just top of large irregular red irregular B in low	angular rectang cube, quartz + red marbled, dist and up, off LHS point of emerg pink lichen B, ulfr + also below rock	no	LC	149	133	100						243	X	Pt	angular rectang cube, quartz + red marbled, dist and up, off LHS point of emerg pink lichen B, ulfr + also below rock							
TR18	243	X	Pt	angular rectang cube, quartz + red marbled, dist and up, off LHS point of emerg pink lichen B, ulfr + also below rock	embedd immov irreg-oval shaped brown B in lichen B	ha = ulfr lines of B + sub in line	MB	560								244	no	7P Pt	embedd immov irreg-oval shaped brown B in lichen B							
TR18	244	no	7P Pt	embedd immov irreg-oval shaped brown B in lichen B	large cream oval B, flatish side facing ulfr, smaller B's packed at dist side	no immov ha	MB	844								245	no	Pt	large cream oval B, flatish side facing ulfr, smaller B's packed at dist side				</			

Second season set-up stone data - May 2004 green shading indicates stones that were lost in 2003 and replaced during setup 2004

Table with columns for stone no., invt sample, Putty (PT), description, hydraulic shelter, Stone Category, Stone Size (x, y, z), Velocity (m/s), and various search dates. Includes detailed descriptions of stones and their characteristics.

FLOOD COLUMN: blue = moved; pink = OUT; Orange shaded = ...

COLUMN: green shade = possible invert / peri sample for after June flood: OLD STONES; pink shade, poss invert samples (must be full samp); NEW STONES, yellow shade, poss invert IMMOV (top surf area only); TICK WHICH ONE ARE STILL SUITABLE

old stone size incl, followed by NEW stone size where replaced. flow depth taken during SETUP (low baseflow) = refers to all initial stones; link to initial Tritan survey. flow depth taken ON 25 JUNE (mid baseflow) = refers to all remaining / new stones; linked to reservoir by Tritan

Main data table with columns: FLOOD 1 - Jun 10 search, BIG FLOOD 2 - Jun 21-23 search, FLOOD 3 - July 2 search, FLOOD 4 - July 18 search, Flood 5, Offset from start, stone no., X invert sample, Putty (P) Paint (PT), Description: original (setup) description, followed by NEW: description where stones have been lost; then (marker has changed (eg putty to paint), new marker type indicated. Stone x (mm), Stone y (mm), Stone z (mm), depth, velocity, depth, velocity, Comment.

FLOOD COLUMN: blue = moved; red = OUT; Orange = FLOOD COLUMN: green shade = possible invert / peri sample for after June flood; OLD STONES: pink shade, poss invert samples (must be full samp); NEW STONES, yellow shade, poss invert IMMOV (top surf area only) - TICK WHICH ONES ARE STILL SUITABLE

flow depth taken during SETUP (low baseflow) - refers to all initial stones; link to initial Tritan survey flow depth taken ON 25 JUNE (med baseflow) in refers to all remaining / new stones; linked to resurvey by Tritan

Main data table with columns: FLOOD 1 - Jun 10 search, BIG FLOOD 2 Jun 21-23 search (7207 moved), FLOOD 3 - July 2 search (in heavy rain), FLOOD 4 - July 18 search, Flood 5, Offset from start stone no., X= invert sample, e = periphyton, imm, emerg = no samp, Putty (P) Paint (PT), Description: original (setup) description, followed by NEW: description where stones have been lost; then if marker has changed (eg putty to paint), new marker type indicated, Stone x (mm), Stone y (mm), Stone z (mm), depth, velocity, depth, velocity, Comment. Rows include items 23-418 with various descriptions and measurements.

BERG RIVER STUDY SITE : FIELD OBSERVATIONS DATABASE

Stellenbosch University <http://scholar.msu.ac.za>

FLOOD COLUMN: blue = moved; pink = OUT; Orange shade = possible invert / peri sample for after June flood; OLD STONES: pink shade, poss invert samples (must be full samp); NEW STONES: yellow shade, poss invert IMMOV (top surf area only) - TICK WHICH ONES ARE STILL SUITABLE

old stone size incl. followed by NEW stone size where replaced

flow/depth taken during SETUP (low baseflow) as refers to all initial stones; link to initial Tritan survey
flow/depth taken ON 25 JUNE (med baseflow) as refers to all remaining / new stones; linked to resurvey by Tritan

FLOOD 1 - Jun 18 search	BIG FLOOD 2 Jun 21-23 search (7207 moved)	FLOOD 3 - July 2 search (in heavy rain)	FLOOD 4 - July 18 search	Flood 5	Offset from start	X# invert sample, # = periphyton, imm, emerg	Putty (P) Paint (PT)	Description: original (setup) description, followed by NEW: description where stones have been lost; then if marker has changed (eg putty to paint), new marker type indicated	Stone x (mm)	Stone y (mm)	Stone z (mm)	depth	velocity	depth	velocity	Comment		
					31	419	too emerg	pt	lc - orange oblong blocky black top: emerges on rhs of tree trunk: #419 = most distr in line of 3 LC/SBs	320	220	205	0			8		
					32	420	full - X#	pt	yellow green round domed MC, betw 1) emergent chisel topped brown sb on rhs, and 2) gold yellow oval knob on lhs and upstr	255	210	95				22	0.08	
					TR 30 Tape start 2													
	OUT: new stone				16	421	full - X#	pt	2-tone red + cream mg, immed distr and left of flat triang embed B w lichen stripe along rmg distr rhs margin NEW 25 June: ac - brown flat (correct number? notes damaged)	70 new: 160	50 new: 100	25 new: 60	0			8	0.01	
					17	422	immov emerg	pt	oval irreg b, white w lichen stripe on distr: dome-shaped but "falling over" on distr side	790	490	emb					emerg	
	OUT: new stone				18	423	full - X#	pt	flat-irreg surface "bean" MC, immed to rhs of square flat SB w large hole on middle of distr edge NEW 25 June: the SB - white embed, angular, hole in its distr = new #	230 new: 640	180 new: 600	85 new: emb	3	0.6				
	OUT: new stone				19	424	full - X#	pt	mc - red and white patches, red tip facing distr, no hs. sits proudly in bw. 10cm distr of orange and cream subm sb	230	200	150	2			8	0.02	
	OUT: new stone				20	425	dry	pt	oval, blockish white LC on in-stream edge of backwater: is on rhs of bar separating bw from main channel. "face" of #425 slopes down to rhs, #425 = 0.75 m distr of v large triang blocky emergent (proud) red/white B, and immed distr of the B = submg white B w taller ridge and rounded distr end. NEW 25 June: emerg dry SB w white striations that = transverse and converging lns	340 new: 505	225 new: 360	emb new: 275					emerg	
	OUT/covered ?? Whats this?			OUT	21	426	dry-bank edge man channel	pt	oval flat pink SB, just distr of orange end of emerg embed B. NEW 25 June: round white SC ?? more	506 new: 90	359 new: 70	166 new: 60	0					
					22	427	full - X#	pt	sc - pink and red, blockish with one longer end pointing distr + across channel, #327 = midway betw 1) on distr rhs, emerg oval sb = orange and white, and 2) on upstr lhs, emerg pinky orange ls	145	100	80	0			12	0.11	
					23	428	full - X#	pt	mc - orange and cream, oval flattish top, orange end facing distr, few cracks on upper surf, esp upstr edge, sed immed to lhs of emerg, whitish + rich domed b distr of #428 = submg white blockish embed B w brown striations nearly // to flow	230	210	70	0			23	0.13	
					24	429	full - X#	pt	brown and grey angular LC/SB, large flat forms seat on upstr side, sits on top of pear-shaped light and dark orange sb which is raised distr	405	275	265	0			20	0.48	
					25	430	full - X#	pt	oval, light and dark orange LC, not embed, submg, on lhs of yellow triang rock - lhs point of this - pointing slightly distr, red line on this perp flow scoop in middle // flow ?? of #430 or other?	395	300	175	8	0.28				
					26	431	sa wire handle net	pu	subm white-yellow triang, flat surface apex upstr = cut off, distr point longer on rhs than lhs, lhs point most elevated, deeply submerged, smooth surface	825	815	emb	5	0.03		27	0.53	
	OUT: new stone				27	432	full - X#	pt	sc in bed of sc = lg, lying betw 1) white/pinky submg pear-shp SB, w submg teardrop B on lhs and 2) dusty pink blockish triang SB w fractured rhs, #432 = creamy-grey retriangl long axis perp flow, no hs. NEW 25 June: mc - round green, immed distr, of brownly orange/grey triang knob with point upstream	not measured new: 215	not measured new: 200	not measured new: 90	14	0.43		36	1.07	
					28	433	full - X#	pt	pink s-mc, mid-one of 3 mc's lodged betw 3 emerg lich b's - 1) upstr and left, 2) distr to left, 3) triang, just emerg, lich b distr and in line w the upstr (1) is -> forms a channel catching these mc's	300	260	130	3	0.36		16	0.12 bubbly	
					29	434	emerg	pt	flat white pink knob, distr end raised and nesting on lichen emerg b distr, another lichen emergent B, long axis perp flow, = to lhs	400	395	185				16	0.45	
					30	435	sa orange alu handle net	immov pu	oval brown pink SB, 2 white lines, transverse-parallel to flow, speckled surface, distr lifted and = perfect arc; upstr of #435 = oval brownly b that partly overlaps it, #435 = also slightly embedd at upstr portion	545	440	emb	6	0.32		54	0.54	
					31	436	emerg	pt	round-oval pink emerg B, embed, on lhs of rif channel	785	495	emb		emerg		26	0.54	
					32	437	tp emerg, but full - X#	pt	oblong brown sbic w concentric brown striations, 2 white eyes just emergent, and raised distr; it rests on upstr lhs of orange and fawn lc which is distr immed of brown and marbled white SB	320	220	135	0			12	0.39	
					33	438	emerg	pt	large red b w green moss, supports tree trunk	1010	780	580	0					emerg under tree
					34	439	dry	pt	triang MB, narrow side up and pointed end up, scoop on lhs, distr end more pointy	790	560	505	0					emerg

Appendix D: Stone Movement for Individual Flood Events



Movement
 No Movement



**Molenaars River 2003
 Stone Movement**

Flood 1

**WRC K5/1411
 The Determination of Substrata
 Maintenance Flows in Cobble
 and Boulder Bed Rivers:
 Ecological and Hydraulic
 Considerations**





MOVED

○ No Movement

● Moved



**Molenaars River 2003
Stone Movement**

Flood 2

**WRC K5/1411
The Determination of Substrata
Maintenance Flows in Cobble
and Boulder Bed Rivers:
Ecological and Hydraulic
Considerations**





MOVED

○ No Movement

● Moved



**Molenaars River 2003
Stone Movement**

Flood 3

**WRC K5/1411
The Determination of Substrata
Maintenance Flows in Cobble
and Boulder Bed Rivers:
Ecological and Hydraulic
Considerations**





MOVED

○ No Movement

● Moved



**Molenaars River 2003
Stone Movement**

Flood 4

**WRC K5/1411
The Determination of Substrata
Maintenance Flows in Cobble
and Boulder Bed Rivers:
Ecological and Hydraulic
Considerations**





MOVED

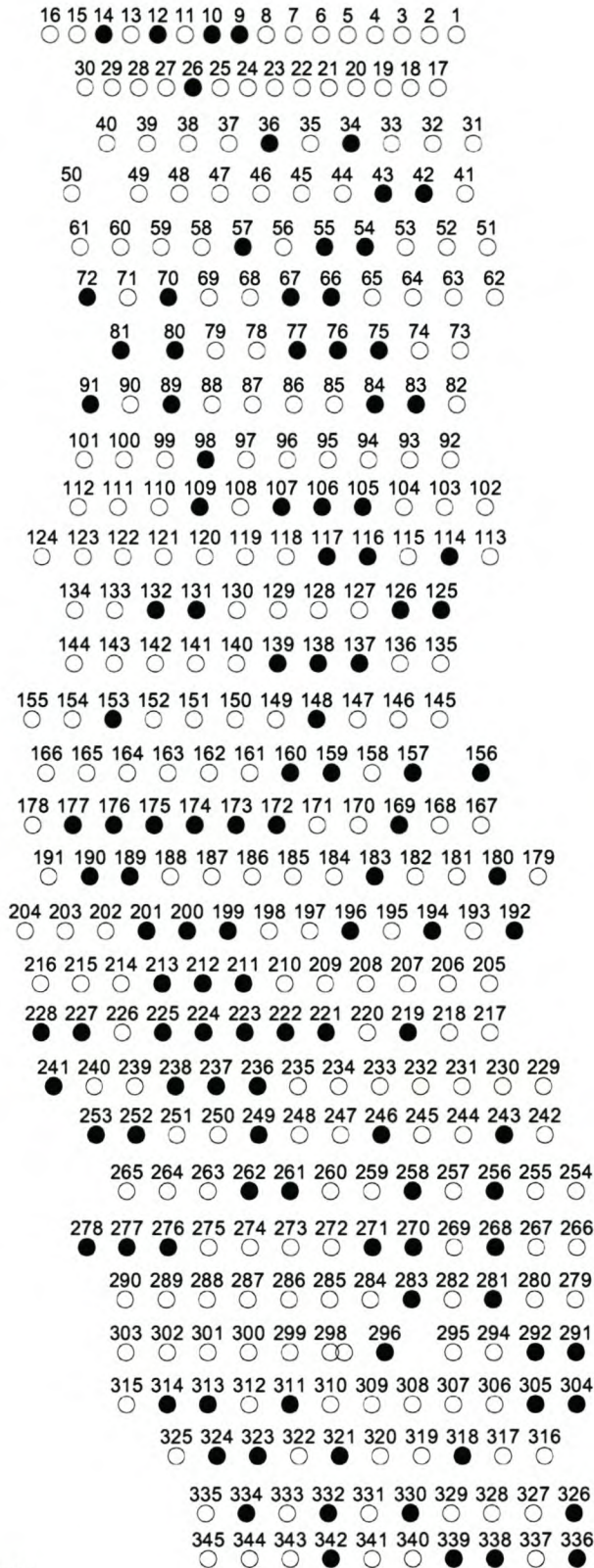
○ No Movement
● Moved



**Molenaars River 2003
Stone Movement
Flood 5**

**WRC K5/1411
The Determination of Substrata
Maintenance Flows in Cobble
and Boulder Bed Rivers:
Ecological and Hydraulic
Considerations**





MOVED
 ○ No Movement
 ● Moved

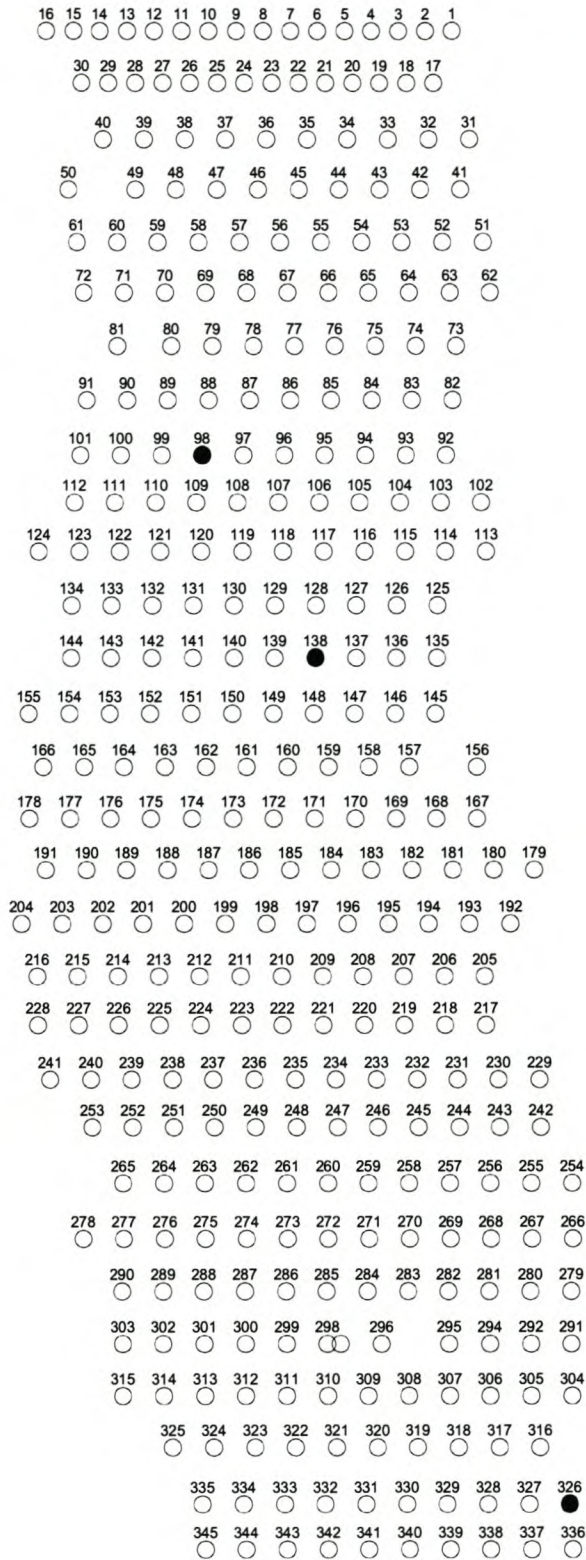


**Molenaars River 2003
 Stone Movement**

Flood 6

**WRC K5/1411
 The Determination of Substrata
 Maintenance Flows in Cobble
 and Boulder Bed Rivers:
 Ecological and Hydraulic
 Considerations**





MOVED

○ No Movement

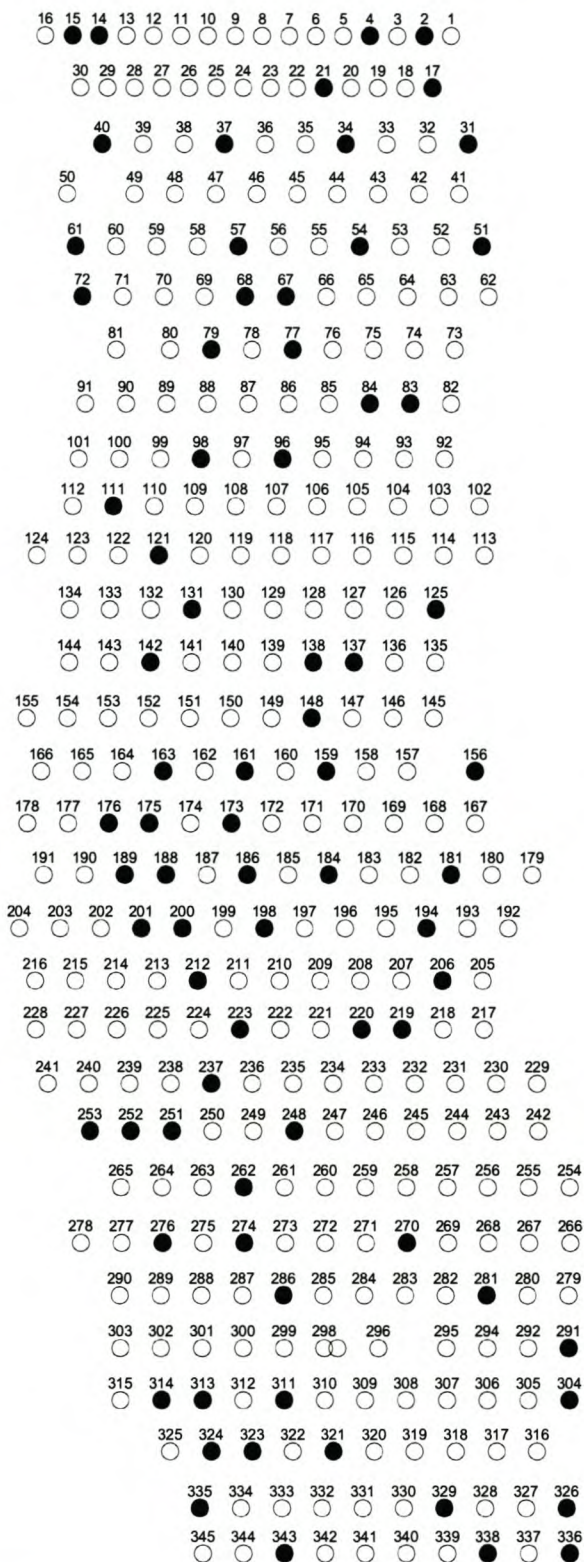
● Moved

**Molenaars River 2004
Stone Movement**

Flood 1

**WRC K5/1411
The Determination of Substrata
Maintenance Flows in Cobble
and Boulder Bed Rivers:
Ecological and Hydraulic
Considerations**





MOVED

○ No Movement

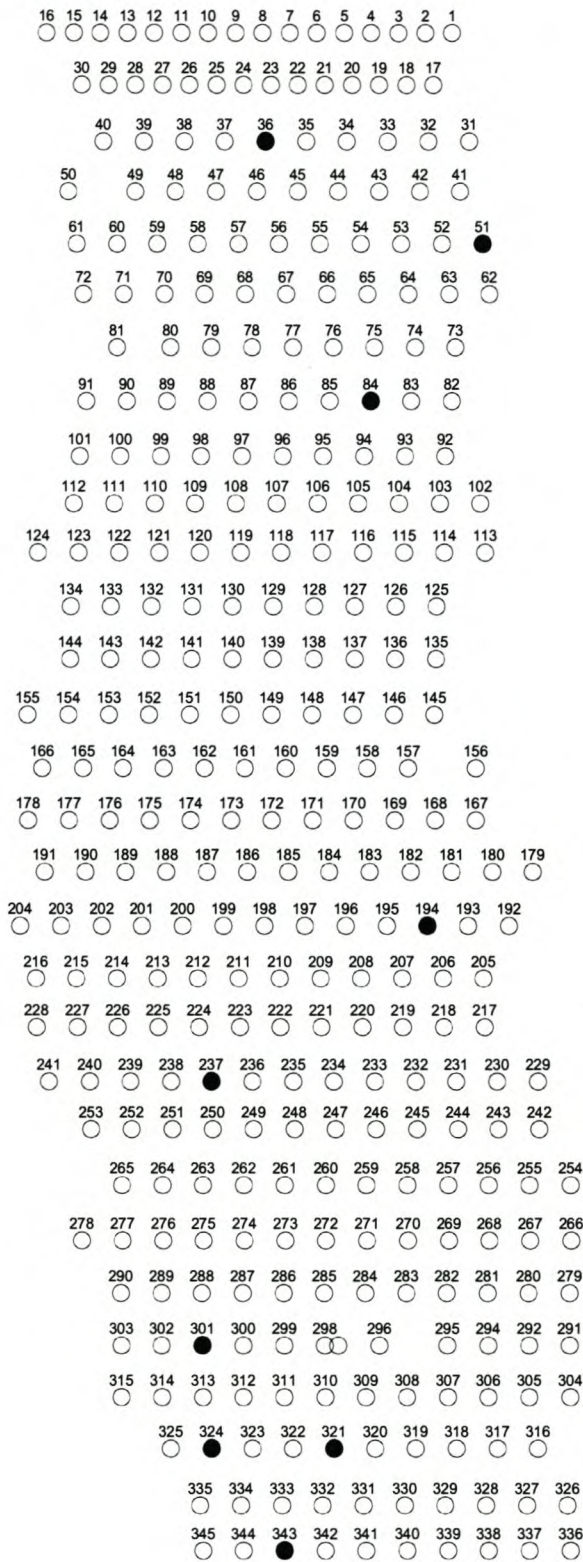
● Moved

**Molenaars River 2004
Stone Movement**

Flood 2

**WRC K5/1411
The Determination of Substrata
Maintenance Flows in Cobble
and Boulder Bed Rivers:
Ecological and Hydraulic
Considerations**





MOVED

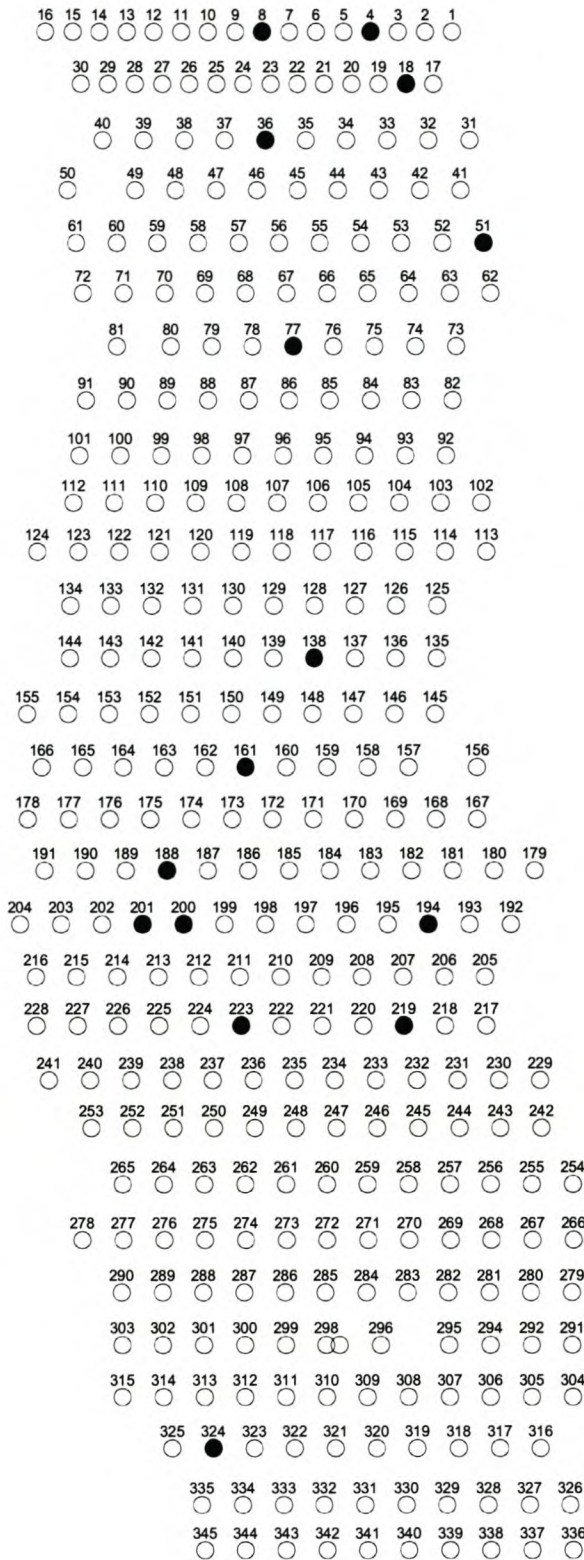
○ No Movement
 ● Moved

**Molenaars River 2004
 Stone Movement**

Flood 3

**WRC K5/1411
 The Determination of Substrata
 Maintenance Flows in Cobble
 and Boulder Bed Rivers:
 Ecological and Hydraulic
 Considerations**





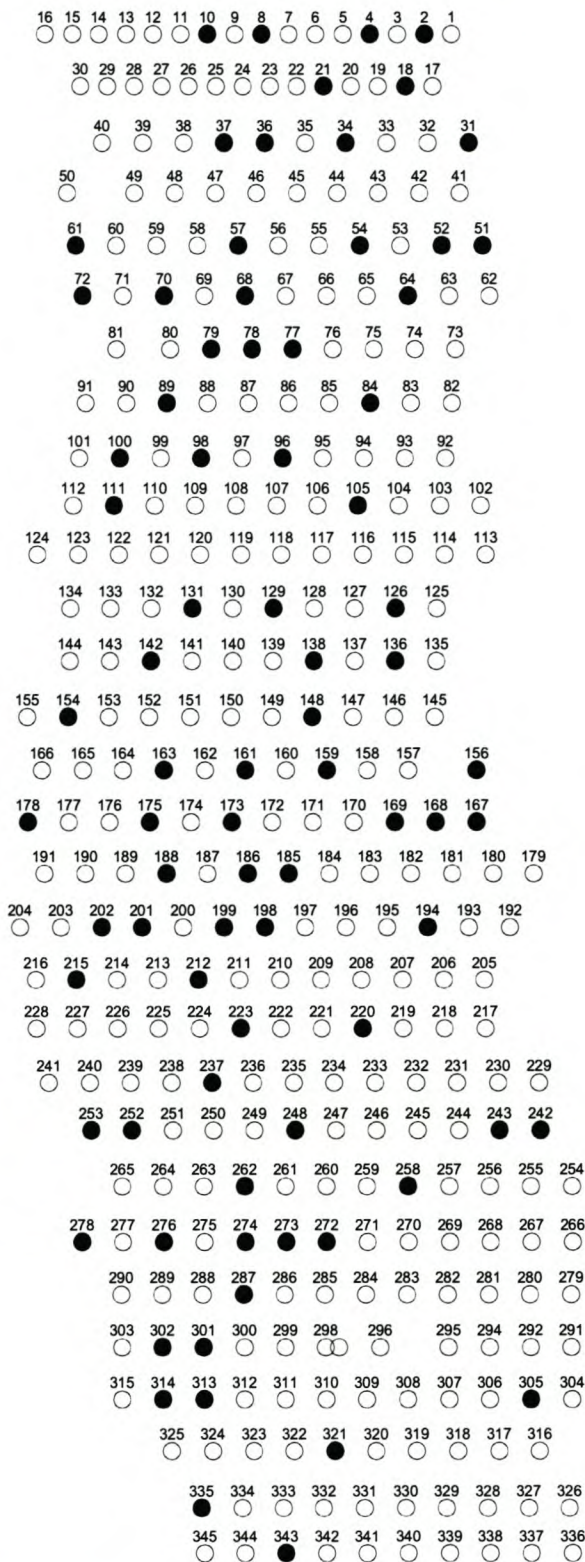
MOVED	
<input type="radio"/>	No Movement
<input checked="" type="radio"/>	Moved

**Molenaars River 2004
Stone Movement**

Flood 4

**WRC K5/1411
The Determination of Substrata
Maintenance Flows in Cobble
and Boulder Bed Rivers:
Ecological and Hydraulic
Considerations**





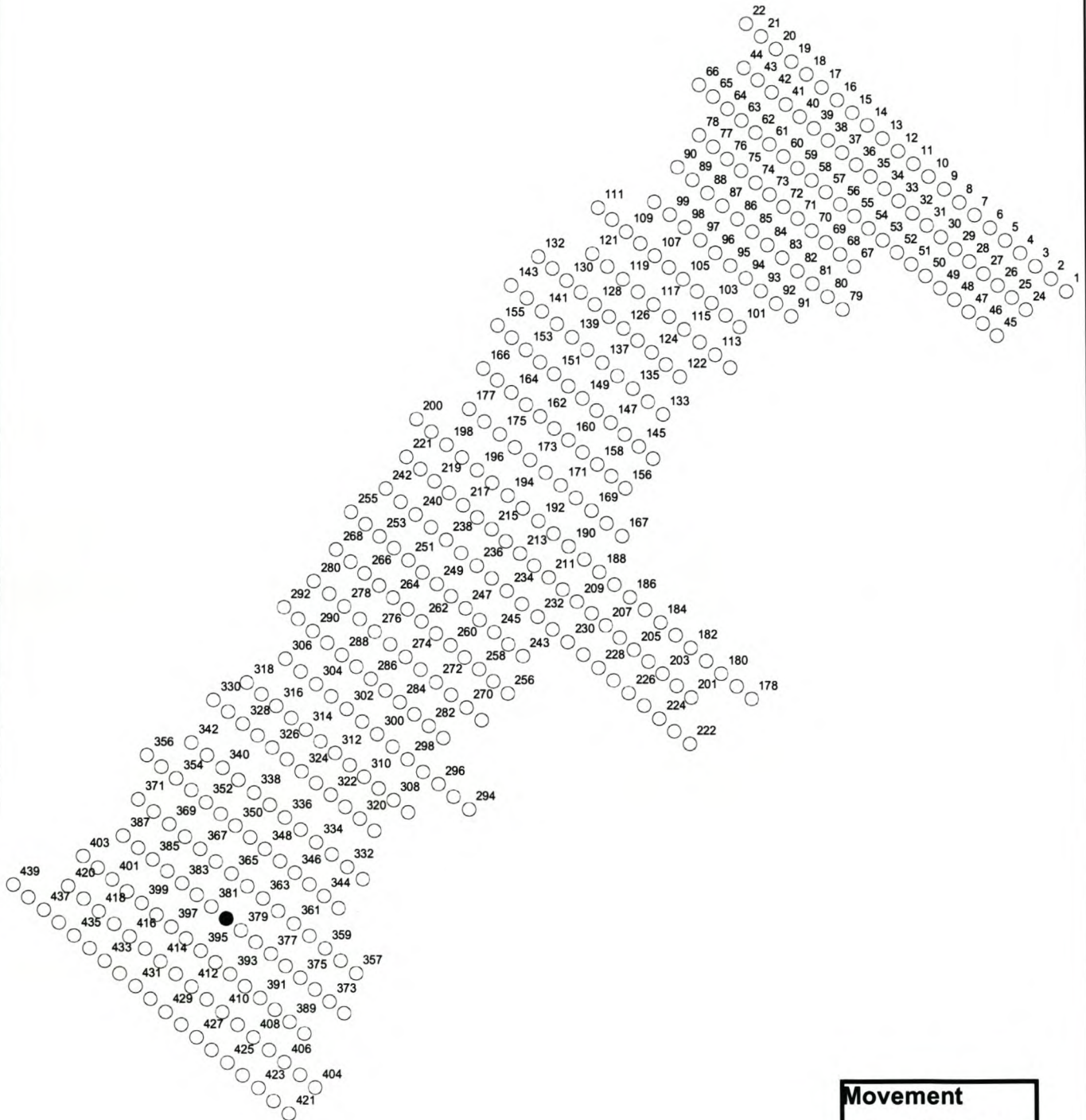
MOVED	
○	No Movement
●	Moved

**Molenaars River 2004
Stone Movement**

Flood 5

**WRC K5/1411
The Determination of Substrata
Maintenance Flows in Cobble
and Boulder Bed Rivers:
Ecological and Hydraulic
Considerations**





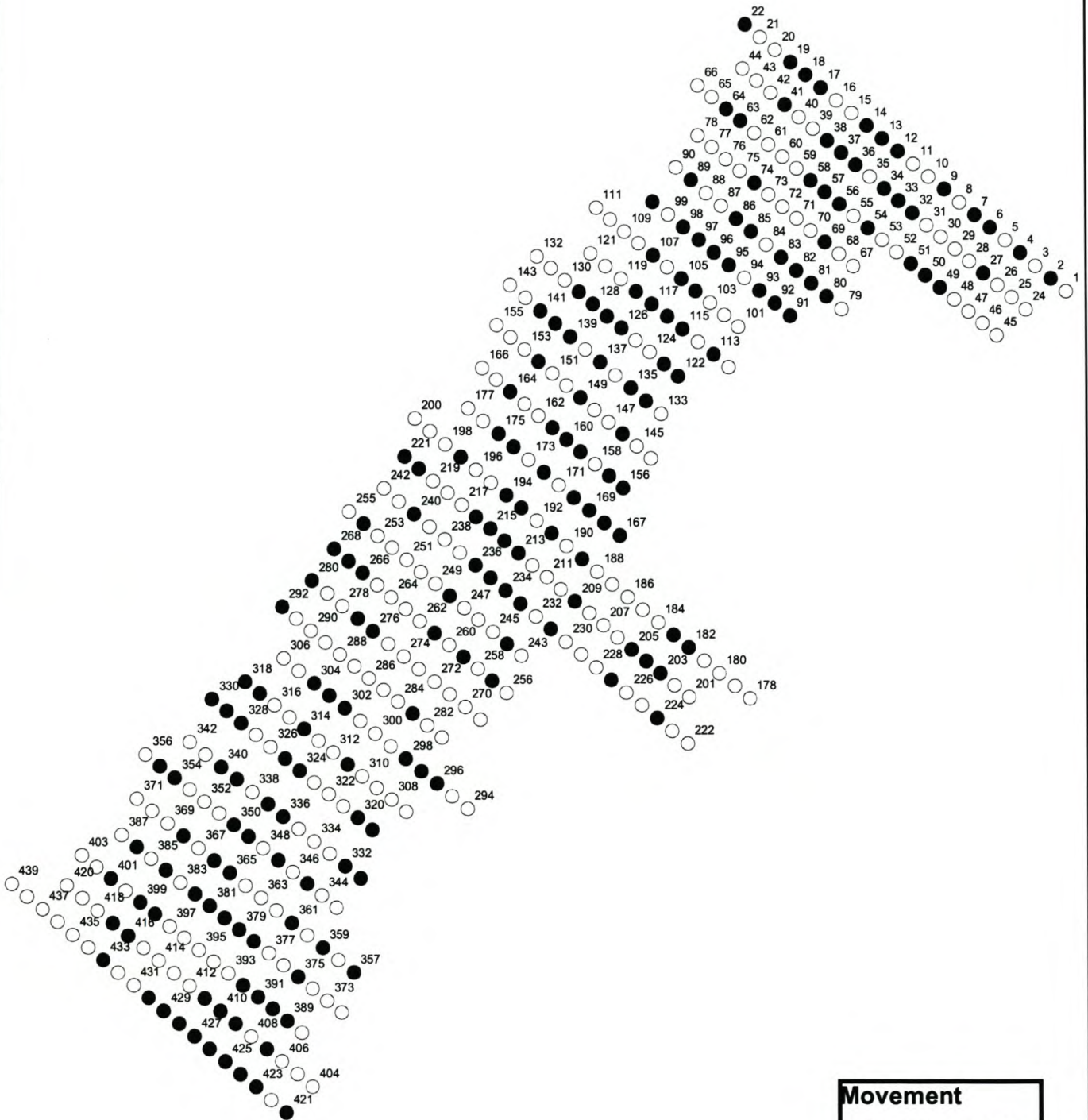
Movement	
○	No Movement
●	Moved

**Berg River 2004
Stone Movement**

Flood 1

**WRC K5/1411
The Determination of Substrata
Maintenance Flows in Cobble
and Boulder Bed Rivers:
Ecological and Hydraulic
Considerations**





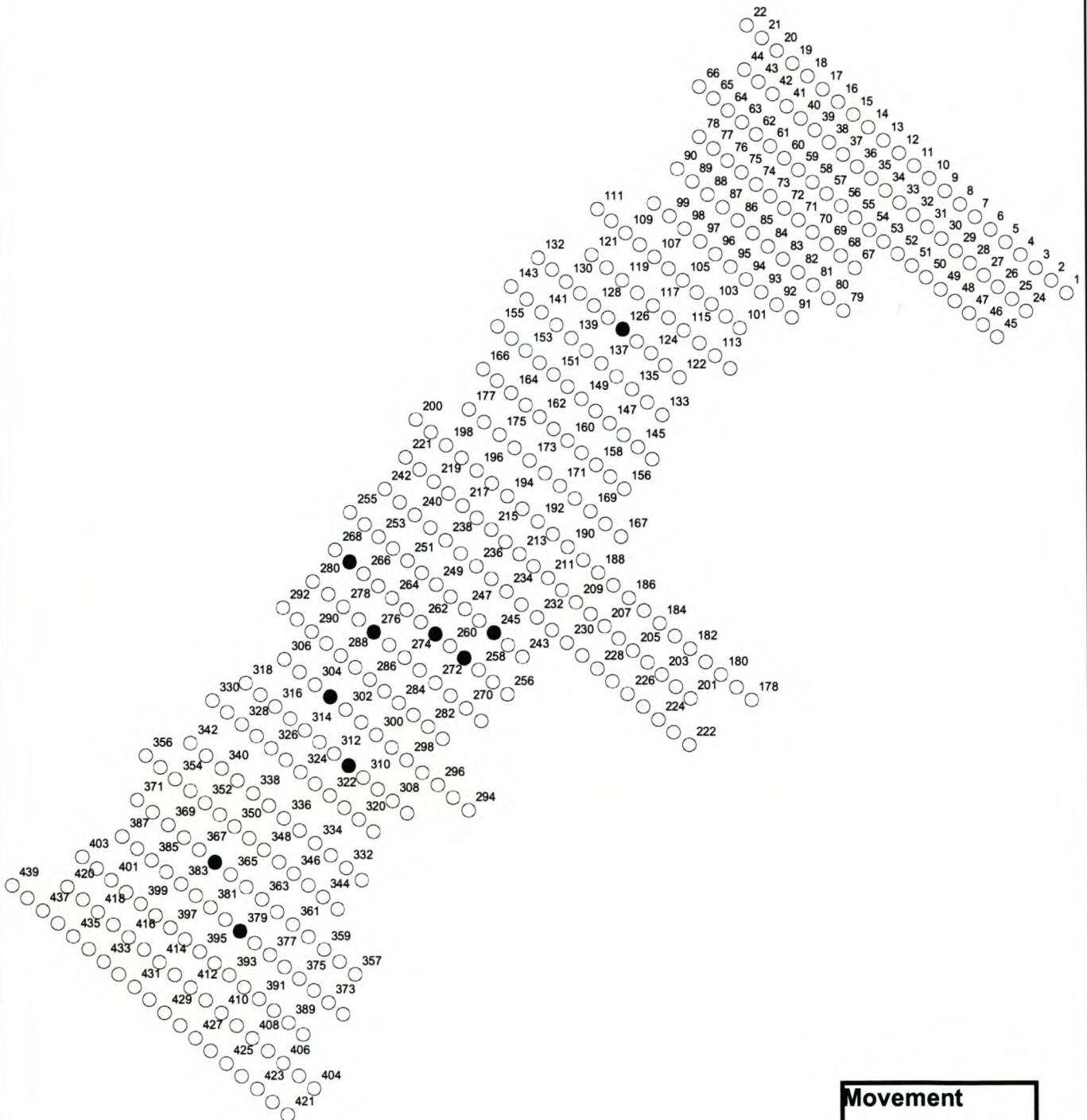
Movement	
○	No Movement
●	Moved

**Berg River 2004
Stone Movement**

Flood 2

**WRC K5/1411
The Determination of Substrata
Maintenance Flows in Cobble
and Boulder Bed Rivers:
Ecological and Hydraulic
Considerations**





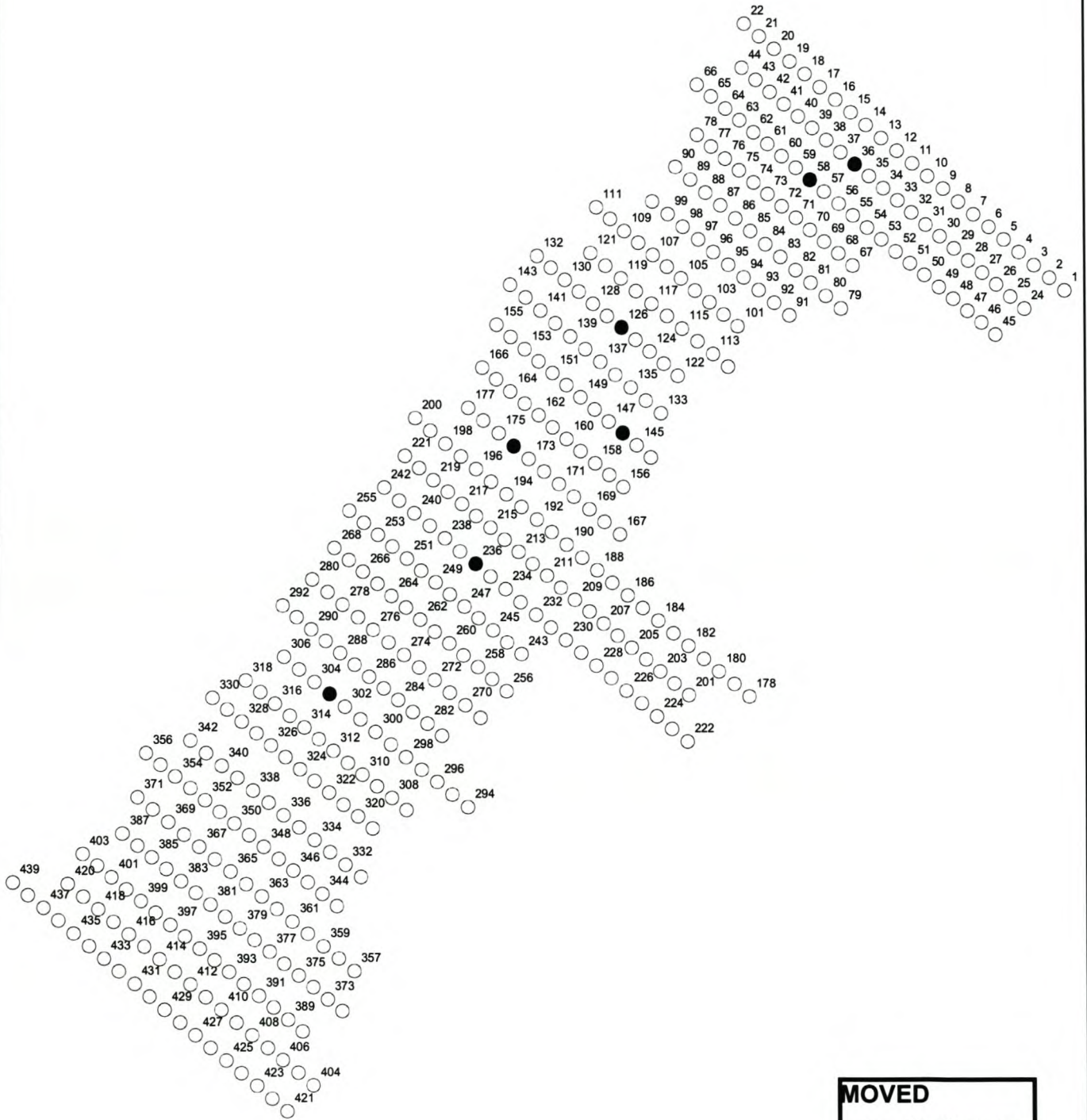
Movement	
○	No Movement
●	Moved

**Berg River 2004
Stone Movement**

Flood 3

**WRC K5/1411
The Determination of Substrata
Maintenance Flows in Cobble
and Boulder Bed Rivers:
Ecological and Hydraulic
Considerations**





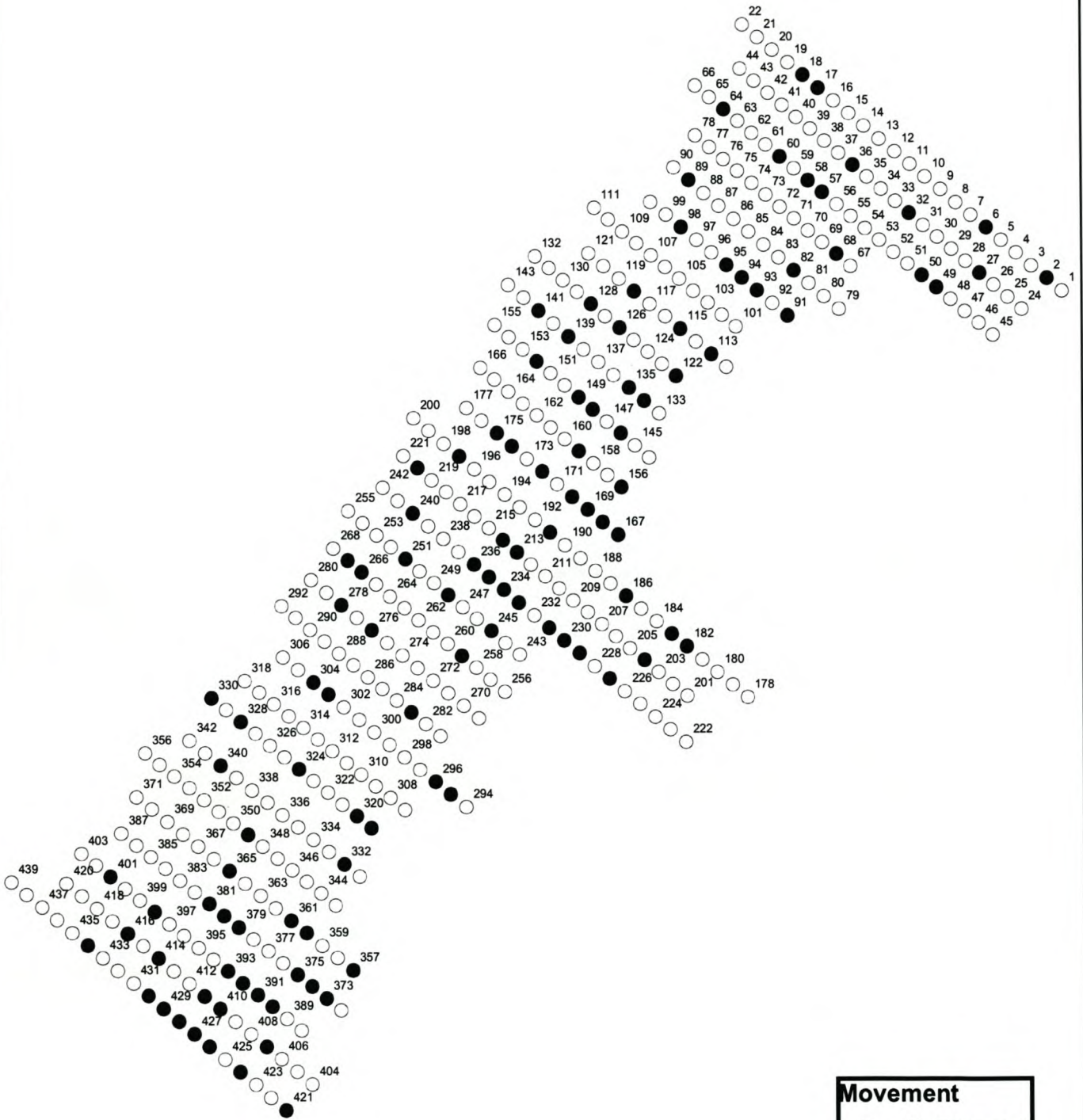
MOVED	
○	No Movement
●	Moved

**Berg River 2004
Stone Movement**

Flood 4

WRC K5/1411
The Determination of Substrata
Maintenance Flows in Cobble
and Boulder Bed Rivers:
Ecological and Hydraulic
Considerations





Movement	
○	No Movement
●	Moved

**Berg River 2004
Stone Movement**

Flood 5

**WRC K5/1411
The Determination of Substrata
Maintenance Flows in Cobble
and Boulder Bed Rivers:
Ecological and Hydraulic
Considerations**

